Multi-Band Fractal Antenna Modeling

Hayder Mazin Makki

Submitted to the
Institute of Graduate Studies and Research
in partial fulfillment of the requirements for the Degree of

Master of Science
in
Electrical and Electronic Engineering

Eastern Mediterranean University
September 2013
Gazimağusa, North Cyprus

Approval of the Institute of Graduate Studies and Research

Prof. Dr. Elvan Yılmaz
Director

I certify that this thesis satisfies the requirements as a thesis for the degree of Master of Science in Electrical and Electronic Engineering.

Prof. Dr. Aykut Hocanın
Chair, Department of Electrical and Electronic Engineering

We certify that we have read this thesis and that in our opinion it is fully adequate in scope and quality as a thesis for the degree of Master of Science in Electrical and Electronic Engineering.

Assist. Prof. Dr. Rasime Uyguroğlu
Supervisor

Examining Committee

1. Prof. Dr. Şener Uysal
2. Assoc. Prof. Dr. Hasan Demirel
3. Asst. Prof. Dr. Rasime Uyguroğlu

ABSTRACT

This thesis demonstrates the design procedure of a multilayer fractal patch antenna to be used. A novel combination structure of fractal geometries arranged in two stacked layers that allows a multiband/wideband operation has been utilized for the proposed antenna. Rectangular and triangular patches are used in layer 1 and layer 2, respectively. A combination of Sierpinski Carpet Fractal (SCF) geometry and Minkowski Fractal (MKF) geometry is used as layer 1; Layer 2 composed of the combination of Koch Snowflake Fractal (KSF) with Sierpinski gasket geometry (SGG). Layers' separation has been achieved by using 4 mm air layer for the purpose of surface wave reduction. Proximity coupled feed technique with 50 Ω microstrip line is used. Both the radiating layers and the feeder are placed on 1.59 mm thick FR4 substrate.

The simulation results show that the antenna can operate at 11 different resonance frequencies 2.08, 2.32, 3.17, 4.04, 4.49, 5.14, 6.20, 7.35, 9.22, 11.1, 11.98 (GHz), with bandwidths of 61, 36, 204, 82, 349, 673, 1142, 1481, 507, 1770 and 530 (MHz) respectively. Gain values up to 6.03 dB were obtained.

Keywords: Multiband/Wideband antenna, Fractal geometries, Multilayer patch antenna, Proximity coupled feed technique.

ÖZ

Çalışma, farklı haberleşme sistemlerinde kullanılabilecek, çok katmanlı fraktal yama anten tasarımı sunmaktadır. Önerilen anten, iki katmanlı fraktal geometrik yapı kullanılarak elde edilmiş çokbantlı / genişbant olarak kullanılabilir.Birinci ve ikinci katmanlarında sırasıyla dikdörtgen ve üçgen yamalar kullanılarak özgün bir anten tasarlanmıştır. Sierpinski Carpet Fractal (SCF) ve Minkowski Fractal (MSF) geometrileri birleşimi birinci katmanda, Sierpinski Gasket Fractal (SGF) ve Koch Snowflake Fractal (KSF) geometri birleşimi ise ikinci katmanda kullanılmıştır. Electromanyetik yüzey dalgalarını ortadan kaldırmak için, katmanlar arasında 4'er mm'lik hava katmanları yaratılmıştır. Anten beslemesi, 50Ω miktoşerit hat ile yakınlık bağdaştırma temassız besleme yöntemi ile gerçekleştirilmiştir. Besleme ve radyasyon katmanları 1.59 mm'lik FR4 maddesi üzerine yerleştirilmiştir.

FEKO simülatörü ile elde edilen sonuçlar, tasarlanan antenin 11 değişik rezonans frekansında, 2.08, 2.32, 3.17, 4.04, 4.49, 5.14, 6.20, 7.35, 9.21, 11.096, 11.98 (GHz), frekans bantgenişlikleri ile 61, 36, 204, 82, 349, 673, 1142, 1481, 507, 1770 and 530 (MHz), çalışabileceğini ve kazanç değerlerinin de 6.03dB'ye kadar ulaşabildiğini göstermektedir.

Anahtar Kelimeler: Çokbant/genişbant anten, fraktal geometriler, çok katmanlı yama anten, yakınlık bağdaştırma temassız besleme.

ACKNOWLEDGMENTS

I wish to express my great thanks, respects and regards to my supervisor Assist. Prof. Dr. Rasime Uyguroğlu for her boundless patience and wonderful help during my research. This thesis wouldn't have been possible without Assist. Prof. Dr. Rasime Uyguroğlu's guidance and priceless supervision.

Special thanks definitely go to Prof. Dr. Aykut Hocanın, the Chair of Electrical and Electronic Engineering. I will also like to thank Assoc. Prof. Dr. Hasan Demirel for his invaluable advice.

I would also want to send my heartfelt estimate to all my teachers especially Prof. Dr. Ozay Gurtug who opened knowledge gates for me, and enriched my thinking capabilities.

Also thanks go to all my dear friends especially my friend Mohammed Khalid Ibraheem for his invaluable assistance.

I would like to express my deepest thankfulness to my pretty family; they gave me a chance for completing my higher education in Cyprus. Without their support, both emotional and financial matters, finalizing this work would be impossible.

TABLE OF CONTENTS

LIST OF TABLES

LIST OF FIGURES

LIST OF SYMBOLS /ABBREVIATIONS

C	Light Speed
D	Antenna Directivity
F	Frequency of Operation
H	Substrate Thickness
L	Patch Length
$Leff$	Effective Length of Patch
L_g	Ground Plane Length
Pin	Input Power
$Prad$	Radiation Power
S	Triangular Patch Side Length
$S11$	Reflection coefficients
W	Patch Antenna Width
W_g	Ground Plane Width
ΔL	Increment Length
ε_o	Free Space Permittivity
ε_r	Dielectric Constant
ε_{reff}	Effective Dielectric Permittivity
η	Antenna Efficiency
λ	Wavelength
π	PI
BGS	Band Gap Structure
CFA	Circular Fractal Antenna
CFG	Circular Fractal Geometry

DCS	Digital Communication System
F-center	Center Frequency
FDTD	Finite Difference Time Domain
FEM	Finite Element Method
F-lower	Lower Frequency
FR4	Flame Retardant 4
F-upper	Upper Frequency
GO	Geometrical Optics
GPA	Giuseppe Peano Antenna
GPF	Giuseppe Peano Fractal
GPG	Giuseppe Peano Geometry
GPS	Global Positioning System
HCG	Hilbert Curve Geometry
HFA	Hilbert Fractal Antenna
HFG	Hilbert Fractal Geometry
HFSS	High Frequency Structures Simulators
IMT	International Mobile Telecommunications
KSA	Koch Snowflake Antenna
KSG	Koch Snowflake Geometry
KSF	Koch Snowflake Fractal
KS-SGF	Koch Snowflake-Sierpinski Gasket Fractal
MKA	Minkowski Antenna
MKF	Minkowski Fractal
MKG	Minkowski Geometry
MLFMM	Multilevel Fast Multiplole Method

MOM	Method of Moment
MSL	Microstrip Line
PBG	Photonic Band Gap
PCF	Proximity Coupled Feed
PCS	Personal Communication System
PO	Physical Optics
RF	Radio Frequency
SCA	Sierpinski Carpet Antenna
SCF	Sierpinski Carpet Fractal
SCG	Sierpinski Carpet Geometry
SC-MKF	Sierpinski Carpet-Minkowski Fractal
SFA	Square Fractal Antenna
SFG	Square Fractal Geometry
SGA	Sierpinski Gasket Antenna
SGF	Sierpinski Gasket Fractal
SGG	Sierpinski Gasket Geometry
UMTS	Universal Mobile Telecommunication System
UTD	Uniform Theory of Diffraction
UWB	Ultra Wide Band
Wi-Fi	Wireless Fidelity
WLAN	Wireless Local Area Network

Chapter 1

INTRODUCTION

Patch antenna is a printed resonant antenna of narrow-bandwidth generally used in microwave frequency bands. It was firstly coined out in 1953 [1], but a considerable attention has been received after the invention of printed circuit technology in 1970 [2]; it was used firstly for military purposes due to its attractive geometry which does not interfere with aerodynamics of the fast moving vehicles such as missiles and aircrafts; the main drawback of using patch antenna is the intrinsic limitations in the bandwidth and gain because of its resonant structure.

Recently, the increased requirements for compact multifunction communication systems prompted the antenna designers to invent new class of compact patch antennas that have a multiband response and relatively high gain; one of the modern techniques that used in this field is the combination the fractal geometries with patch antenna.

The fractal geometries are structures with no specific size constructed from multiple exactly similar segments with different size scales; it was firstly demonstrated in 1983 by Mandelbrot [3]. Innovative class of antennas has been produced by combining fractal shapes and electromagnetic theory that has a superior performance than their peers. Applying fractal shapes to the patch leads to introduce an antenna

with multiband frequency operation due to the capacitive and inductive loads appended to the patch surface.

Many fractal shapes have been developed recently, which are suitable for the antenna designs, to produce patch antennas with high gain radiation pattern or wide bandwidth.

1.1 Thesis Objectives

This thesis aims to demonstrate the fractal geometries application on the planar antenna structures, present their effects on the antenna performance, and model a new compact multiband/wideband antenna with moderate gain and single feed.

1.2 Thesis Contribution

Multiband/wideband planar antenna has been modeled and simulated using FEKO software. The modeled antenna has 6.1 dB gain. Ten different resonance frequencies of 1.77 GHz bandwidth have been achieved.

1.3 Thesis Organization

Chapter 2 demonstrates several antenna topics, where primitive antenna definitions are presented in section 2.1; section 2.2 demonstrates the most important parameters that generally used for the antennas such as radiation pattern, gain, and bandwidth. Depending on the structural geometry of the antennas, they can be classified into two types, which presented in section 2.3, the protrude antennas (conventional antennas) and planar antennas (patch antenna). A brief summary of the most used fractal shapes to reduce the size of the antenna and to provide multiband operation is presented in section 2.4.

Chapter 3 demonstrates the design procedure of multilayer fractal antenna. Section 3.2.1 describes and presents the basic rectangular patch and Sierpinski Carpet Fractal (SCF) antennas with different orders. Section 3.2.2 shows the design of triangular patch, Koch snowflake fractal (KSF) and Sierpinski Gasket Fractal (SGF) with different orders. The stacking of the triangular and triangular patch is presented in section 3.3.

Conclusion section and suggested future work are discussed in Chapter 4 in the sections 4.1 and 4.2, respectively.

Chapter 2

PLANAR ANTENNAS AND FRACTAL GEOMETRIES

2.1 Antenna Definition

An antenna is a device whose function is to radiate and/or intercept electromagnetic radiation, or it is defined as a matching device between the transmission line or wave guide and the surrounding medium. The first antenna was originally designed by Heinrich Hertz around 1886. This antenna is called dipole antenna, which consists of two conductors with a center fed element for receiving and transmitting radio frequencies. The result of removing one of the two conductors of the dipole antenna is the monopole antenna, which developed by Marconi in 1896, these antennas were the simplest forms.

Because of the increased demands especially after the use of the submarines in World War II in 1939 the complexity of the antennas grow up with time, where this event prompting the scientists to develop a new classes of antennas that have the ability to receive electromagnetic signals in depth of seas and make the information recovery process available for submarine, such that planar antenna.

2.2 Some Antenna Parameters

Radiation Pattern: It demonstrates how well an antenna transmits and receives in all directions; generally it described by a polar graph such that in Figure 2.1.

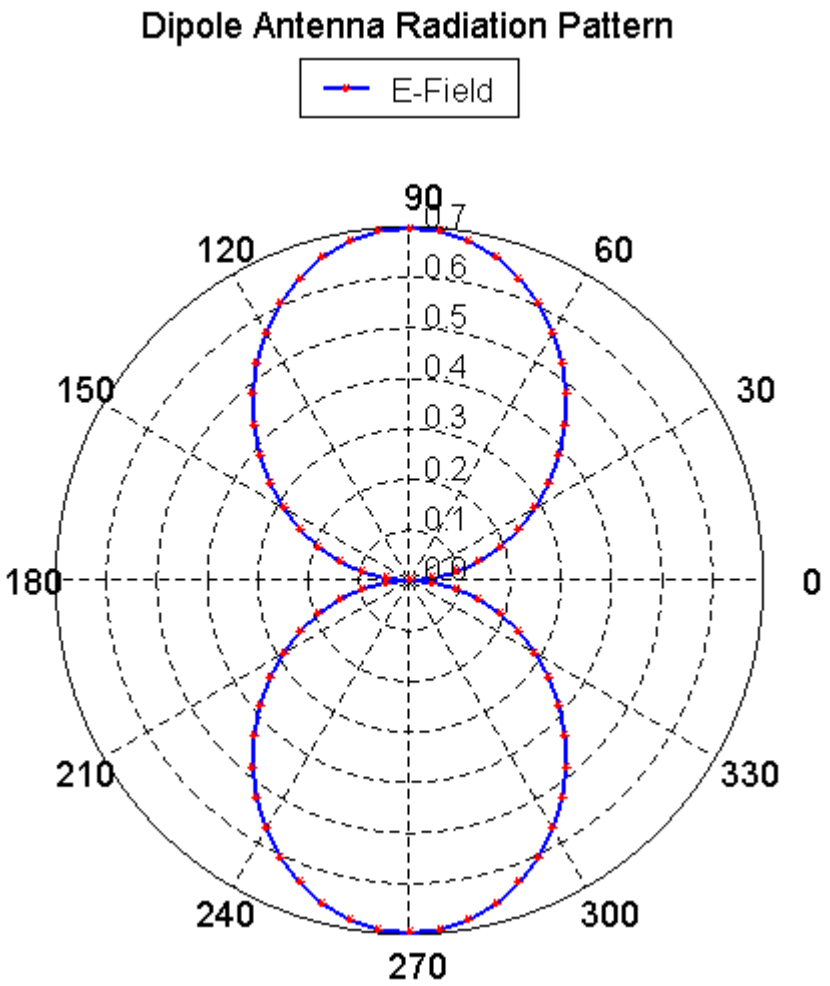

Figure 2-1: Dipole antenna radiation pattern simulated in FEKO

Directivity: A comparison between the antenna radiation in particular direction and the radiation of a reference antenna, usually the reference antenna represented an omnidirectional or isotropic antenna. Mathematically it can be calculated using equation 2.1.

$$D = 4\pi \frac{radiation\,intensity}{total\,radiated\ power} = 4\pi \frac{U}{P_{rad}} \tag{2.1}$$

Efficiency: It represents the measure of how much input have been translated to useful radiation. It can be calculated using equation 2.2.

$$\eta = \frac{P_{rad}}{P_{in}} \times 100\% \quad (2.2)$$

Gain: This parameter describes the practical value for the directivity after antenna losses calculation. Gain is equal the directivity in ideal antenna (no losses). Equation 2.3 calculates the antenna gain according to the directivity.

$$G = \eta D \quad (2.3)$$

Where: *G* is the antenna gain, *D* antenna directivity, and η is the efficiency of the antenna.

Impedance: it is the ratio of voltage to the current at the input terminal of the antenna; usually it consists of two parts, real and imaginary part.

Bandwidth: It represents the range of frequencies in which the reflection coefficient (S11) is < -10 dB. Figure 2.2 illustrates the frequency response for patch antenna.

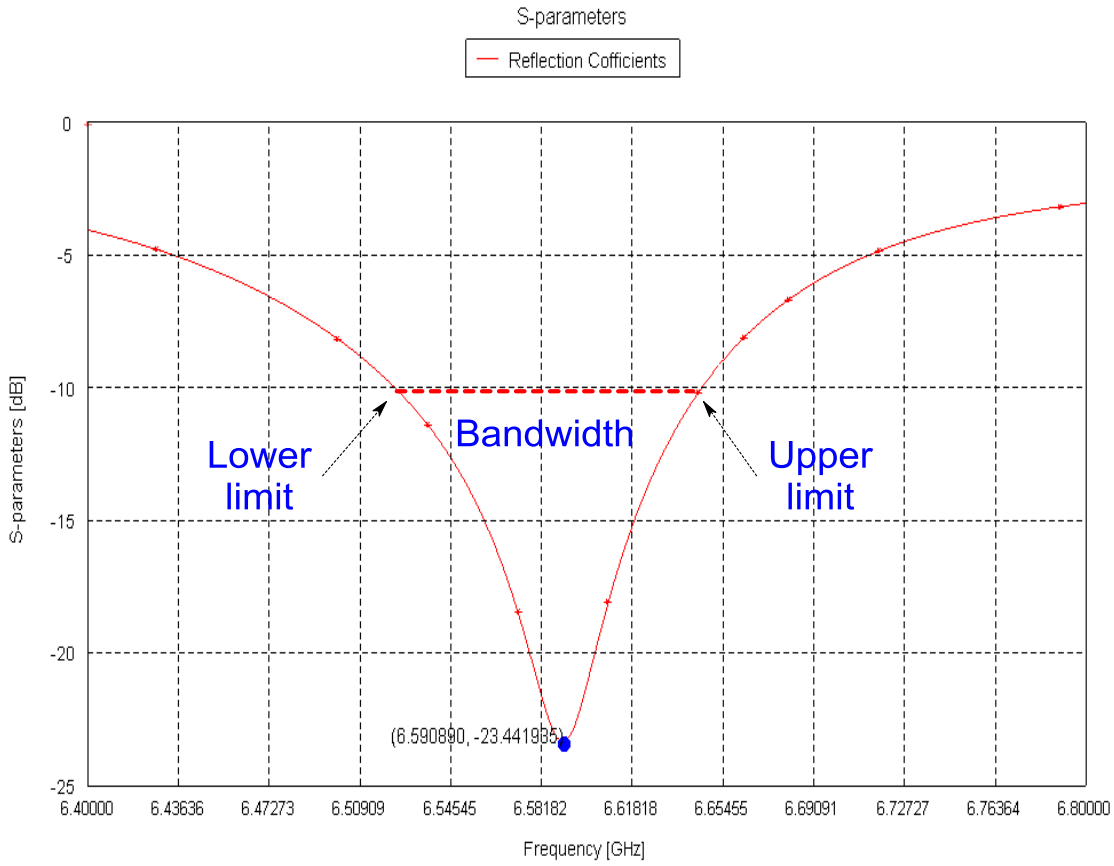

Figure 2-2: Patch antenna frequency response produced by FEKO

Percentage value of the bandwidth in terms of the center frequency can be calculated by equation 2.4.

$$Bandwidth = \frac{f_{upper} - f_{lower}}{f_{center}} \times 100\% \qquad (2.4)$$

2.3 Antenna Classification

Geometrically antennas can be classified into protrude (conventional antennas) and not protrude antenna (planar antennas); Figure 2.3 mentions the most well-known antennas.

Figure 2-3: Hierarchical Antenna classification

2.3.1 Patch Antenna

The antennas that cannot protrude from their surfaces are very attractive for applications that used in fast moving vehicles like missiles, spacecraft and airplanes. This attractiveness arises due to the zero interference between the antenna structure and the aerodynamics of these vehicles, in other word the antenna should be mounted on the vehicle body with perfect conformance and patch antenna supports this property.

Patch antenna was invented at 1950 [1], but practical fabrication and considerable attention has been received after the printed technology invention at 1970 [2], when the scientists start using the printed circuit technology in radiator components. Tables (1&2) illustrate the advantages and disadvantages of the patch antenna [4].

Table 2-1 Patch antenna advantages

Advantages of Patch Antenna
• Solid and difficult to fracture
• Integration within the devices itself is possible
• Achieves size reduction for the portable systems
• Conformal shape to the supporting structures.
• Multiple bands mode operation can be achieved.
• Supports the monolithic Microwave Integrated Circuits fabrication methods.
• Linear and circular polarization can be made by changing feed position.

Table 2-2 Patch antenna disadvantages

Disadvantages of Patch Antenna
• Limited bandwidth
• Low radiation efficiency especially for high thickness
• Have a low level of the power capabilities
• Level of cross polarization is too high
• Limited gain
• High losses due to the surface waves.
• Limited scan performance.

A comparison between patch antenna and other conventional antennas is presented in Table 2.3. Although the patch antenna is not the best one but it still possesses some unique properties that cannot be obtained using other types of antenna. Depending on the Table 2.3 it is clear that patch antenna is very conformal and has a good interference with other electronic components [5].

Table 2-3 Comparison of patch and conventional antennas

Antenna type	Gain dB	Conform-ability	Mechanical Stability	Interference Compatibility	Size	Cost
Patch	3-8	Excellent	Excellent	Excellent	Small	Low
Horn	10-20	Bad	Average	Bad	Medium	High
Dipole	1.7	Good	Bad	Average	Small	Low
Dish	>10	Bad	Bad	Bad	Large	High
Yagi	5-15	Bad	Bad	Bad	Large	High

The most important purpose of using fractal techniques is to enhance the patch antenna gain and bandwidth.

2.4 Fractal Antennas Overview

The concept of fractal which means irregular fragments or broken was firstly described by Mandelbrot in “The Fractal Geometry of Nature” around 1983, where the cloud boundaries, coastlines, and mountain ranges are examples for the fractal shapes that described by him. Fractal shapes usually consist of copies of themselves but with different scales, and have no specific size. Due to pioneering work to Mandelbrot, variety applications for fractals in different science are consistently to be found, one of these applications is the fractal electrodynamics, which is the combination of fractal geometries with electromagnetic theory.

Several attempts have been carried out to obtain suitable fractal geometry for the antenna designs, which can be employed to enhance the bandwidth, reduce the overall size and obtain high-gain.

Applying fractal geometry to the structure of the patch antenna adds inductive and/ or capacitive loads to the antenna which results in different resonance frequencies that provide the multiband/ wide band antennas and enhanced the gain.

2.4.1 Sierpinski Carpet Geometry (SCG)

2.4.1.1 Sierpinski Carpet Fractal Antenna for Multiband Applications

R. Mohanamurali and T. Shanmuganantham designed and simulated the first three orders of patch fractal carpet antenna for multiband applications [6]. Figure 2.4 shows the antenna layout.

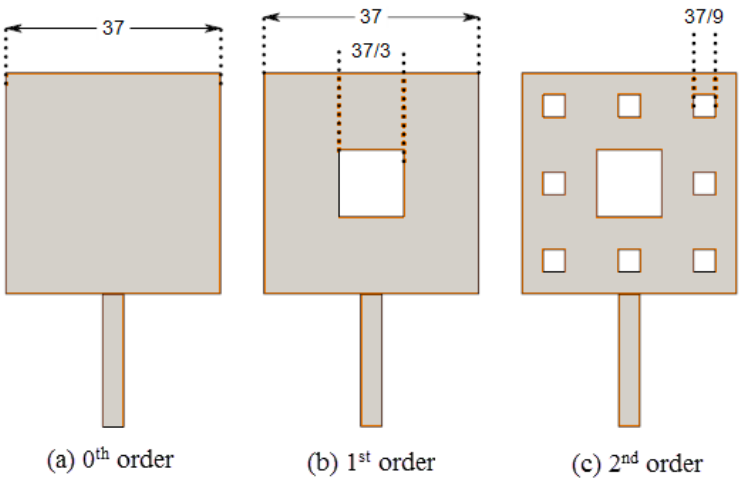

Figure 2-4: SCF antenna layouts [6]

The antenna has side length of 37 mm; placed on a substrate of 1.59 mm thickness and dielectric constant of 4.5 with $\tan\delta = 0.012$. The antenna has been fed by using the MSL, to reduce the Reflection coefficient; an optimization process has been carried out for better matching between the antenna and the line. The Reflection coefficient that obtained by the IE3D software for the antenna shows that the antenna is convenient to operate at the frequency bands 1.8/ 5.59/ 5.78/ 6.4/ 6.63/ 7.84 GHz. These three designs has been simulated using FEKO software as part of software testing, where good agreement has been observed between FEKO and IE3D software. Simulation designs are comprehensively explained in chapter 3.

2.4.1.2 Small Size Edge-Fed Sierpinski Carpet Microstrip Patch Antenna

In modern mobile communication systems, the size of the antenna is very important design parameter, where the system size should be small and compact enough for easy mobility during the connection. Generally two methods have been used in size reduction of the patch antenna are adding inductive loads to the edge of the patch, and loading the patch antenna surface with capacitive loads.

A capacitive load was appended to the patch surface by Chen and Wang by applying the SCG, as shown in Figure 2.5 [7].

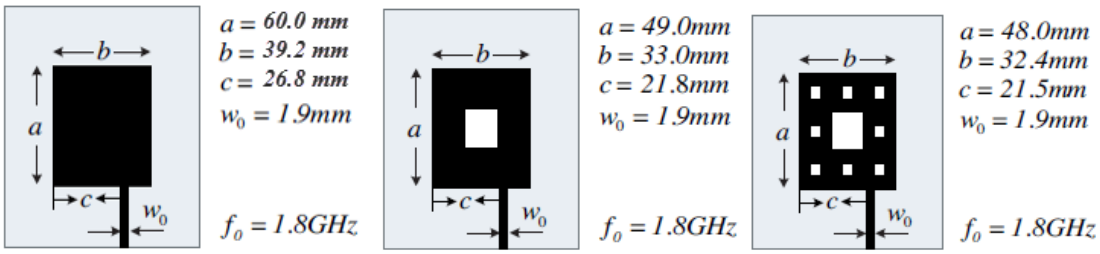

Figure 2-5: SCF antenna size reduction steps [7]

This antenna was designed to operate at 1.8GHz; with a substrate of 4.3 dielectric constant and one mm thickness. Corresponding to these values the physical parameters are found to be 60 mm, 39.2 mm, and 26.8 mm, as the antenna length, width, and feed position respectively.

The obtained simulation and measurement results show that the patch antenna size can be reduced to 31.25% from its original size at the 1st order and 33.9% at the 2nd order of the SCF, where the resonant frequency, reflection coefficient, radiation pattern and other performances are virtually unchanged.

2.4.1.3 Analysis and Bandwidth Enhancement of Sierpinski Carpet Antenna

Numerical methods used in solving electromagnetic problems such as Finite Difference Time Domain (FDTD) and Finite-Element method are computationally exhausted due to their memory and time requirements, so in [8] S. Wong and B. L. Ooi used the Boundary Integral method coupled with Segmentation Method to analyze the behavior of the SCA. Figure2.6 shows the analyzed antenna.

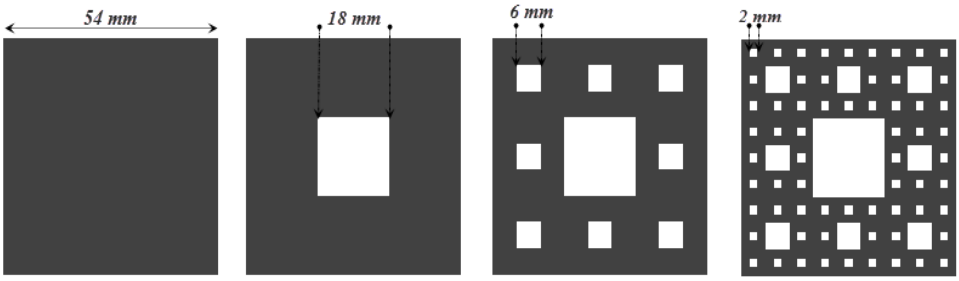

Figure 2-6: First four steps of SCF antenna [8]

The initial patch length is 54 mm×54 mm and the iteration factor used is 3; the patch antenna is imprinted on Duroid substrate of dielectric constant 2.2 and thickness 0.25 mm. For all antenna orders the theoretical results are obtained and compared with empirical results. The theoretical results show agreed well with empirical results, especially when taking the dielectric losses into account and this due to the losses of the surface wave or the radiation losses.

S. Wong and B. L. Ooi further endeavored to extend the antenna bandwidth by stacking the SCA orders as a sandwich. Figure 2.7, illustrates the antenna geometry with the photonic band gap (PBG) structure that used in suppression the unwanted waves.

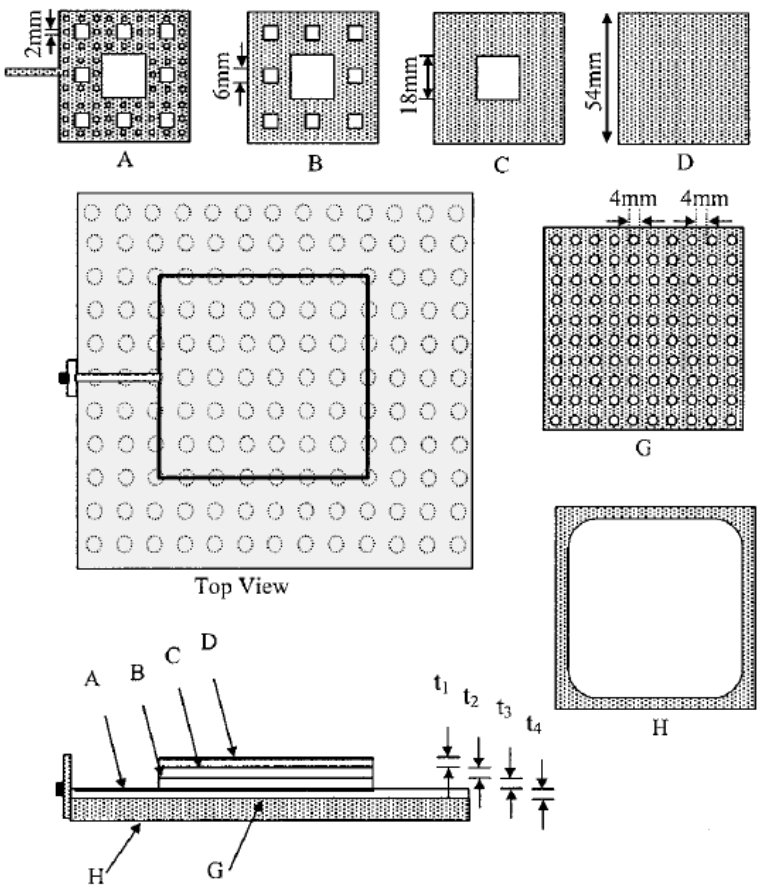

Figure 2-7: Multilayer stacked SCF antenna [8]

The antenna orders are etched together from the higher order up to the lower one and separated by 0.25 mm thickness of 2.2 dielectric constant substrate. The entire geometry is printed on photonic band gap structure composed of square lattices with circular holes; the total geometry thickness is 1.54 mm.

Antenna performance which tested by using HP-8510A network shows that the stacking technique improved the reflection coefficient, impedance bandwidth as well as the other parameters.

2.4.1.4 Flexible SCF Antenna on a Hilbert Slot Patterned Ground

The emergence of adjustable shape electronics paved the way for the integration of wireless systems into the animated objects or the animals for the purposes of monitoring their behaviors. Although the components produced by using the flexible

technology can bend without adversely effect on the performance of the system, bending can significantly spoil the performance of the wireless components, especially the antenna.

A novel flexible fractal antenna has been studied for UMTS based on the SCG coupled with Hilbert's curve shown in Figure 2.8 [9].

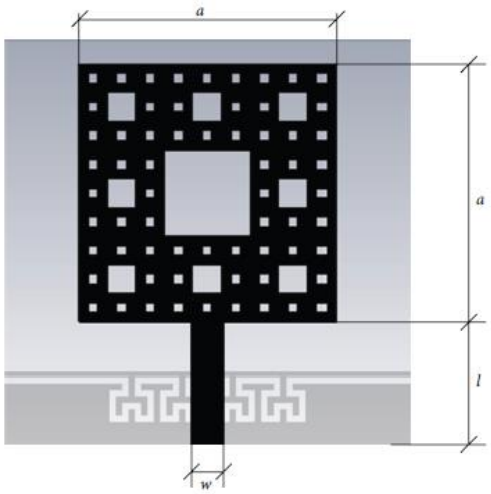

Figure 2-8: Flexible SCF antenna configuration [9]

The designed antenna has 20 mm×20 mm 3rd order SCF plate that used as a radiator, which implanted on the top of 0.075 mm thick Kapton substrate with a permittivity of 3.2 and ground layer has the shape of Hilbert's slot that used for matching purposes. The antenna has been fed by a MSL with 2.6 mm and 10 mm width and length respectively.

Several folded antenna cases have been simulated in CST Microwave Studio to see the effects of the bending on the antenna performance. The results show that there is a frequency shift of less than 20 MHz when bending the antenna, which can be

neglected because the UMTS works in the band of frequencies that includes that shift.

The antenna has been fabricated By using the Dimatix material deposition printer DMP-3000, and the results show a good agreement with simulated one.

2.4.2 Sierpinski Gasket Geometry (SGG)

2.4.2.1 Design Formula for S GF Planar Monopole Antennas

Fractal monopole SGA has been studied in [10]; the antenna is constructed through three iterations. Figure 2.9 shows the last stage of the design.

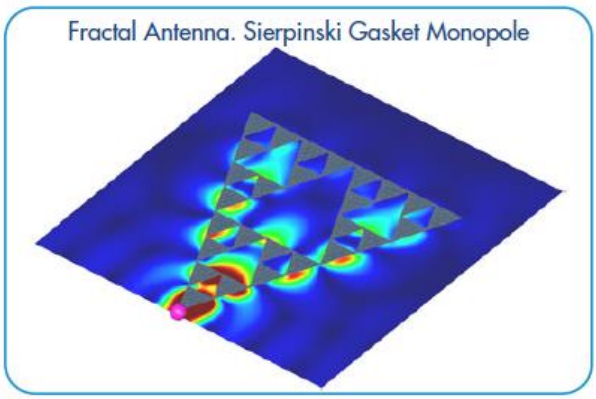

Figure 2-9: SGF monopole antenna geometry [10]

As shown in the above figure the antenna has side length and height of 102.77 mm, 89 mm respectively, which implanted on FR4 substrate of 1mm thickness.

The antenna has been simulated and fabricated; a good agreement has been shown between the simulation results and the fabricated antenna, which explained that the antenna could operate at 5 different resonant frequencies 0.520, 1.740, 3.510, 6.950, 13.890 GHz with reasonable radiation.

2.4.2.2 Sectoral Sierpinski Gasket Fractal Antenna for Wireless LANs

The swift evolution in wireless communications and the appearance of the multifunction systems, paved the way for the scientists to develop a new class of antennas based on fractal techniques to produce a multi behavior antenna.

Y. K. Choukiker and R. Jyoti studied the Sectoral SGG on the antenna behavior [11], where they invented an antenna with a dual broadband frequency response based on SSG. Figure 2.10 shows the stages of the designed antenna.

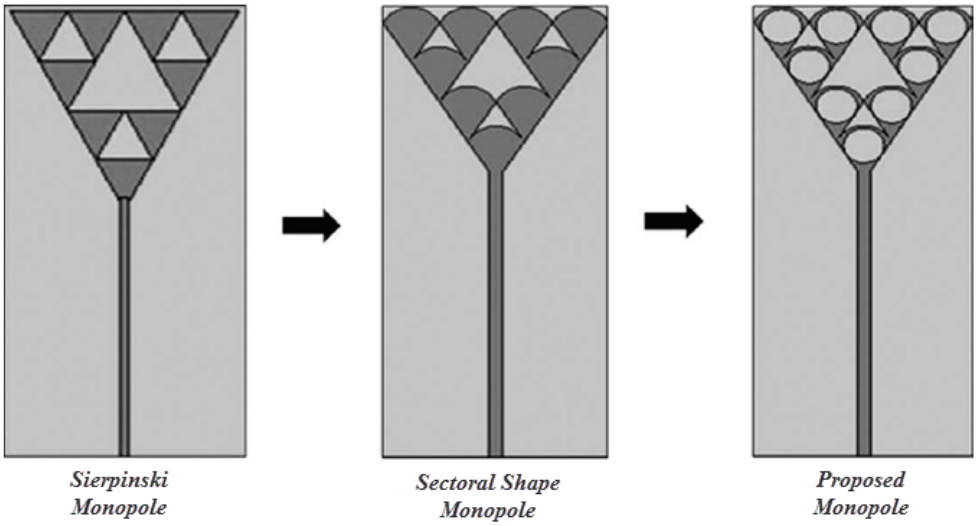

Figure 2-10: Sectoral SGF antenna layouts [11]

As shown in the figure above, a simple triangular gasket antenna is converted to a sectoral shape antenna and a circle of diameter D is drilled out from the antenna surface. Dimensions of the antenna are shown in Figure 2.11 and Table 2.4.

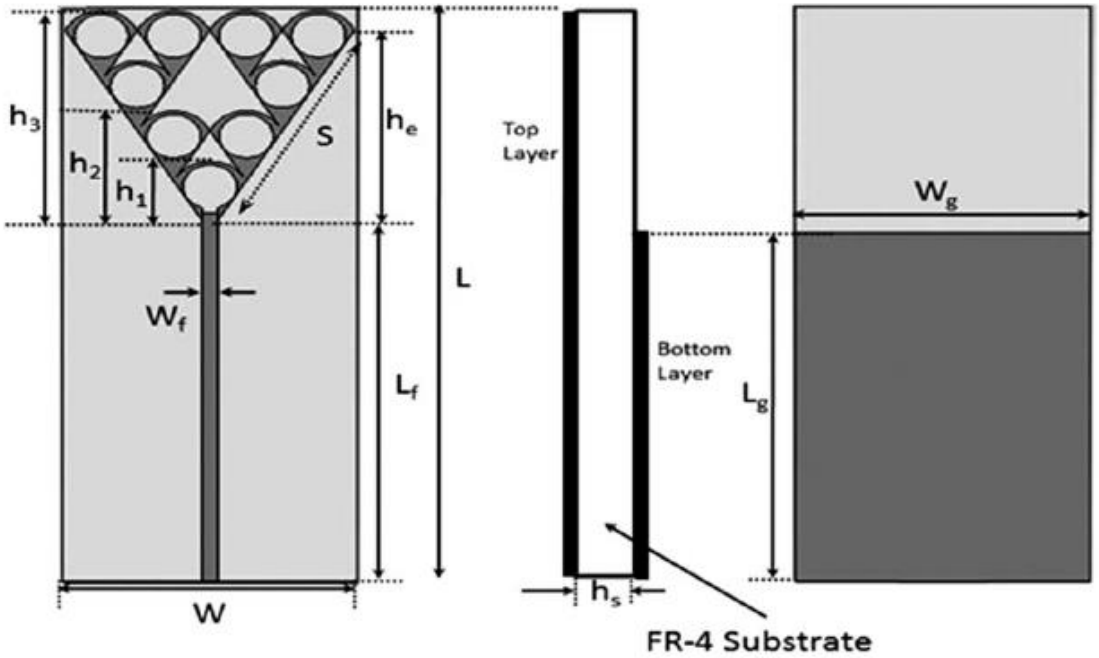

Figure 2-11: Sectoral SGF antenna (Side view) [11]

Table 2-4 Sectoral SGF antenna dimensions

h_1	h_2	h_3	D	W_f	L_f	W	L	L_g	W_g	S
8	13.74	25.24	2.5	1.5	42	27	65.5	40.3	27	26.55

Good agreement has been obtained between the fabricated antenna and simulated one, where the results show that the antenna has two broad-band responses, the first one is 1.51-3.39 GHz, and the other is 5.31-6.32 GHz. The designed antenna is suitable for GPS, DCS-1800, PCS-1800, UMTS, IMT-2000, WLAN, and Bluetooth.

2.4.3 Giuseppe Peano Geometry

2.4.3.1 Miniaturization of MPA by the Novel Application of the GPF Geometries

Applying the GPF to the patch antenna for the size reduction purposes has been investigated and studied by Homayoon Oraizi and Shahram Hedayati; they found that patch antenna size can be reduced by applying these geometries to the patch edges as shown in Figure 2.12 below [12].

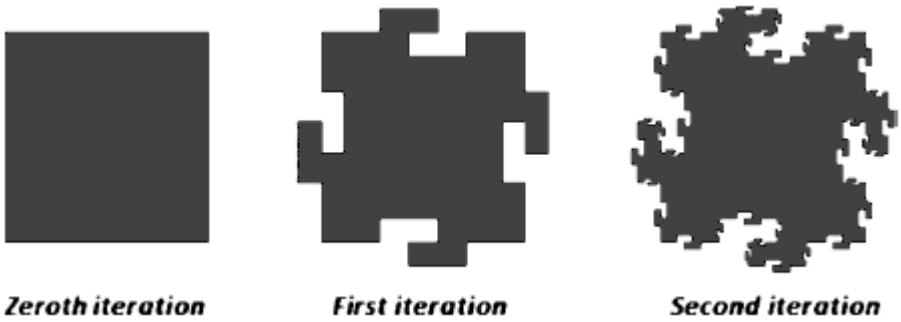

Figure 2-12: GPF antenna configurations [12]

The antenna uses FR4 substrate with dielectric constant equal to 4.4 and tangential losses of 0.02646, substrate height equal to 1.6 mm; the initial patch has lengths of 30 mm.

The antenna is simulated and optimized by using the High-Frequency Structure Simulator (HFSS); the results show that applying fractal geometry to the antenna reduced the overall size, enhanced the gain and broaden the frequency bandwidth.

2.4.3.2 Circularly Polarized Multiband MPA Using the Square and GPFs

Combination of two types of fractal antenna has been elaborated under large investigation by Homayoon Oraizi [13], where he studied the combination of GPF and square fractal effects on the antenna. Figure 2.13 shown below describes the antenna geometry.

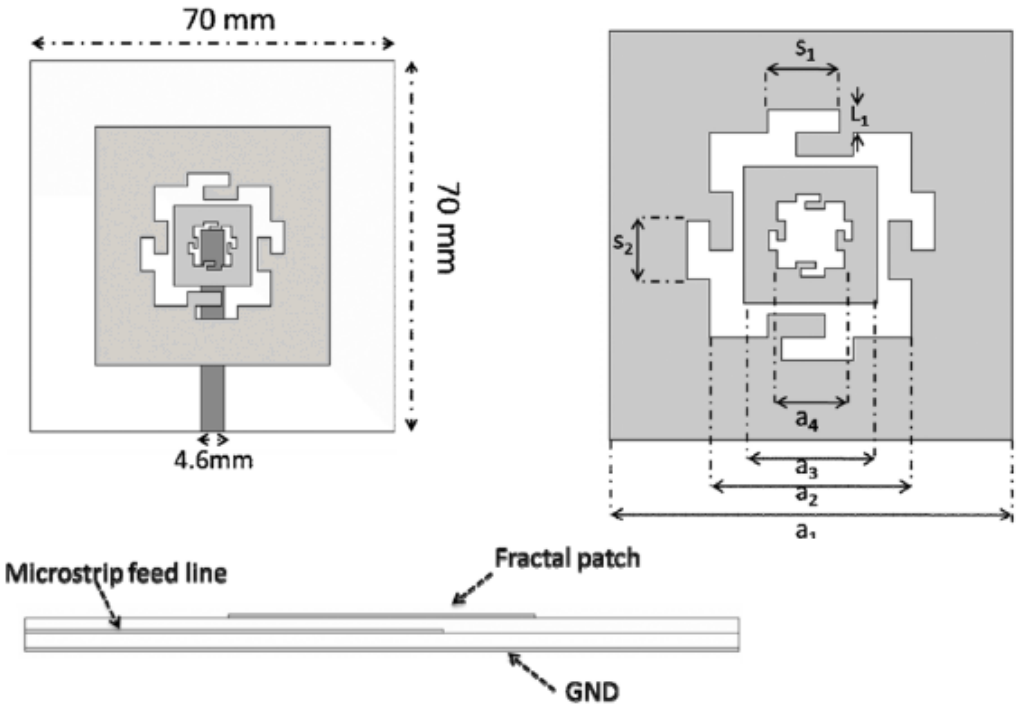

Figure 2-13: Combination of GPF and square fractal Antenna [13]

The antenna is composed of two layers; the lower layer has a 2.2 dielectric constant and 1.524 mm thickness with tangential losses 0.0009; the upper layer consists of FR4 substrate of 1 mm thickness and 0.02 losses. The fractal patch geometry is implanted on top of the upper substrate and fed by 3.4 mm width, 38mm length MSL, printed on the top of lower layer (proximity coupled feed). By using a computer full wave simulator the antenna has been optimized to get better parameter values as shown in Table 2.5 below.

Table 2-5: Dimensions of GPF and square fractal antenna

a_1	a_2	a_3	a_4	s_1	s_2	L_1
30 mm	15 mm	10 mm	5 mm	4.3 mm	3.9 mm	1.7 mm

Approximately, 400 MHz frequency bandwidth and 4.5 dB gain has been achieved by the designed antenna.

2.4.4 Minkowski Curve

2.4.4.1 MKF Patch antenna for Size and Radar Cross Section Reduction

In the modern communication systems antenna size is the main obstacle during the designing, where antenna geometry plays a vital role in enhancing the bandwidth and size reduction of the overall system.

MKF geometry has been proposed by Chen and Chang to reduce the size and increase the radiation efficiency of the antenna [14]. Figure 2.14 shown below illustrates the first four orders of the antenna.

A substrate of 2.62 dielectric constant and 1.8 mm thickness has been used; the antenna has 37 mm×30.79 mm side lengths. Coaxial cable of 50 Ω impedance has been used as a feeder.

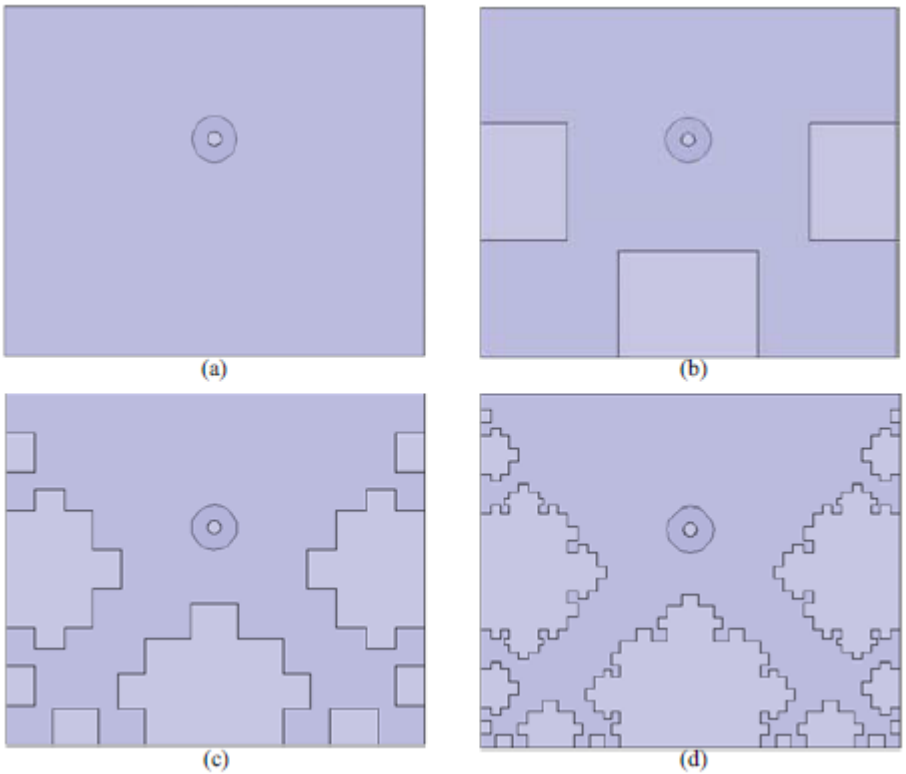

Figure 2-14: MKF antenna configuration [14]

62% and 49.76% size reduction has been achieved in the 4th and 3rd orders of the antenna, and these results show that MKG is valid for patch antenna size reduction purposes.

2.4.4.2 Analysis of Multiband Behavior on Square Patch Fractal Antenna

In the telecommunication sector, there are many devices that possess multifunction capacities such as satellite systems, radio determination applications, broadband wireless access, navigation systems and many other applications. In order to meet the capabilities of these devices they should be provided by a multiband antenna.

A multiband antenna based on MKF geometry has been presented in [15]. Figure 2.15 shown below illustrates the first four iterations.

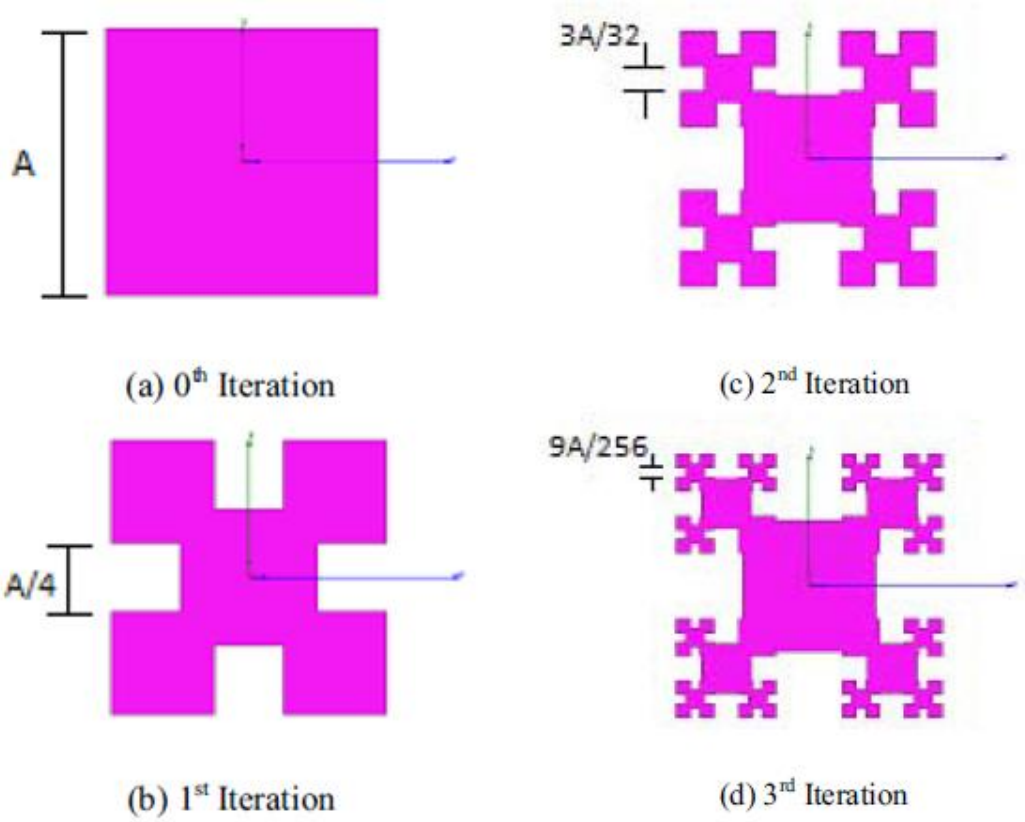

Figure 2-15: First four iterations of MKF antenna [15]

The antenna has 5 cm side lengths implanted on a substrate of 2.2 dielectric constant and 0.32 cm thickness. The antenna has been fed by a coaxial cable at the center. Computer simulator is used to test the antenna performance; Table 2.6 shown below represents the frequency response of this antenna.

Table 2-6: MKF antenna frequency response

Iteration	Resonant Frequency (GHz)	Reflection coefficients (dB)
1st	6.15	-19.39
	9.40	-27.02
	11.40	-15.33
2nd	3.86	-26.72
	7.96	-19.69
	9.40	-26.85
3rd	3.00	-22.20
	7.49	-18.70
	9.68	30.96
	11.21	-15.82

2.4.4.3 A New Ultra-Wideband Fractal Monopole Antenna

The main difference of the modern wireless communication systems is the need of a vast bandwidth; especially when talking about the UWB applications. Abolfazl Azari proposed an antenna with a super wide band; Figure 2.16 shows the antenna configuration [16].

The antenna has been simulated using NEC electromagnetic simulator [17]; it has length of 16 mm, and wire diameter of 0.25 mm, which is attached over 16 mm × 6

mm ground plane. The reflection coefficient results show that the antenna is suitable for the operation in the frequency band 10 GHz up to 40 GHz and have 12 dB gain.

The antenna has been fabricated, where the monopole is made of copper, and the ground plane is made of aluminum; good agreement has been achieved between the fabrication and simulation results.

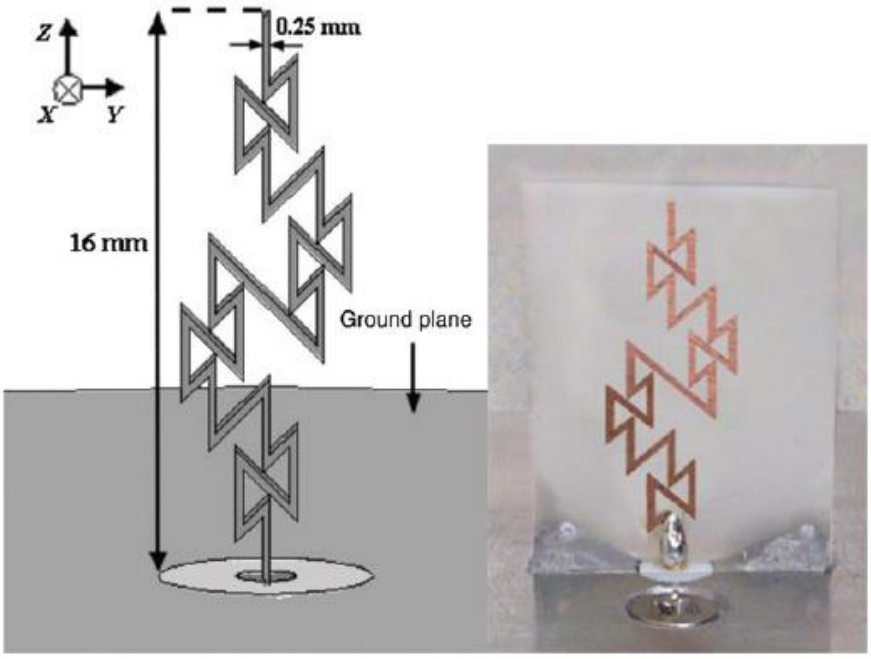

Figure 2-16: Monopole fractal antenna configuration [16]

2.4.5 Koch Snowflake Fractal Geometry

2.4.5.1 Bandwidth Enhancement of a MSL Fed Printed Wide-Slot Antenna

Bandwidth enhancement of the planar antennas is the topic that takes a lot of attention of the antenna researchers and designers. An antenna composed of planner metal with a cut out wide slot has been studied and experimentally tested in [18]. Figure 2.17 shows the antenna design.

As shown in the figure below, the slot has the shape of KSF with initial perimeter of 22 mm etched on the surface; the planner metal is implanted on 1.5 mm substrate thickness of 4.1 dielectric constant. Antenna feed has been achieved by a 50 Ω MSL in the bottom that operates depending on the coupling property.

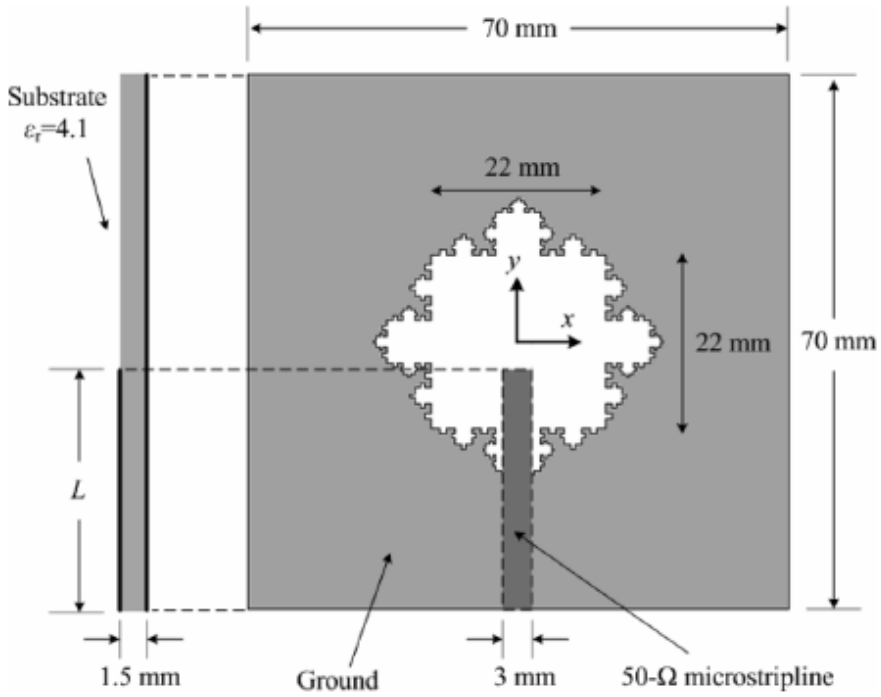

Figure 2-17: Fractal shaped printed slot antenna [18]

The obtained reflection coefficient shows that the antenna has 2.4 GHz bandwidth at 4 GHz operating frequency, which is better than the bandwidth obtained by the conventional slotted antenna. Good agreement has been observed between experimental and simulation results. 2 dB gain is obtained at the operating frequency.

2.4.5.2 A New High-Directivity Fractal Antenna Based on the Modified KSF

The high directivity as well as bandwidth enhancement is intended in many applications; it was found that applying some fractal shapes to the antennas such as Koch's curve provide dual frequency responses as well as directivity with high levels. A modified KSF antenna has been presented in [19] by Abbas Bin Younas

that possess a high dB level of directivity and wide bandwidth. Figure 2.18 shown below describe the antenna configuration.

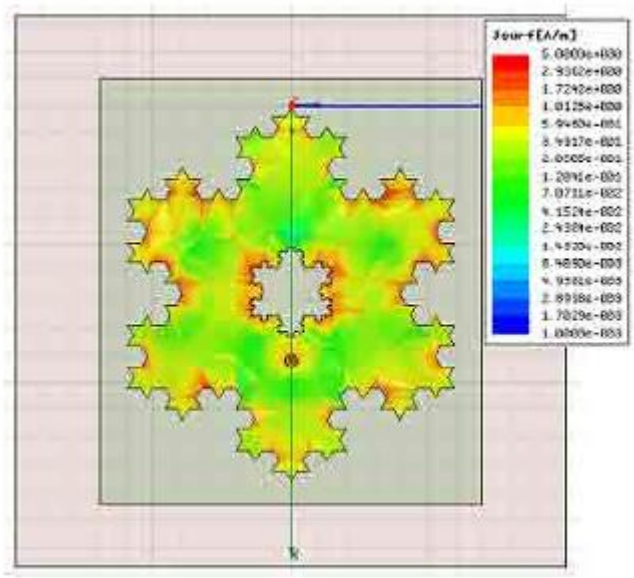

Figure 2-18: Slotted KSF antenna configuration [19]

The designed antenna has been implanted on the top of 1.5 mm thickness substrate of 4.5 permittivity; the side length of the antenna is 118 mm. Combination of the substrate as well as Koch shaped antenna are printed on a 20 mm×20 mm ground plane.

The fabrication as well as simulation results, which are in good agreement, proved that the antenna has dual frequency response and high directivity of more than 14 dB at the operating frequency.

2.4.5.3 CPW-Fed Fractal Slot Antenna for UWB Application

Conventional antennas have been designed to operate in narrow bandwidth of frequencies and owing to the swift growth in communication systems, especially in UWB applications; antennas with a wide range of operation frequencies are intended.

Koch's curve slot shape planar antenna with enhanced band width has been presented in [20], which can be used in UWB; Figure 2.19 describes the antenna configuration.

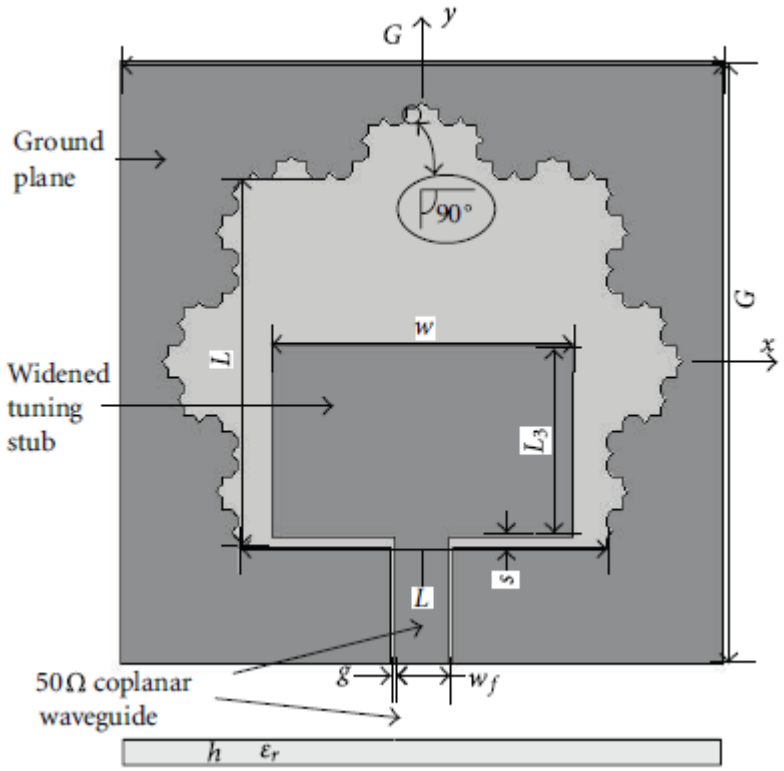

Figure 2-19: CPW-fed fractal slot antenna configuration [20]

The antenna consists of 72 mm×72 mm ground plane printed of FR4 substrate of dielectric constant 4.6 and thickness of 1.6 mm, and fed by 50 Ω coplanar MSL.

The simulation results show that the antenna appropriate to work in the frequency range of 1270 MHz to 4670 MHz, with 5.7 dB maximum gain. Fabrication process was carried out, and good agreement has been obtained.

2.4.6 Circular Fractal Geometry

2.4.6.1 On the design of Inscribed triangle-circular fractal antenna for UWB

Circular fractal antennas play an important role, especially in UWB applications in the frequency range of 3.1 to 10.6 GHz; where a lot of efforts have been spent by the researchers to design a new class of antennas that meet the requirements of the swift progress in communications. One of those researchers is Dhananjay Magar, who designed a new type of fractal circular antenna in [21].

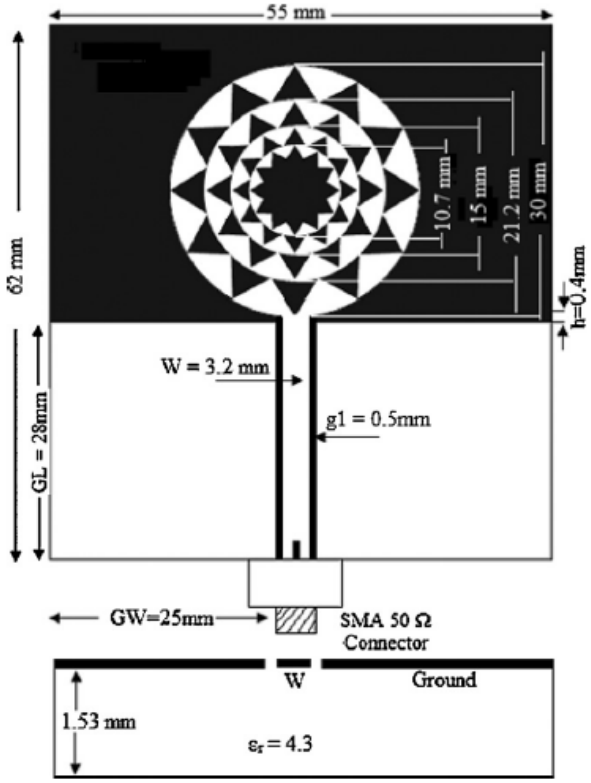

Figure 2-20: Circular fractal antenna configuration [21]

Figure 2.20 describes the antenna structure, where it consists of circular monopole antenna with triangular elements that inscribed on its surface as shown above; the circular monopole is implanted then on 1.53 mm thickness substrate with dielectric permittivity of 4.3. The antenna has been fed by coplanar waveguide of 50 Ω impedance.

Simulation as well as the fabrication process has been carried out, which shows good agreement, and proved that the antenna is suitable to operate in the frequency range of 2.25 GHz to 15 GHz, with unidirectional radiation patterns.

2.4.7 Hilbert's Curve Geometry

2.4.7.1 Modified HFG patch antenna for UWB wireless communication

Multimedia services advancement currently attracting a lot of considerable attention also the new mobility lifestyle offered by the wireless personal area networks paved for the appearance of new classes of antennas that have larger bandwidths.

UWB patch antenna has been designed based on the second iteration Hilbert curve as shown in Figure 2.21, then a slot of yagi shape, as shown in Figure 2.22, cut out from the 2nd iteration Hilbert's surface, and hexagonal plane cut out from the ground plane as shown in Figure 2.23 [22].

The antenna has 39 mm length, 30 mm width, Y_1=14 mm, Y_2=7 mm, Y_3= 4.67 mm, a_1=7.6 mm, a_2= 18.4 mm, W_a= 7 mm, K_a= 5.5 mm, and d_a=2.9 mm. The antenna was fed by a MSL with matching elements that have the dimensions W_d = 2.1mm, l_a= 9.2 mm, W_c =3.2 mm, and l_c = 3.7 mm to ensure 50Ω matching.

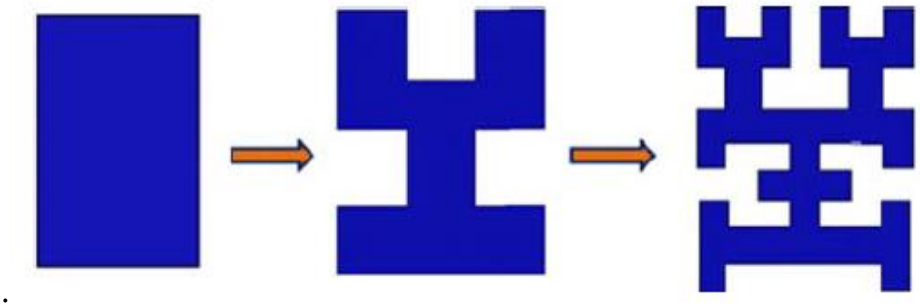

Figure 2-21: HCF antenna layouts [22]

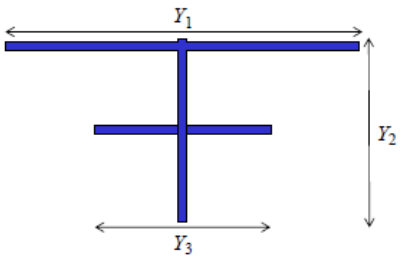

Figure 2-22: Yagi shaped slot

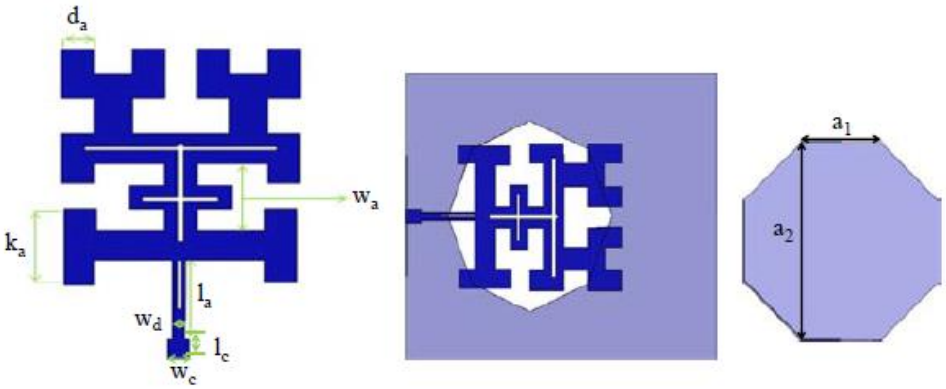

Figure 2-23: HCF antenna with yagi shaped slot

Simulation process is carried out by using HFSS software; the antenna results show reflection coefficient < -10 dB for the frequency range 3.1 GHz to 4 GHz and < -15 dB for the frequency range 4 GHz up to 10.6 GHz.

2.5 Conclusions

A summarized review about the mostly used fractal antennas has been introduced in this chapter. The calculated reflection coefficient, radiation, gain and other parameters show that applying fractal techniques acquired the patch a multi frequency response. Next chapter presents the design steps of a novel stacked patch antenna, based on fractal techniques.

Chapter 3

SIMULATION AND DESIGN

3.1 FEKO Simulation Package Overview

FEKO is a full wave electromagnetic software, based on advanced numerical method; it represents a comprehensive simulation tool for the complex electromagnetic engineering problems and it is an applicable solver to a wide range of complex problems due to the multiple solution techniques that are built within it, where firstly method of moment (MOM) was the only solution method that used, but later MOM hybrids with following methods:

- Multi-Level Fast Multiplole Method (MLFMM).
- Physical Optics (PO).
- Geometrical Optics (GO).
- Uniform Theory of Diffraction (UTD).
- Finite Element Method (FEM).

All of these techniques make FEKO one of the most appropriate packages to be used for solving the engineering problems related to the electromagnetics such as, antenna placement and designing, bio-electromagnetics, 3-D electromagnetic circuit design, RF structures analysis, scattering problems, as well as analysis of multi dielectric structures and coupling problems [23].

3.2 Antenna Designing

A novel stacked patch antenna of two layers based on fractal geometry is presented with simulation results computed by FEKO. Figure 3.1 describes the design procedure for the proposed antenna. As shown in the figure, the proposed antenna consists of two layers of different dimensions.

SCF and MKF geometries are applied to a rectangular shaped patch antenna which composes the first layer. The second layer is the result of applying the combination of KSG and SGG to a triangular shape patch. Each layer has a preferable behavior than the other one, where the wide bandwidth with multiband response and relatively low gain obtained by the first layer, on the other hand a multiband response of the narrow bandwidth and high gain are obtained from the second layer. So in order to obtain a multiband/wideband high gain antenna, stacking technique is proposed here.

A substrate is used to separate the antenna layers in order to prevent the interference between them. FR4 substrate of dielectric constant 4.6 has been chosen in this work due to its suitable characteristics, where a comprehensive study has been done on the substrate materials in order to choose the suitable one for the planar antennas.

It has been shown that FR4 substrate has better reflection coefficient; RT-Duroid has wider bandwidth and Liquid Crystal Polymer has better radiation pattern [24].

A detailed explanation for each stage shown in Figure 3.1 will be described in next sections with the FEKO simulation results.

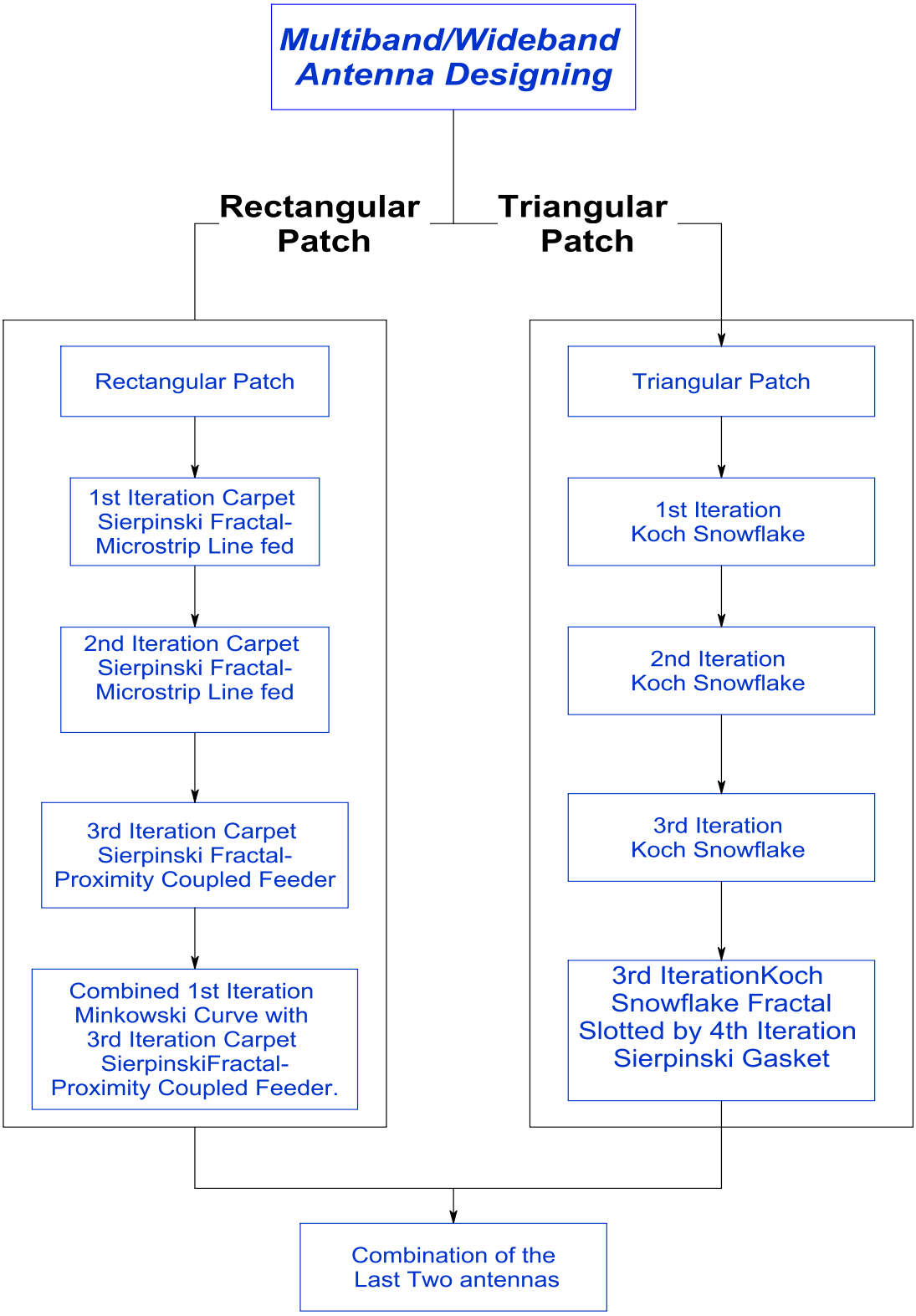

Figure 3-1: Multiband/ Wideband antenna designing flow chart

3.2.1 Rectangular Patch

3.2.1.1 Rectangular Patch Antenna

Based on transmission line theory, which was used to analyze the patch antenna behavior, three main parameters should be determined. These are the operating frequency (*f*), dielectric constant (ε_r), and substrate height (*h*) to calculate the actual physical length and width of the patch antenna that represents the designing process. Characteristics impedance is mainly affected by the patch width, where the patch length effects on the resonance frequency. Patch antenna design procedure is shown below [25].

Design procedure:

Step 1: **Width calculation (W)**

W, can be calculated by using the following equation:

$$W = \frac{c}{2 f_o} \sqrt{\frac{2}{\varepsilon_r + 1}} \tag{3.1}$$

Step 2: **Effective Length Calculation (L_{eff})**

The electrical length of the patch antenna is known as effective length, where this value closely related to the resonance frequency; due to the fringing effects, (which are electromagnetic fields that propagate outside the conductor towards the ground plane through the dielectric layer). The effective length is slightly larger than the

actual physical length. Calculation of this parameter can be done using Equation 3.2 below.

$$L_{eff} = \frac{c}{2 f_o \sqrt{\varepsilon_{reff}}} \tag{3.2}$$

Where ε_{reff} represents the effective dielectric constant, which is less than the actual dielectric constant due to the presence of fringing fields. It can be calculated by using Equation 3.3.

$$\varepsilon_{reff} = \frac{\varepsilon_r + 1}{2} + \frac{\varepsilon_r - 1}{2}\left(1 + 12\frac{h}{W}\right)^{-\frac{1}{2}} \tag{3.3}$$

Step3: **Length Extension Calculation (ΔL)**

This parameter appears due to the fringing fields which can be calculated by using Equation 3.4 shown below.

$$\Delta L = \frac{(\varepsilon_{reff} + 0.3)\left(\frac{W}{h} + 0.264\right)}{(\varepsilon_{reff} - 0.258)\left(\frac{W}{h} + 0.8\right)} \tag{3.4}$$

Step 4: **Actual Length Calculation (L)**

Subtracting the extension length value from the effective length, the actual antenna length will be, as follows.

$$L = L_{eff} - 2\Delta L \quad (3.5)$$

Step5: **Ground Plane Dimensions Calculation (W_g and L_g)**

Infinite ground plane has been assumed in the transmission line analyzing theory to explicate the patch antenna behavior, but for practical cases finite ground plane should be used. So to keep transmission line theory valid a finite ground plane will be used but at the same time, it will be large enough to act as an infinite plane, where ground plane length and width, can be calculated using the following formulas:

$$L_g = L + 6h \quad (3.6)$$

$$W_g = W + 6h \quad (3.7)$$

Design Calculations:

Step1: Substituting c= 3*10^8 m/s, ε_r = 4.6, and f_o= 1.884 GHz in Equation 3.1, to get W= 47.58 mm.

Step 2: Effective permittivity is calculated by substituting ε_r = 4.6, W= 47.58 mm and h=1.59 mm in Equation 3.3, which equals to ε_{reff} = 3.82, then substituting it in equation 3.2 to get the effective length L_{eff} = 40.73 mm

Step 3: Length extension has been calculated in this step by substituting ε_{reff} =3.82, W= 47.58 mm, and h=1.59 mm to get ΔL = 1.14.

Step 4: Actual patch physical length is calculated by substituting the parameter values in equation 3.5 to get L= 38.45 mm.

Step 5: Substituting *W*= 47.58, *L*= 38.46 mm, and *h*= 1.59 mm to get the ground physical length and width, which is equal to *L*g=44.46 mm and *Wg*=53.58 mm.

In this case a square patch has been considered and the following formula is used to calculate the width and length of the patch antenna:

$$L = W = \frac{c}{2 f_o \sqrt{\varepsilon_r}} \tag{3.8}$$

Whish results *W*=*L*= 37mm.

The designed antenna is modeled and simulated with FEKO as shown in Figure 3.2; MSL of 50 Ω characteristic impedance is used to feed the antenna. Figure 3.3 shows the real and imaginary parts of the input impedance at the feeding terminal.

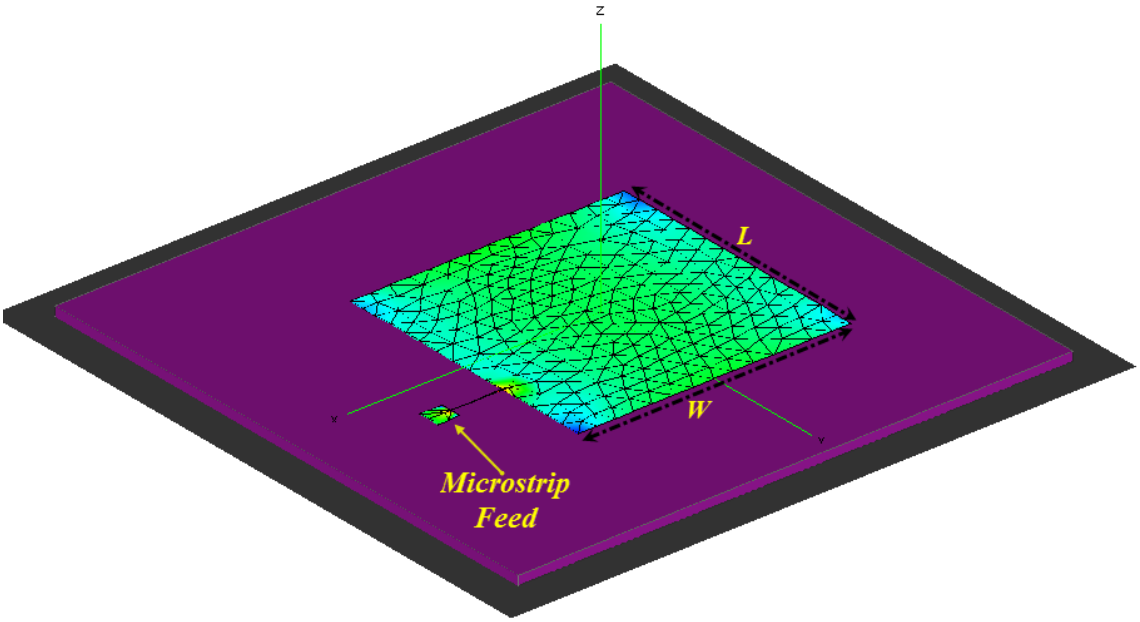

Figure 3-2: Patch antenna geometry with MSF line simulated by FEKO

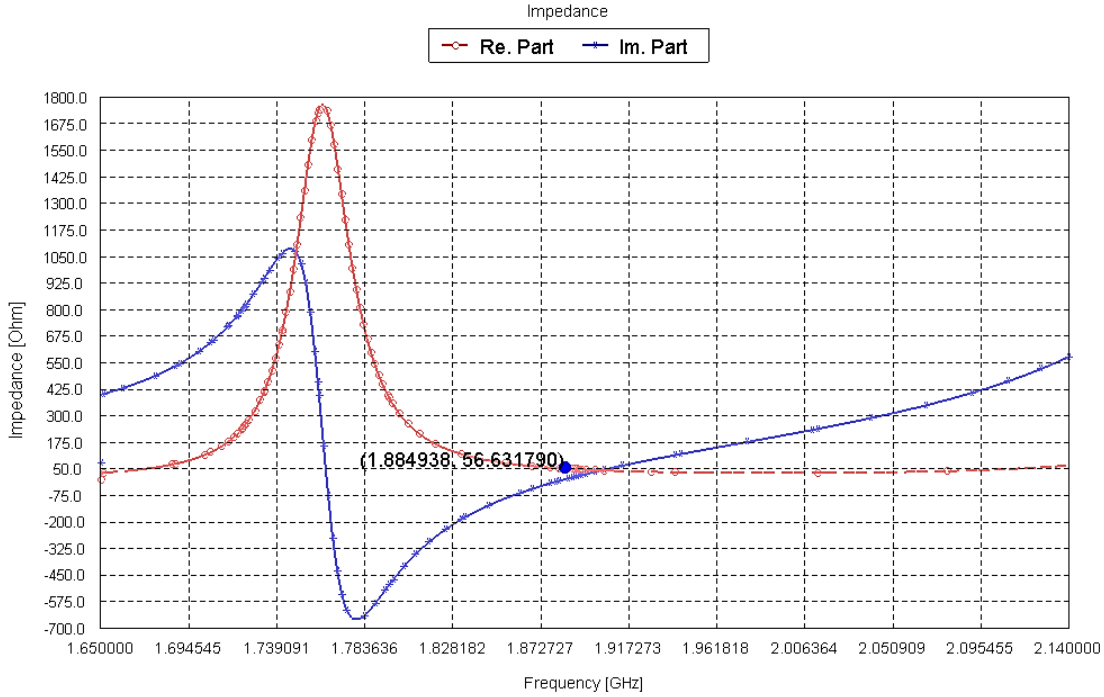

Figure 3-3: FEKO input impedance result for the rectangular patch antenna

FEKO reflection coefficient result of the antenna is presented in Figure 3.4a, where it shows a bandwidth of 32 MHz, which calculated for the frequencies of < -10 dB S11.

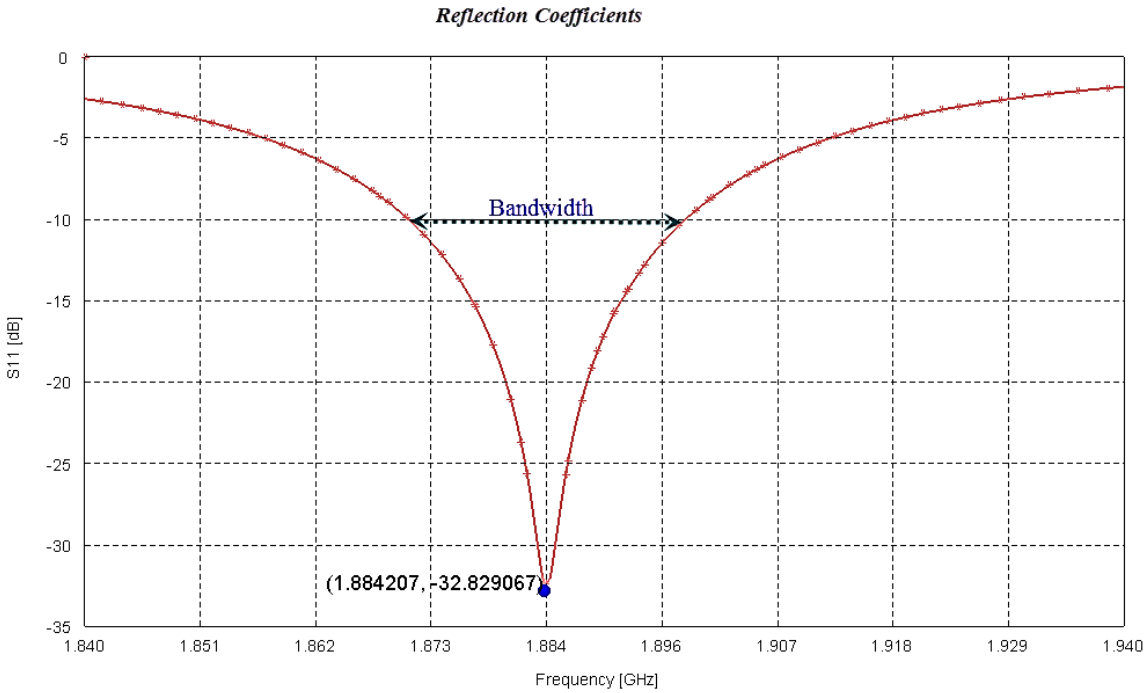

Figure 3-4: Patch antenna reflection coefficient computed by FEKO

For FEKO result validation, same antenna has been designed and simulated using IE3D by R. Mohanamurali and T. Shanmuganantham [6], Figure 3.5 shows the reflection coefficient calculation. Good agreement has been observed between FEKO result and IE3D results.

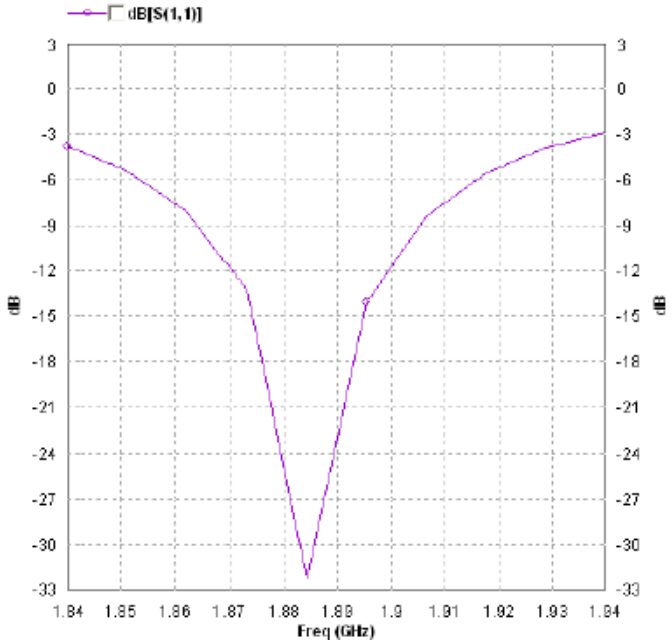

Figure 3-5: Patch antenna reflection coefficient [6]

The antenna has a resonance frequency of approximately 1.884 GHz with -32 dB reflection coefficients. 3-D radiation pattern and antenna gain are shown in Figure 3.6 and 3.7 respectively.

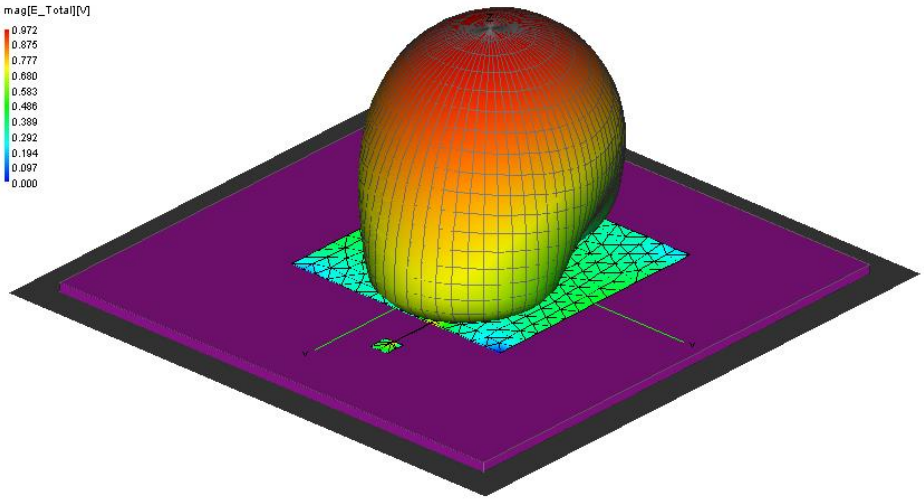

Figure 3-6: 3-D rectangular patch antenna radiation pattern

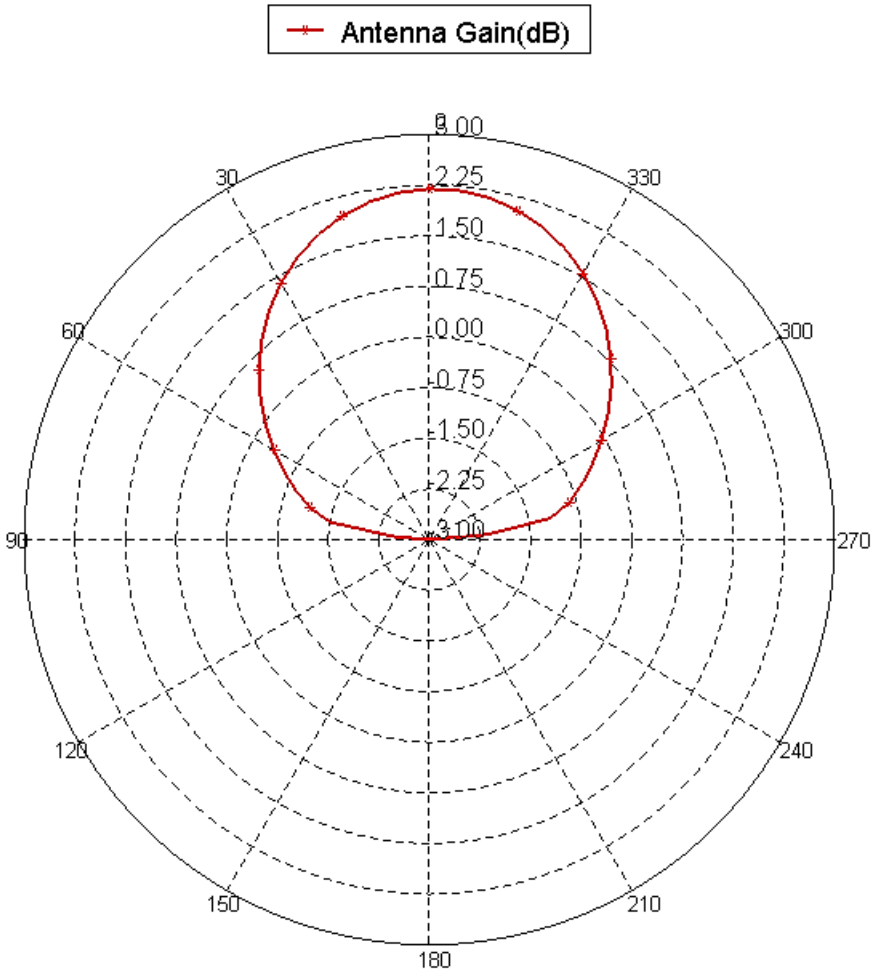

Figure 3-7: 2-D graph patch antenna gain

Antenna performance is summarized in Table 3.1. As shown in the table and in the figure the bandwidth is relatively narrow, so SCF geometry will be applied to the patch surface to get multiband response with relatively wider bandwidth.

Table 3-1: Patch Antenna Performance

Band no.	Center freq.(GHz)	Reflection coef. (dB)	Upper freq.(GHz)	Lower freq.(GHz)	Bandwidth (MHz)	Gain dB
1	1.884	-32.4944	1.900245	1.868174	32.071	2.214981

3.2.1.2 1st Iteration SCF Antenna

First iteration SCF geometry has been applied to the designed patch antenna (previous step). The iteration factor is 1/3, where the patch surface is divided into nine equal sub-squares. The middle sub-square has been removed forming an air gap in the center of dimensions 12.33 mm×12.33 mm, as shown in the FEKO Figure 3.8 below.

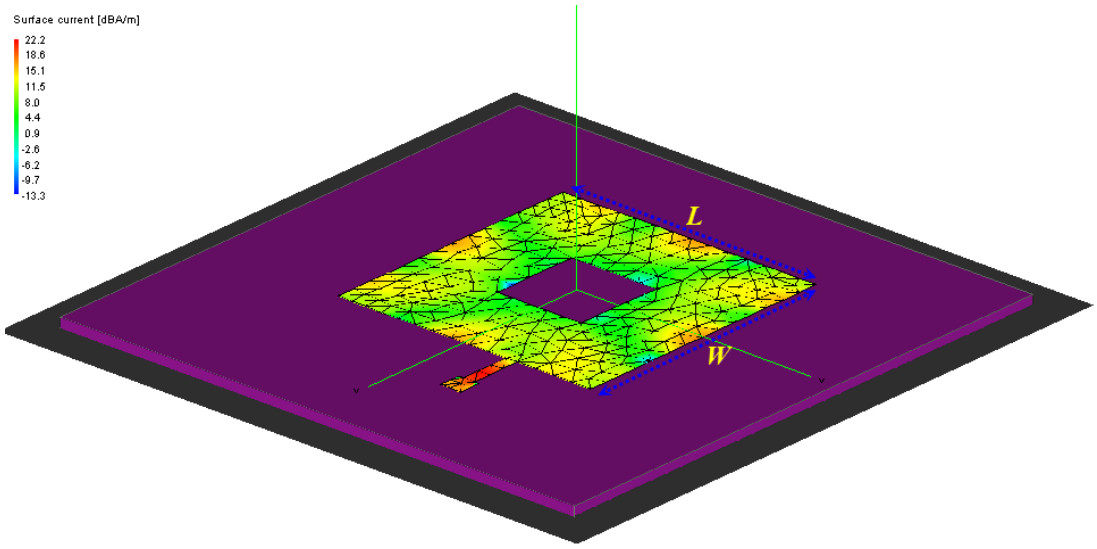

Figure 3-8: 1st iteration SCF antenna configuration fed by MSL

Input impedance at the feeding point is shown in Figure 3.9, where this figure shows that there are two resonance frequencies, the first one is at 5.78 GHz and the second one is at 6.625GHz.

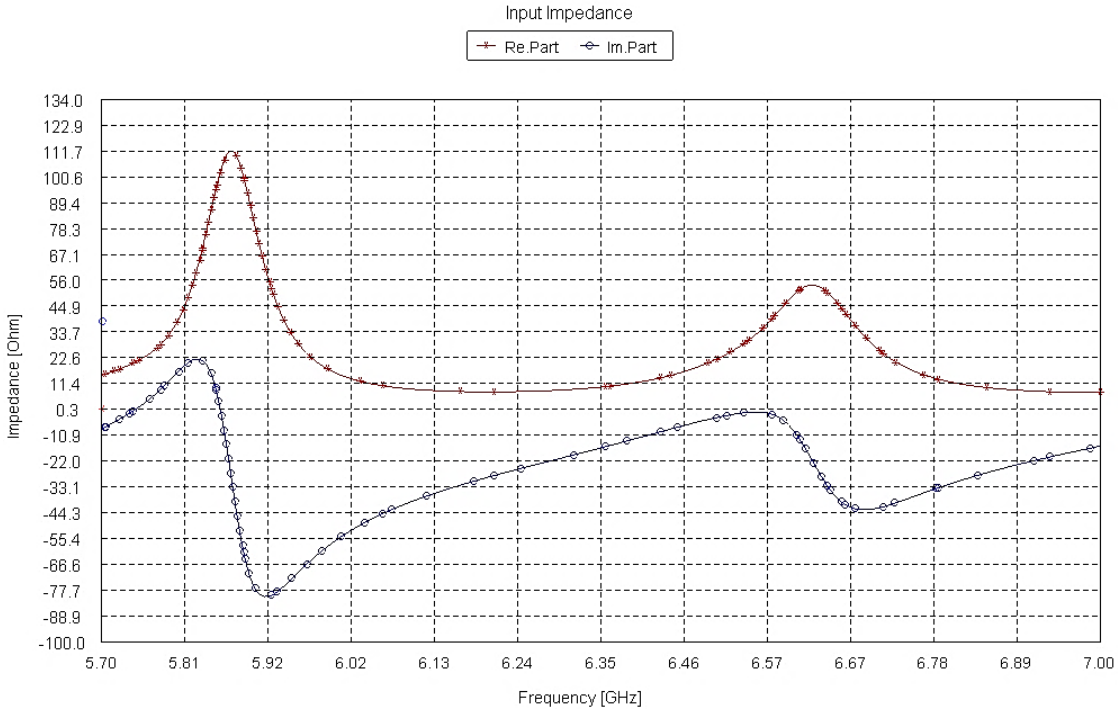

Figure 3-9: 1st iteration SCF antenna input impedance by FEKO

Reflection coefficient curve for this antenna is shown in Figure 3.10. Reflection coefficients of less than -10 dB has been observed at two different resonance frequencies, which means that applying SCF geometry to the patch antenna acquire it a multiband behavior.

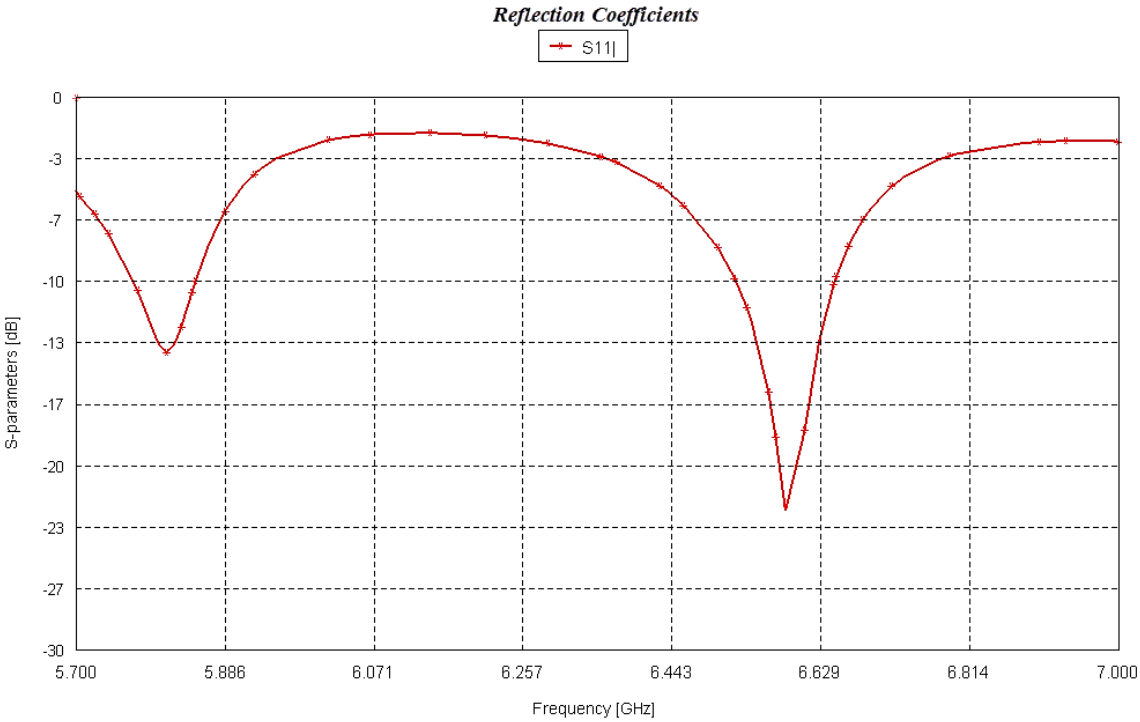

Figure 3-10: 1st iteration SCF antenna reflection coefficient produced by FEKO

Figures 3.11 and 3.12 show the 3-D radiation pattern and antenna gain computed by FEKO, where maximum gain of 2.34 has been registered in -45 degree direction; all of these results are clearly described in Table 3.2.

Table 3-2: 1st iteration SCF antenna performance

Band no.	Center freq. (GHz)	Ref. coeff. (dB)	Upper freq. (GHz)	Lower freq. (GHz)	Bandwidth (MHz)	Radiation Pattern (dB)	
						Gain	Atten.
1	5.81	-14.03	5.86	5.77	87.74	--------	-0.325
2	6.59	-23.42	6.65	6.52	132.42	2.459	-------

We can conclude from this antenna that multiband frequency response with wider bandwidth can be obtained by applying fractal geometries in random or systematic motif.

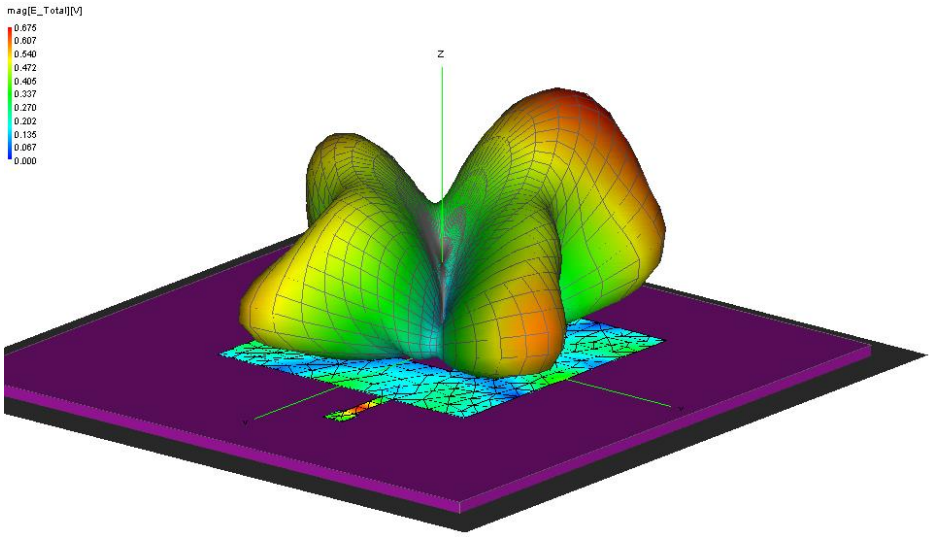

Figure 3-11: 3-D radiation pattern of 1st iteration SCF antenna

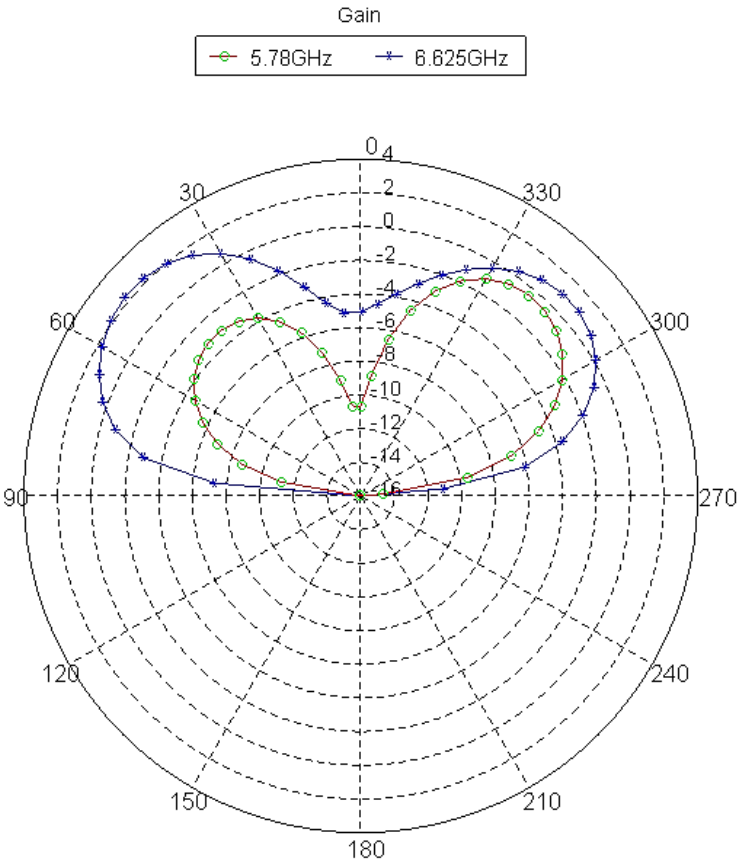

Figure 3-12: 2-D gain graph of 1st iteration SCF antenna

3.2.1.3 2nd Iteration SCF Antenna

2nd iteration of SCA is presented; a new 4.11 mm×4.11 mm air gaps has been etched on the 1st iteration SCA as shown in Figure 3.13 below.

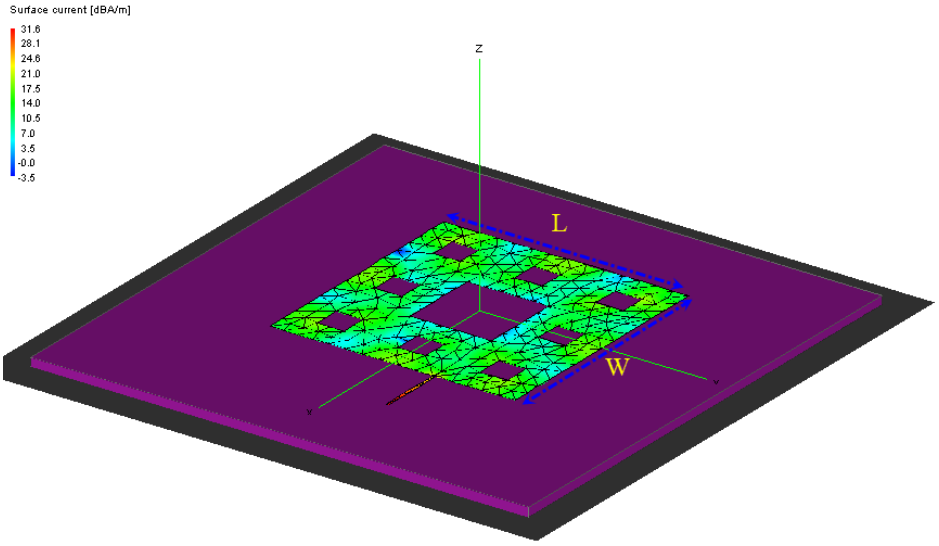

Figure 3-13: MSL fed 2nd iteration SCF antenna configuration constructed by FEKO

This antenna is modeled and simulated; input impedance, reflection coefficient are shown in Figure 3.14 and 3.15 respectively. Easily we can conclude that this antenna is suitable to operate in 3 different frequencies, which are 5.6 GHz, 6.47 GHz, and 7.6 GHz. Figure 3.16 and 3.17 show the 3-D radiation pattern and antenna gain respectively at the resonance frequencies. A 2.5 dB gain is obtained at the 6.47 GHz frequency in the -45^{o} direction. Table 3.3 summarizes the results.

Table 3-3: 2nd Iteration SCF antenna performance

Band no.	Center freq. (GHz)	Ref. coeff. (dB)	Upper freq. (GHz)	Lower freq. (GHz)	Bandwidth (MHz)	Radiation Pattern (dB)	
						Gain	Attenuation
1	5.592	-17.09	5.618	5.57	54.117	-------	-0.815
2	6.456	-13.61	6.486	6.43	59.562	1.87	--------
3	7.654	-20.30	7.708	7.601	107.425	-------	-5.78

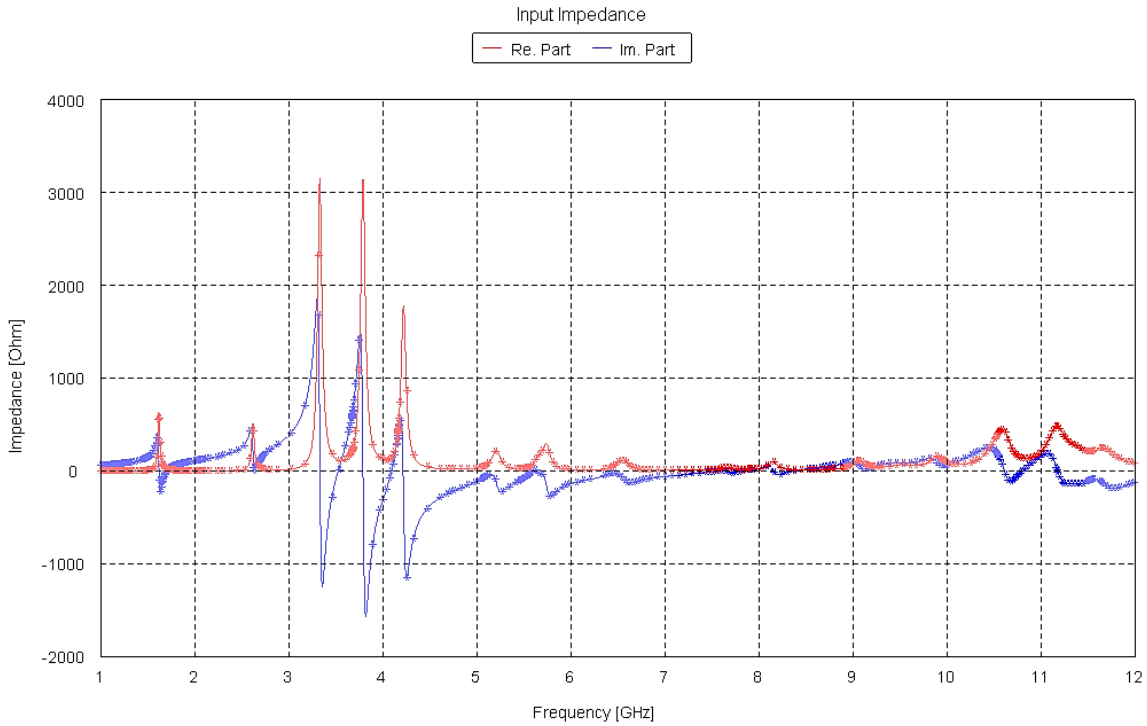

Figure 3-14: FEKO Input impedance result for the 2nd iteration SCF antenna

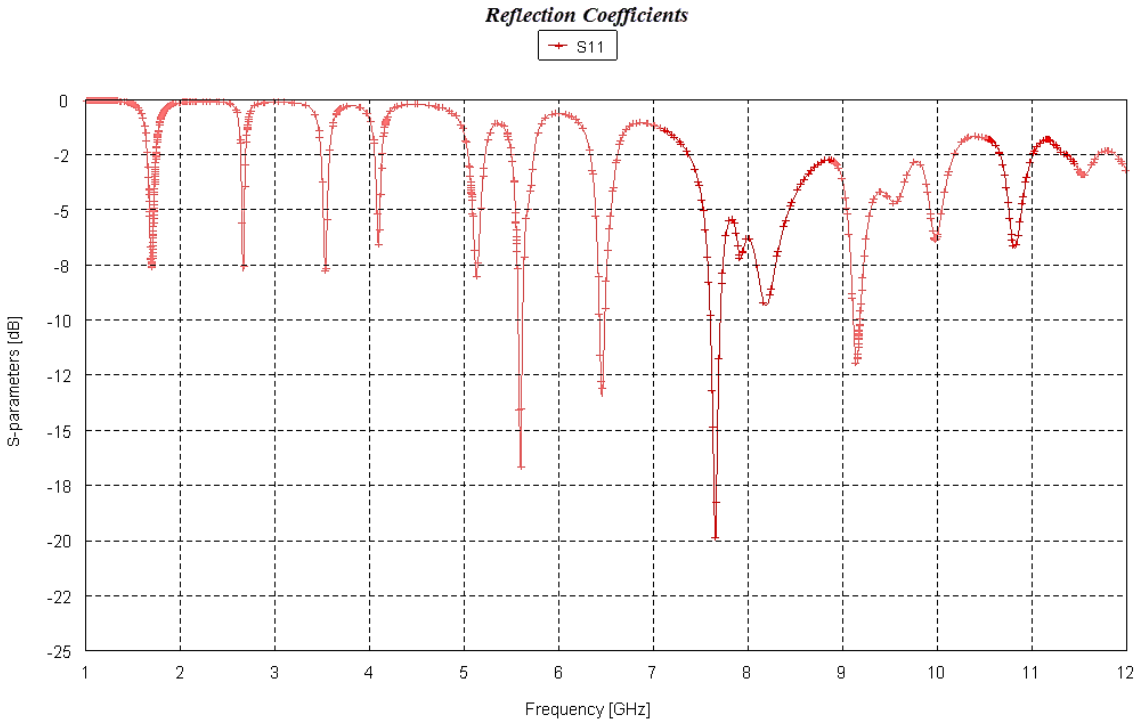

Figure 3-15: 2nd iteration SCF antenna reflection coefficient

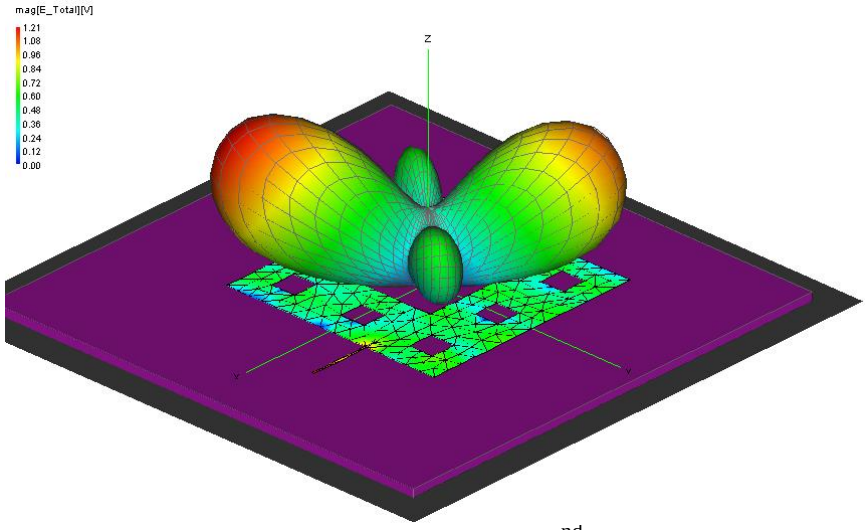

Figure 3-16: 3-D Radiation pattern of the 2nd iteration SCF antenna

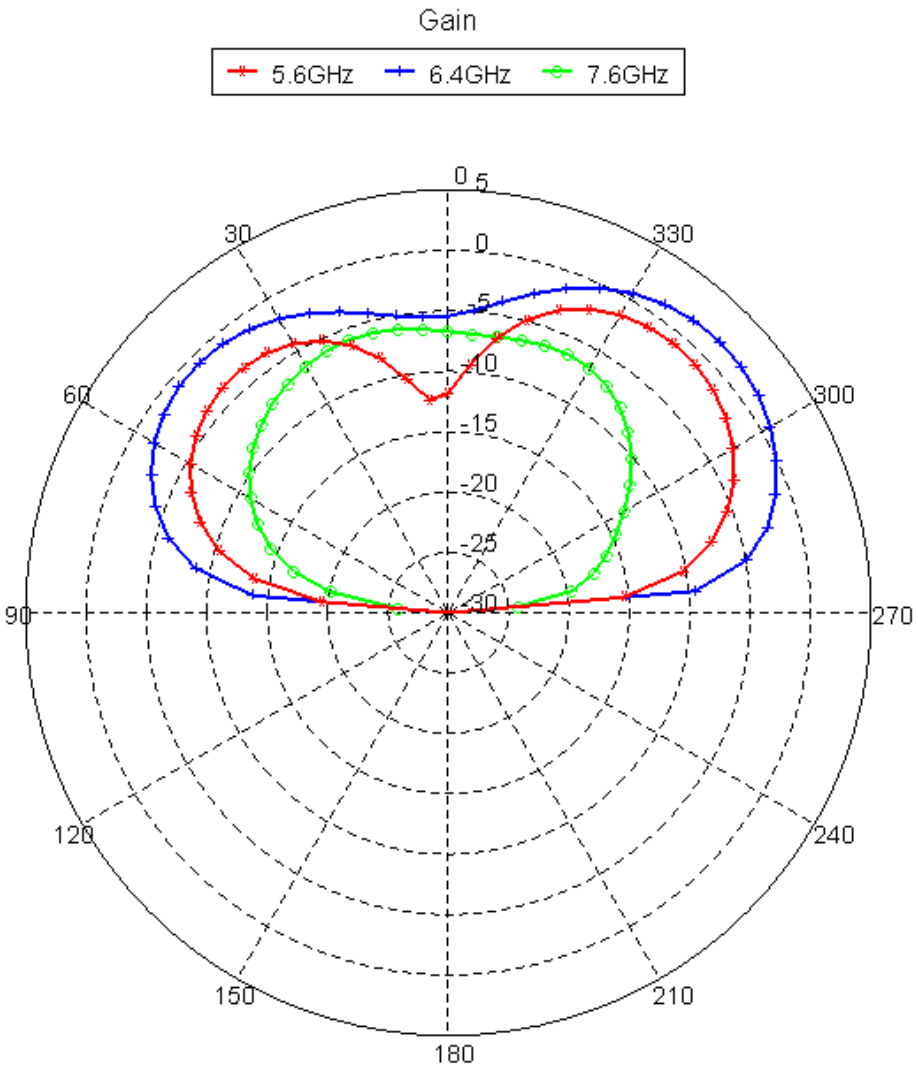

Figure 3-17: 2-D gain graph of the 2nd iteration SCF antenna

3.2.1.4 3rd Iteration SCF Antenna

In order to increase the antenna electrical lengths, 3rd iteration SCA in suggested. The antenna has air gaps of dimensions 12.33 mm×12.33 mm, 4.111 mm×4.111 mm and 1.37 mm×1.37 mm arranged by the size from largest to smallest one, as shown in Figure 3.18.

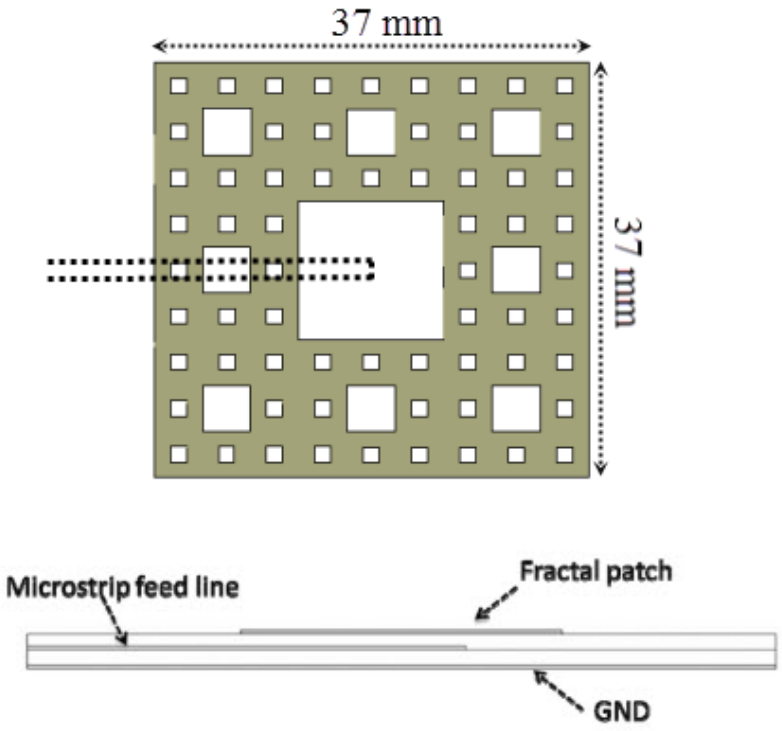

Figure 3-18: 3rd iteration SCF antenna fed by PCF line produced by FEKO

Due to the difficulty in positioning of the MSF line connection with antenna, proximity coupled feeding technique has been used. The antenna was implanted on FR4 substrate of 3.2 mm thickness. In the middle of the substrate a 50 Ω characteristics impedance feeding line was embedded. The reason of choosing this feeding method is due to its flexibility and its resistance against the oxidation problems between the line and the antenna.

The optimization process is carried out in order to determine the proper distance between the antenna center and far edge of the feeder. Using FEKO the optimization process has been carried out for different feed positions in which the reflection coefficient is calculated as shown in Figure 3.19.

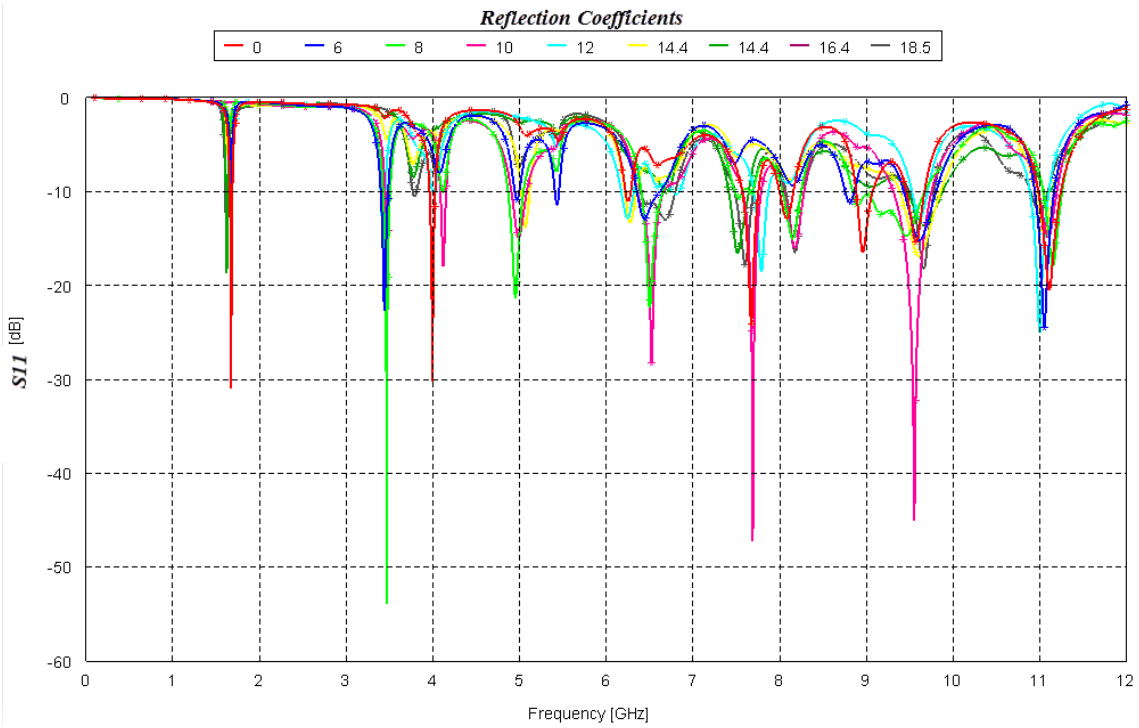

Figure 3-19: FEKO optimization reflection coefficients results for 3rd iteration SCF antenna

Table 3.4 below summarizes the contents of the optimization figure; we can conclude that 10 mm is the optimal feeding point, because it has minimum reflection coefficient and wider frequency bands.

Table 3-4: Optimization of the feed position

Proximity Coupled-3rd Iteration	Feed = 0 mm	Feed= 6 mm	Feed= 8 mm	Feed= 10 mm	Feed= 12 mm	Feed= 14.4mm	Feed= 16.4 mm	Feed= 18.5 mm
F1(GHz)	1.676	3.426	3.478	3.471	1.673	5.063	1.624	1.622
RL(dB)	-31.1	-22.9	56.98	-14.459	-20.8	-13.94	-18.814	-17.39
BW(MHz)	39.66	120	140	350.16	45	140	506	34
F2(GHz)	3.996	4.97	4.089	4.125	3.4	6.291	6.676	3.787
RL(dB)	-30.4	11.1	-10	-18.264	-14.45	-13.46	-10.25	-10.68
BW(MHz)	110	92	------	74.466	78	170	--------	--------
F3(GHz)	6.250	5.431	4.931	4.988	4.024	9.590	7.53	6.666
RL(dB)	-11.3	-11.56	-21.63	-15.172	-19.31	-16.9	-16.722	-13.1
BW(MHz)	92	83	235	188.35	-------	523	279	499
F4(GHz)	7.666	6.443	6.52	5.51	6.246	11.06	8.161	7.587
RL(dB)	-24.5	-13.1	-22.63	-28.727	-13.1	-14.28	-14.86	-17.96
BW(MHz)	240	304	300	326.33	230	230	231	290
F5(GHz)	8.078	8.816	7.52	7.686	6.8		9.674	8.179
RL(dB)	-13.1	-11.31	-11.21	-46.44	-10.35		-13.77	-16.63
BW(MHz)	221	175	331	266783	-------		455	276
F6(GHz)	8.962	9.616	8.149	8.181	7.767		11.094	9.651
RL(dB)	-16.7	-15.36	-15.35	-16.36	-18.67		-10.3	-13.34
BW(MHz)	260	441	278	248.58	233		-------	355
F7(GHz)	9.560	11.04	9.458	9.567	9.625			11.02
RL(dB)	-15.7	-24.73	-15.06	-43.7	-13.01			-12.3
BW(MHz)	260	258	919	458.59	273			249
F8(GHz)	11.11		11.16	11.114	11.00			
RL(dB)	-20.8		-18.20	-15.172	-25.29			
BW(MHz)	325		296	222.25	287			

Table 3.5 shows the reflection coefficient, bandwidth, and gain, Figures 3.20 and 3.21 shows the 3-d radiation pattern and gain respectively computed by FEKO for the optimal feed point.

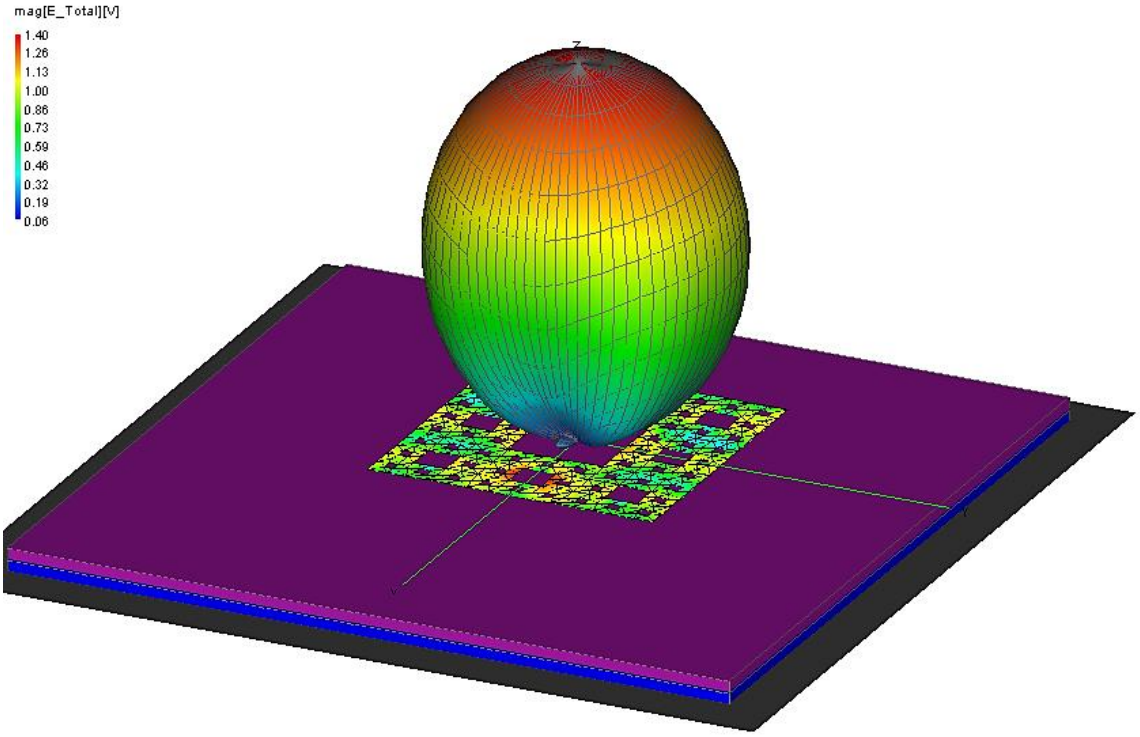

Figure 3-20: 3-D radiation pattern of 3rd iteration SCF antenna at 4.9GHz

Table 3-5: 3rd Iteration SCF antenna performance

Band no.	Center freq. (GHz)	Ref. coeff. (dB)	Upper freq. (GHz)	Lower freq. (GHz)	Bandwidth (MHz)	Radiation Pattern (dB)	
						Gain	Attenuation
1	3.471	-14.459	3.51	3.16	350.16	1.70	--------
2	4.125	-18.264	4.15	4.08	74.46	0.40	--------
3	4.988	-15.172	5.09	4.90	188.35	7.85	--------
4	5.51	-28.727	6.68	6.34	326.33	4.68	--------
5	7.686	-46.44	7.81	7.54	266.78	4.37	--------
6	8.181	-16.36	8.29	8.03	248.58	------	-2.408
7	9.567	-43.7	9.76	9.3	458.59	6.77	--------
8	11.114	-15.172	11.2	10.98	222.25	8.14	--------

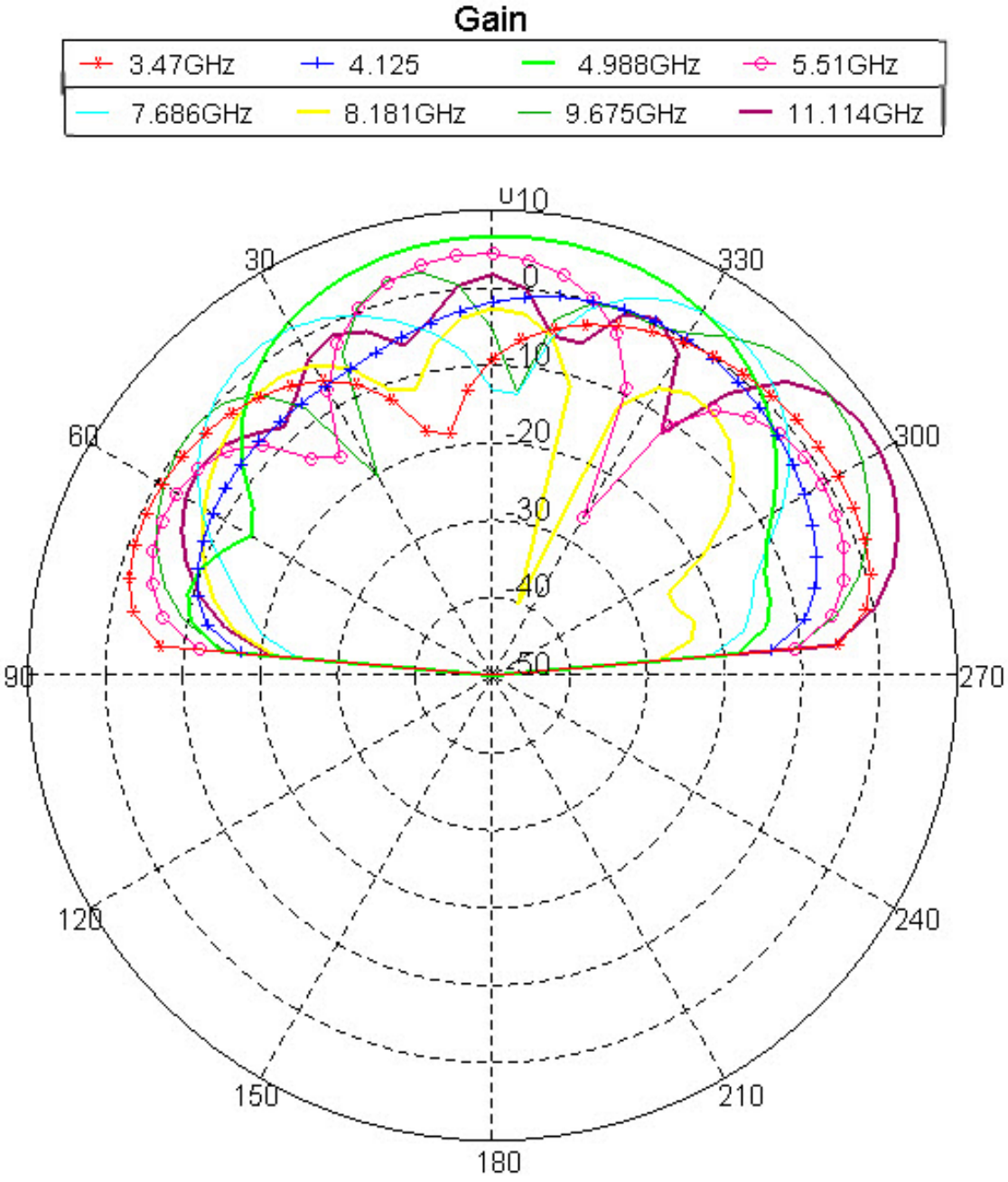

Figure 3-21: 3rd SCF antenna gain graph at the resonance frequencies

Gain enhancement has been achieved by this antenna, where 8.12 dB 7.85 dB and 6.76 dB are obtained at -60^{o}, 0^{o}, -45^{o} directions respectively.

3.2.1.5 Combination of 3rd Iteration SCF and 1st Iteration MKF (SC-MKF)

The antenna structure in this step is shown in Figure 3.22, where 1st MKF has been applied for the 3rd iteration SCA to add some electrical lengths. Feeding technique and substrate material are kept intact. Antenna dimensions are shown in the following figure.

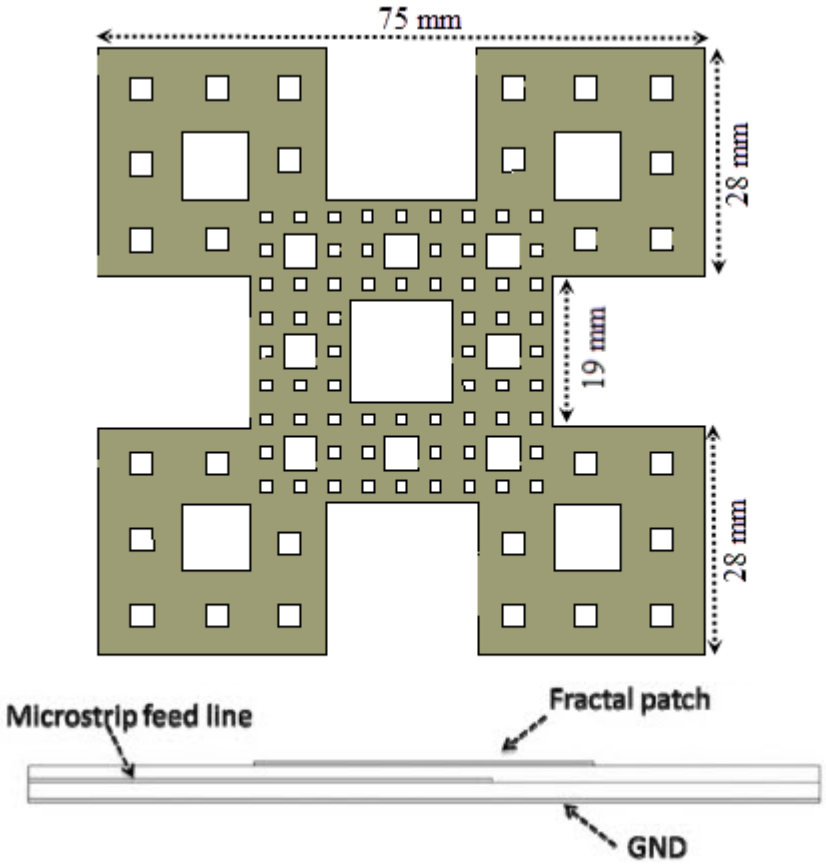

Figure 3-22: FEKO image for SC-MKF antenna

The input impedance of this antenna shows that, it has 9 resonance frequencies with suitable gain dB level as shown in Figure 3.23. The reflection coefficients calculation is given in Figure 3.24.

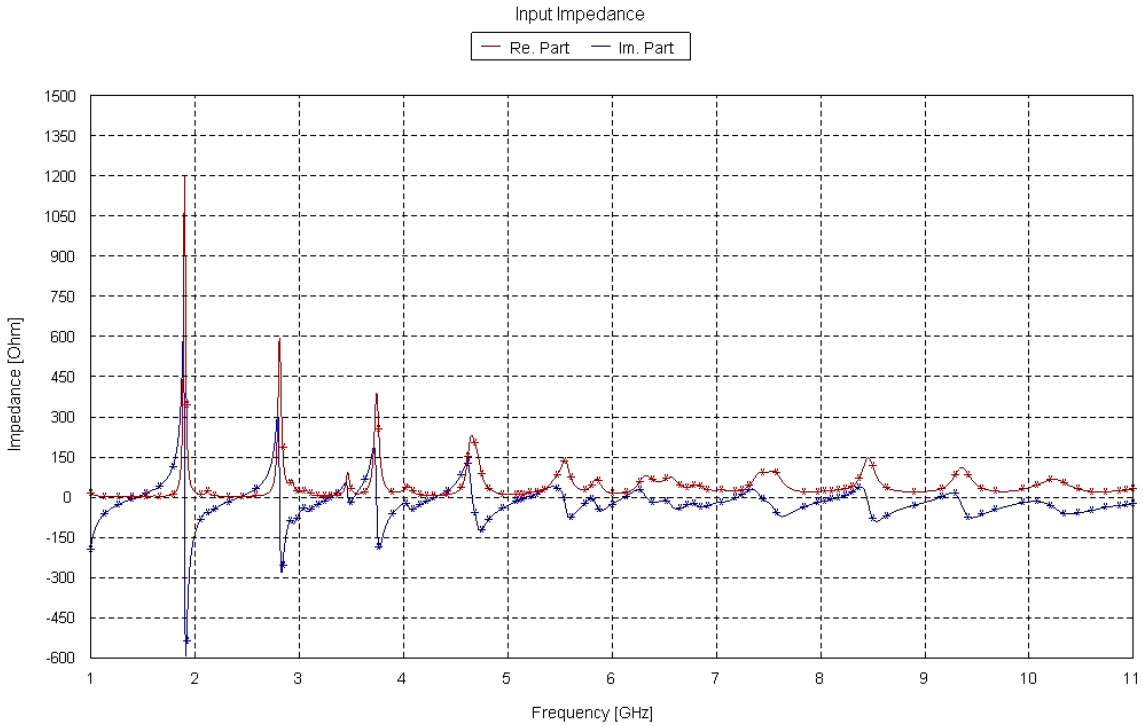

Figure 3-23: SC-MKF antenna input impedance

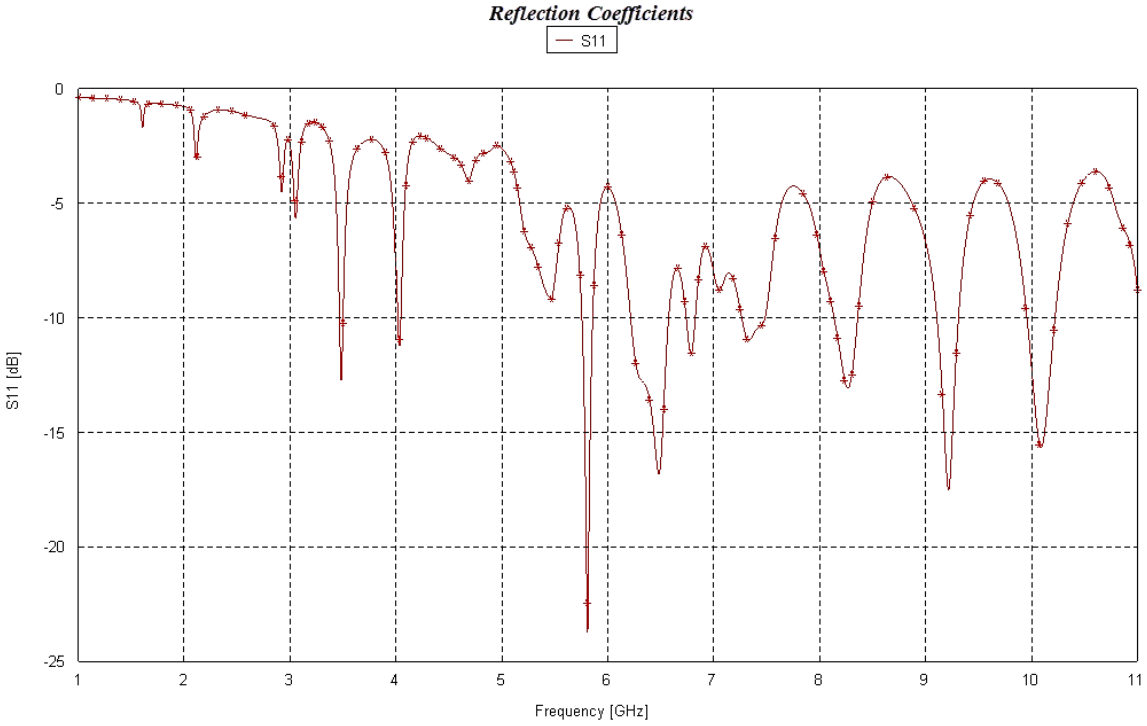

Figure 3-24: SC-MKF antenna reflection coefficients

Antenna radiation pattern at 6.484 GHz is shown in Figure 3.25 as example, and Figure 3.26 shows the antenna gain at the resonance frequencies in 2-D graph.

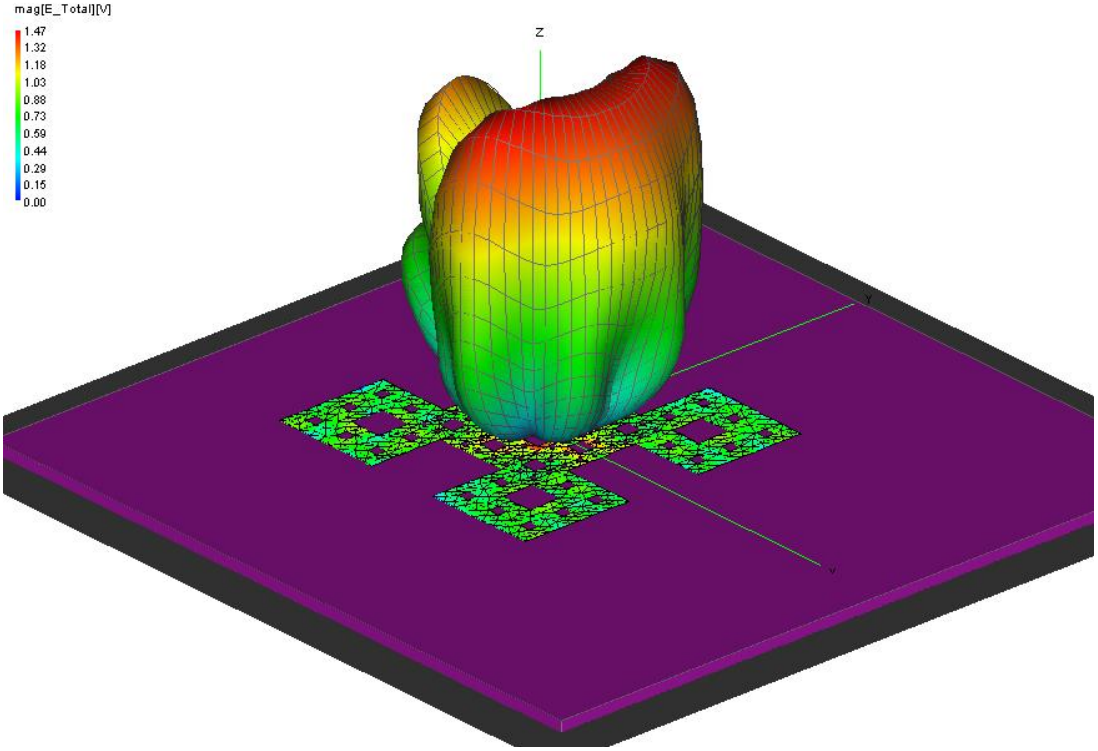

Figure 3-25: SC-MKF antenna 3-D radiation pattern at 6.4 GHz

Table 3.6 describes the antenna reflection coefficients, bandwidth, and gain.

Table 3-6: SC-MKF antenna performance

Band no.	Center freq. (GHz)	Ref. coeff. (dB)	Upper freq. (GHz)	Lower freq. (GHz)	Bandwidth (MHz)	Radiation Pattern (dB)	
						Gain	Attenuation
1	3.48	-12.85	3.51	3.46	45.20	-------	-2.95
2	4.03	-11.35	4.05	4.02	34.98	------	-2.92
3	5.81	-23.78	5.86	5.75	112.71	3.663	--------
4	6.48	-16.92	6.58	6.21	366.20	6.59	--------
5	6.79	-11.80	6.83	6.73	94.94	2.46	--------
6	7.32	-11.15	7.47	7.26	212.83	------	-0.38
7	8.27	-13.21	8.36	8.13	237.35	4.01	--------
8	9.21	-17.62	9.31	9.09	213.83	2.79	--------
9	10.09	-15.72	10.23	9.95	272.97	2.04	--------

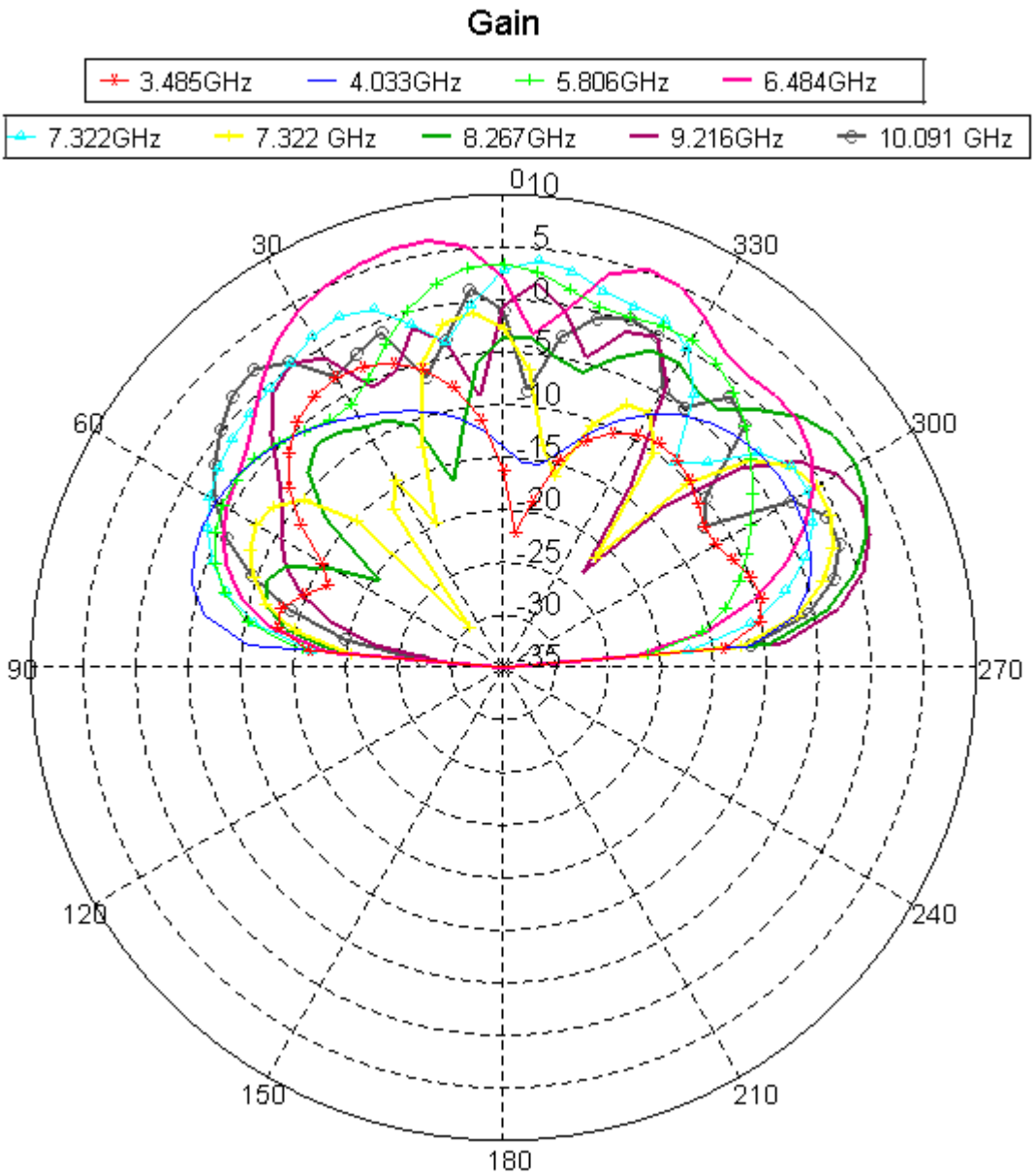

Figure 3-26: SC-MKF antenna gain graph at the resonance frequencies

2-D gain level shows that the antenna has 6.51 dB, 4.001 dB, and 3.66 dB at 25^{o}, -60^{o}, and 0^{o} directions respectively.

3.2.2 Triangular Patch

3.2.2.1 Triangular Antenna

The design procedure for 1.6 GHz triangular patch antenna is presented in this section; according to the cavity model the rectangular and triangular patch have the same design parameters except the use of the side length (*S*) with triangular patch instead of the length and width of the rectangular patch. The side length can be calculated by using equation 3.9 shown below [26].

$$f_{mn} = \frac{2c}{3S\sqrt{\varepsilon_r}}\sqrt{m^2 + mn + n^2} \qquad (3.9)$$

Substituting c=3×10^8 m/s, f= 1.623 GHz, m=n=1, εr = 4.5; we get S=100.568 mm.

Cavity model is not a perfectly accurate method for the analysis of planar antennas [2], where a percentage of error must be exist; but the result obtained from the formula can be considered as starting point for further calculations and simulations; FEKO simulations are carried out by considering the obtained values; Figure 3.27 shows the proposed antenna geometry, where it implanted on FR4 substrate (ε_r = 4.5) of 1.59 mm thickness. The antenna was fed by coaxial cable of 50 Ω characteristics impedance in the center of the patch.

Figure 3.28 shows the input impedance curve, the antenna is suitable for 1.63 GHz operation frequency which means that there is 30 MHz deviation as expected. Antenna reflection coefficients has also been simulated and presented in Figure 3.29.

3-D antenna radiation pattern and 2-D gain graph are illustrated in Figures 3.30 and 3.31 respectively.

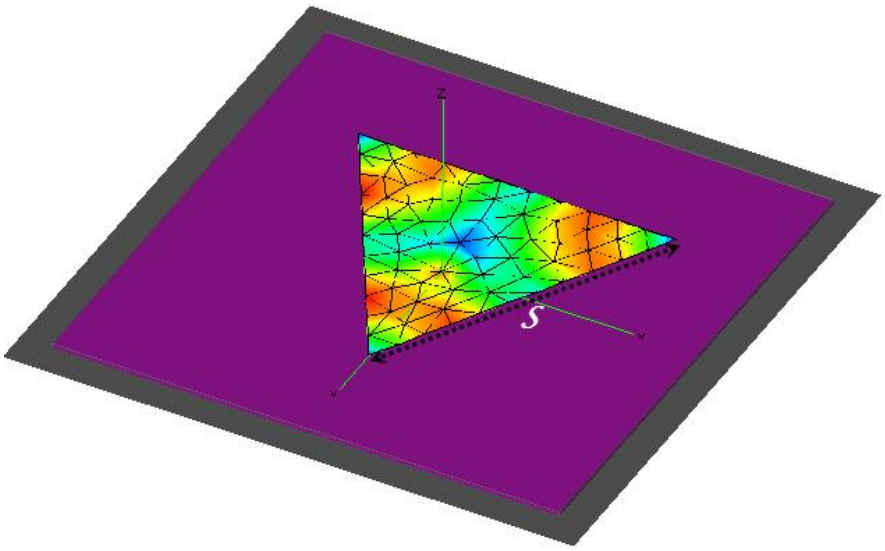

Figure 3-27: Triangular patch antenna with pin feed configuration in FEKO

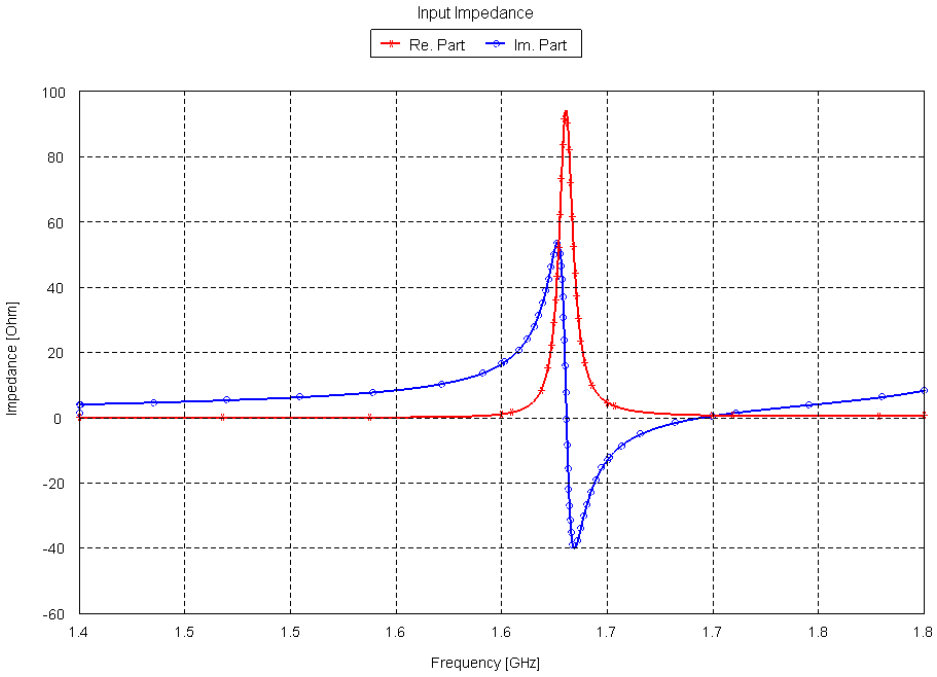

Figure 3-28: Triangular patch antenna input impedance (FEKO)

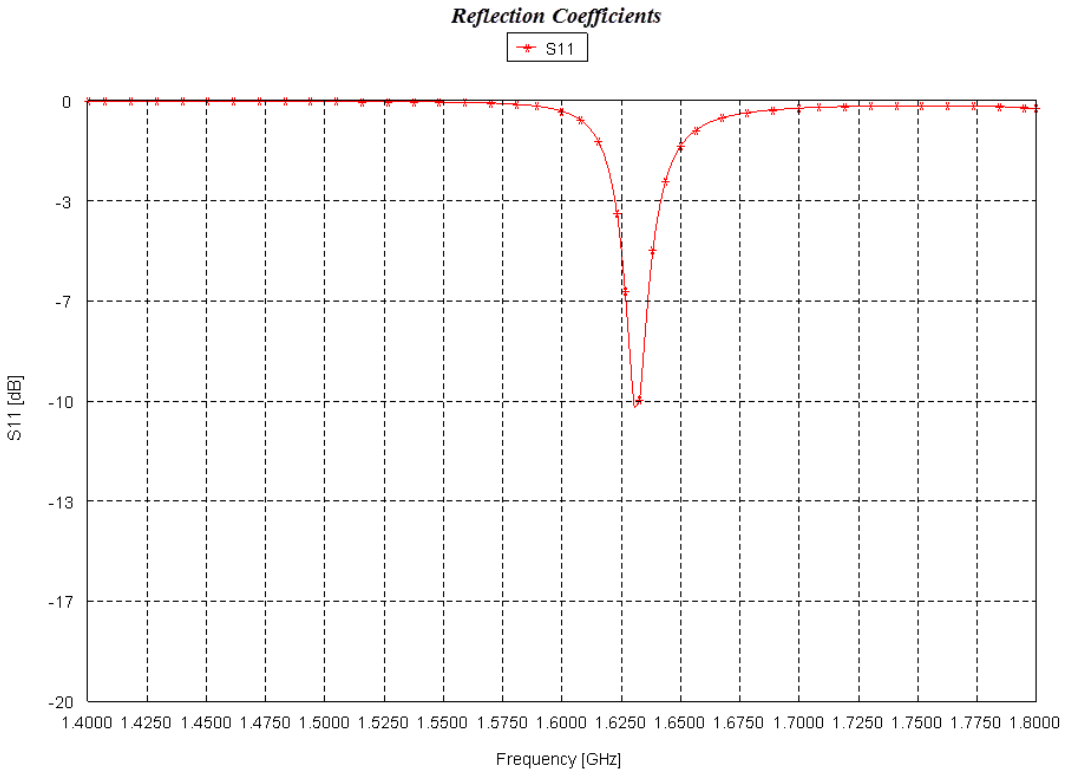

Figure 3-29: Triangular patch antenna reflection coefficients (FEKO)

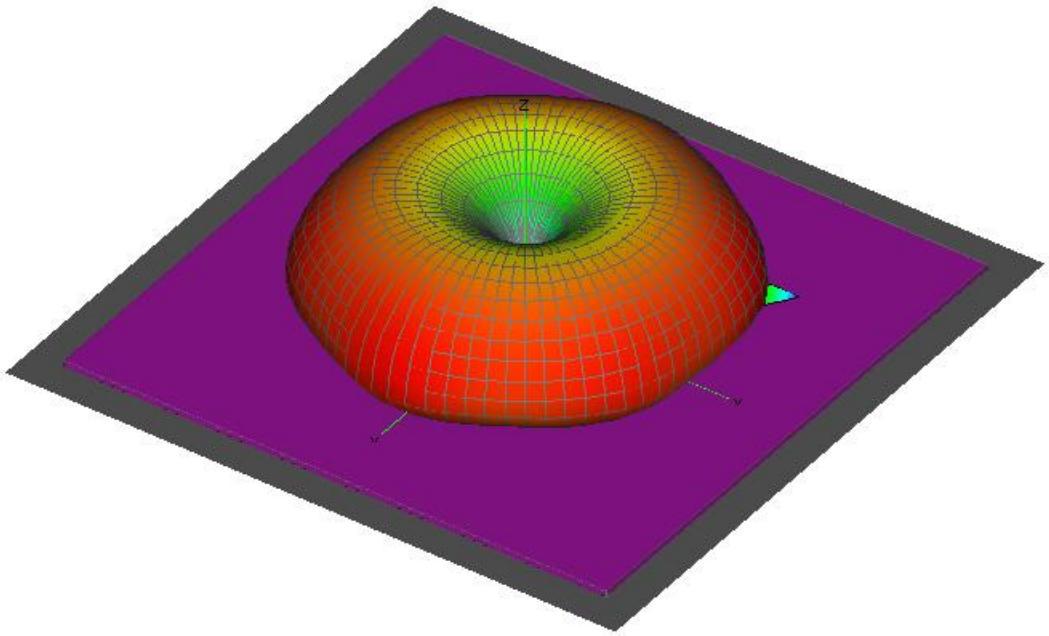

Figure 3-30: 3-D Triangular patch antenna radiation pattern (FEKO)

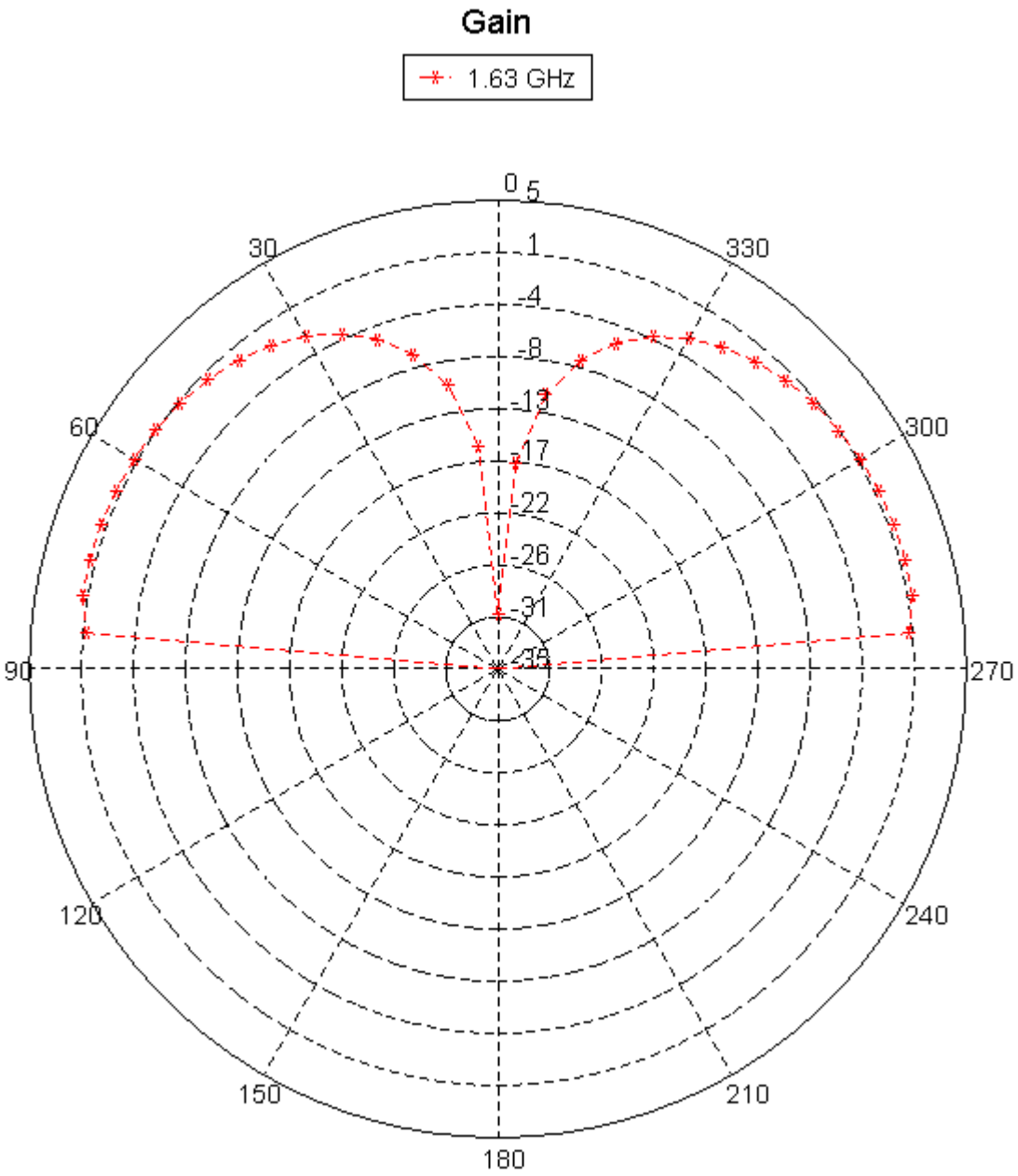

Figure 3-31: Triangular patch antenna gain (FEKO)

Maximum gain is obtained in -75^{o} of 1.5 dB, which will be enhanced by applying KSG to the edges of the triangular patch. KSF geometry acquires the antenna multiband frequency response with relatively high gain.

3.2.2.2 1st Iteration KSF Antenna

1st Iteration KSF geometry is presented in this section. KSF geometry creation has the following procedure:

1. Dividing the patch sides into three segments of equal lengths (S/3 mm)
2. Adding an equilateral triangle that goes outward the middle segment as its base
3. Removing the middle line segment. Figure 3.32 shows the antenna geometry.

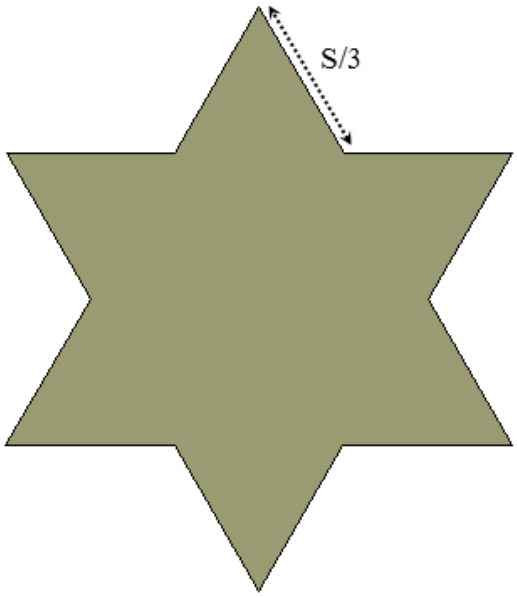

Figure 3-32: 1st iteration KSF antenna with pin feed (FEKO)

The metallic plane is implanted on FR4 substrate of 4.5 dielectric constant having 1.59 mm thickness with commercial coaxial cable for feeding in the middle of the antenna.

Input impedance and reflection coefficients, which show a multiband behavior, are shown in Figure 3.33 and 3.34 respectively. Figure 3.35 shows the antenna 3-D radiation pattern and 2-D gain graph is demonstrated in Figure 3.36.

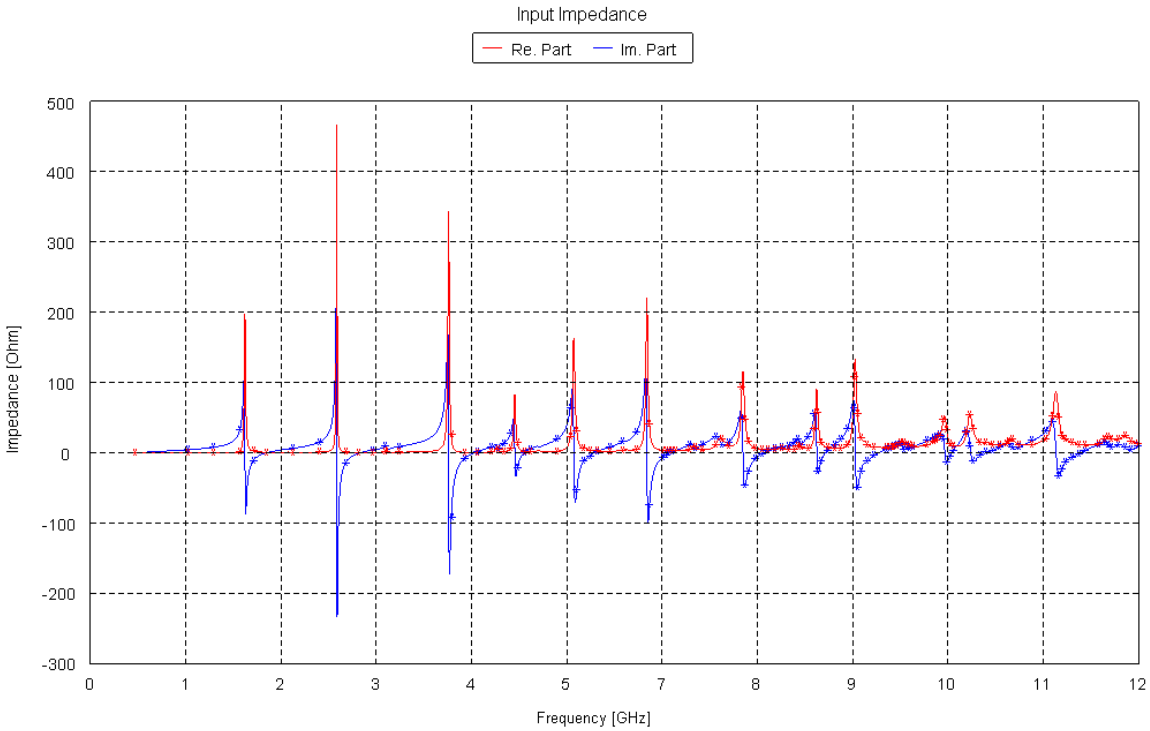

Figure 3-33: 1st iteration KSF antenna input impedance (FEKO)

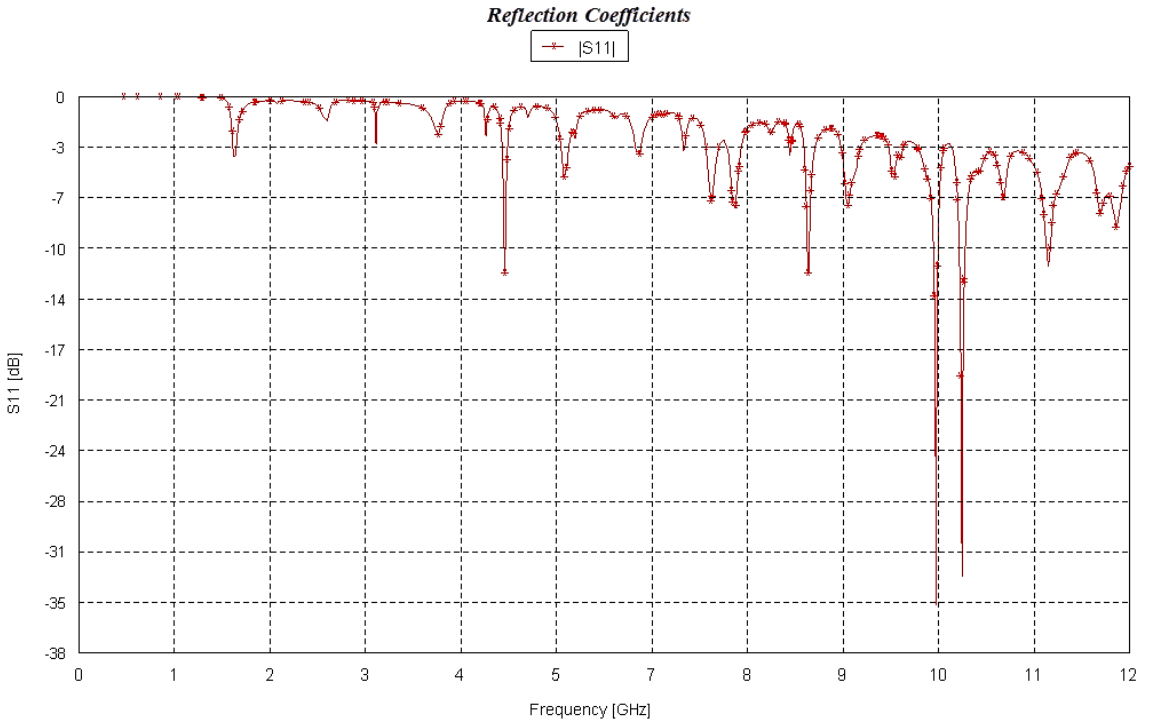

Figure 3-34: 1st iteration KSF antenna reflection coefficients (FEKO)

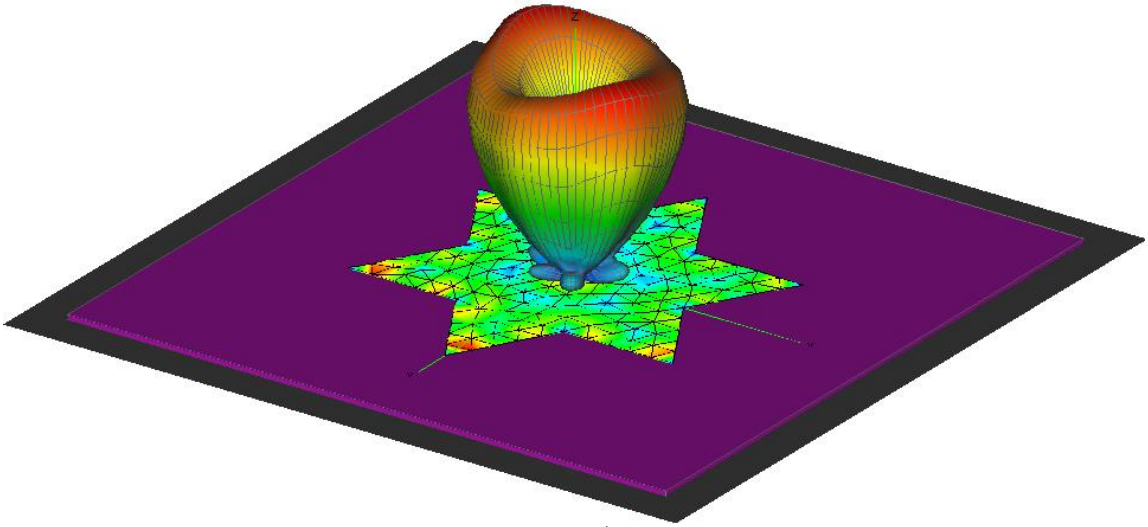

Figure 3-35: 3-D Radiation pattern of 1st iteration KSF antenna (FEKO)

Table 3.7 summarizes the antenna reflection coefficients, bandwidth, gain and resonant frequencies as shown below:

Table 3-7: 1st iteration KSF antenna performance

Band no.	Center freq. (GHz)	Ref. coeff. (dB)	Upper freq. (GHz)	Lower freq. (GHz)	Bandwidth (MHz)	Radiation Pattern (dB)	
						Gain	Attenuation
1	4.87	-12.26	4.87	4.85	16	7.063	--------
2	8.31	-12.34	8.34	8.31	25	4.298	--------
3	9.79	-34.96	9.81	9.76	55	-------	-1.561
4	10.09	-32.93	10.12	10.05	71	4.655	--------
5	11.07	-11.79	11.09	11.04	51	-------	-1.124

From the table, it can be observe that antenna gain has been enhanced after applying KSF to the antenna edges. Higher KSF iterations will be discussed in the next sections.

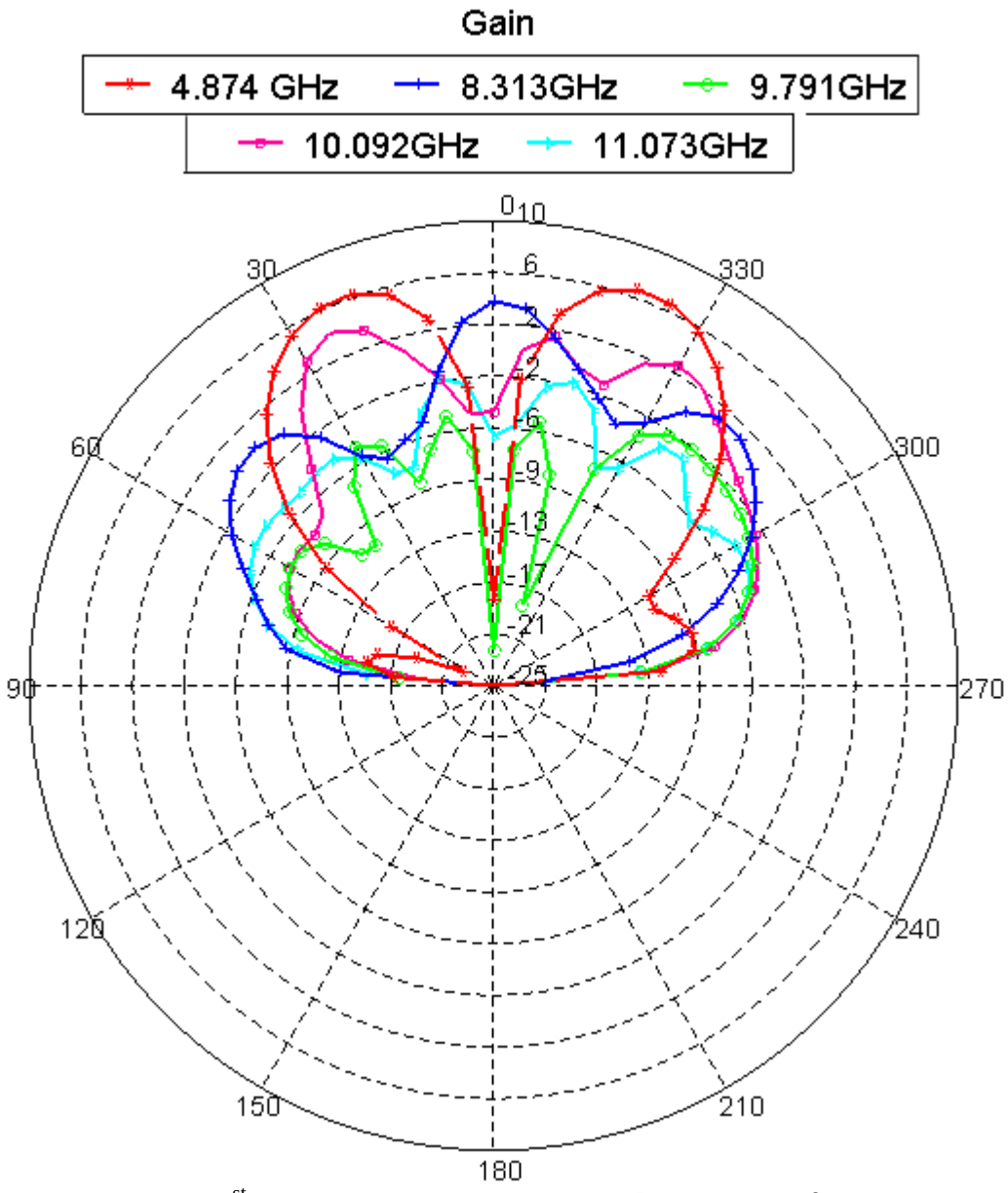

Figure 3-36: 1st Iteration KSF antenna gain at the resonance frequencies

3.2.2.3 2nd Iteration KSF Antenna

Second iteration KSF with same dielectric layer specifications is presented and simulated in this section; Figure 3.37 shows the antenna geometry.

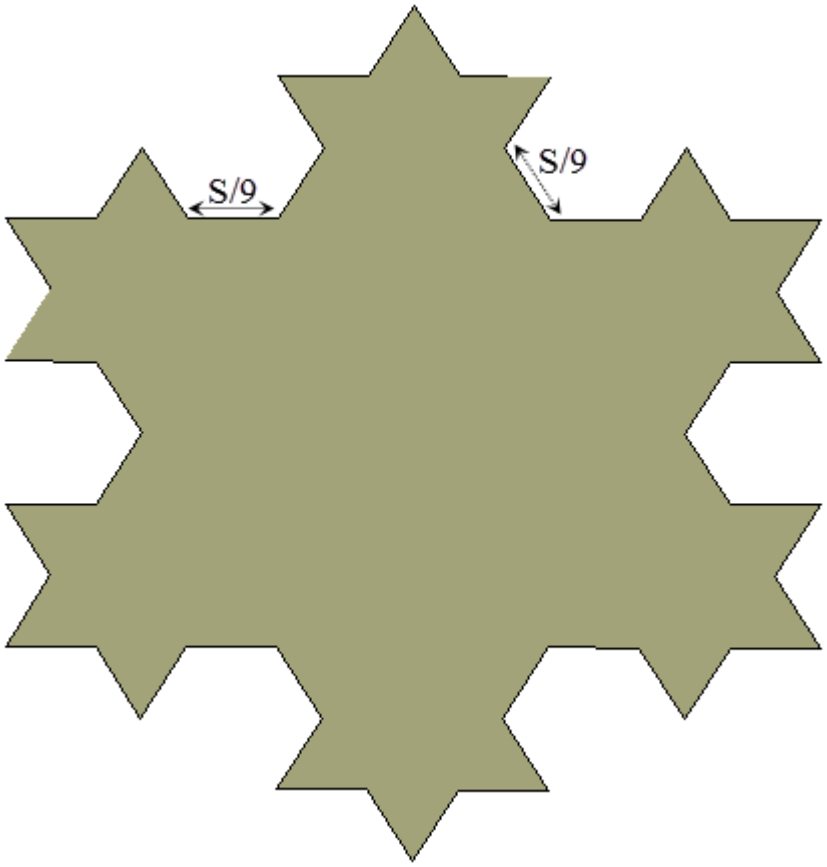

Figure 3-37: Pin feed 2nd iteration KSF antenna configuration simulated by FEKO

Five resonance frequencies are obtained by this antenna. Input impedance and reflection coefficients curves are demonstrated respectively in Figures 3.38 and 3.39.

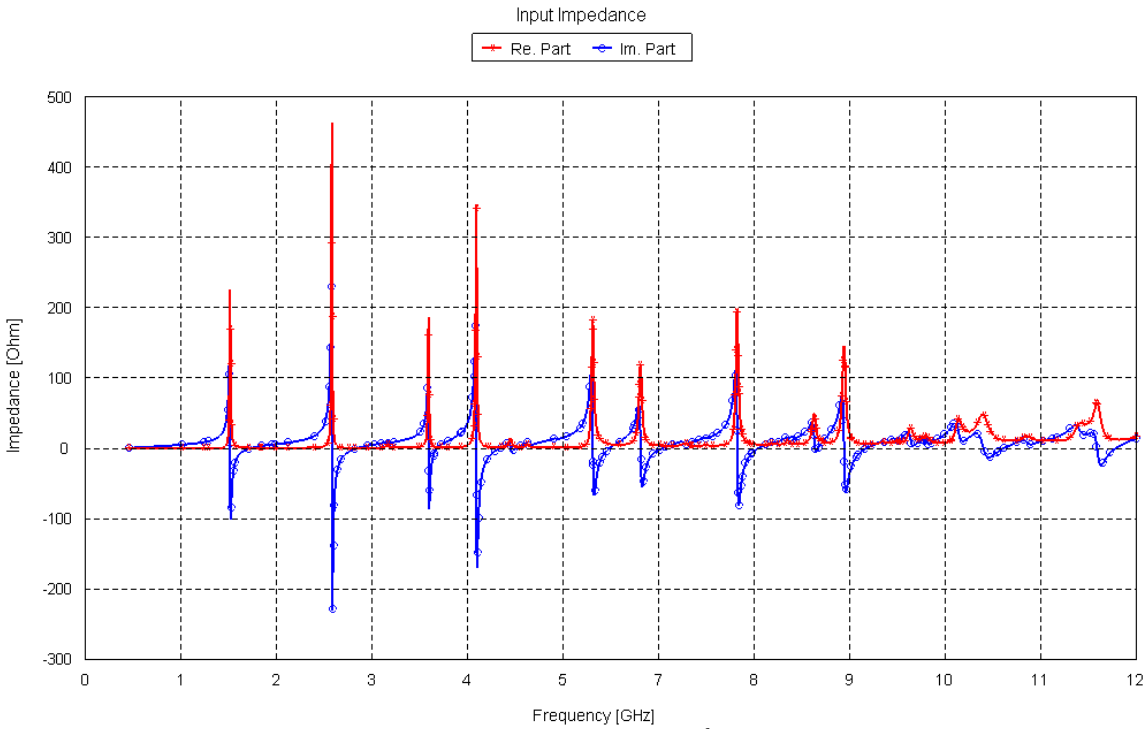

Figure 3-38: FEKO input impedance for the 2nd Iteration KSF antenna

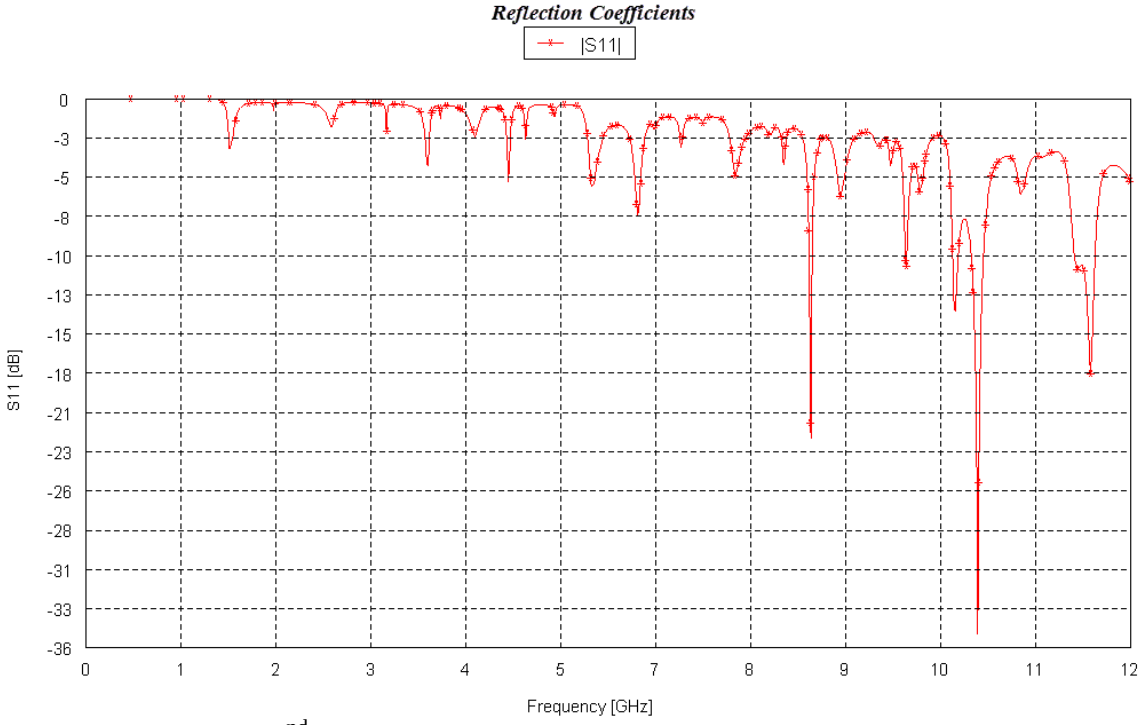

Figure 3-39: 2nd Iteration KSF antenna reflection coefficients (FEKO)

Antenna radiation pattern at 9.425 GHz operating frequency has been calculated by FEKO and presented in Figure 3.40 below.

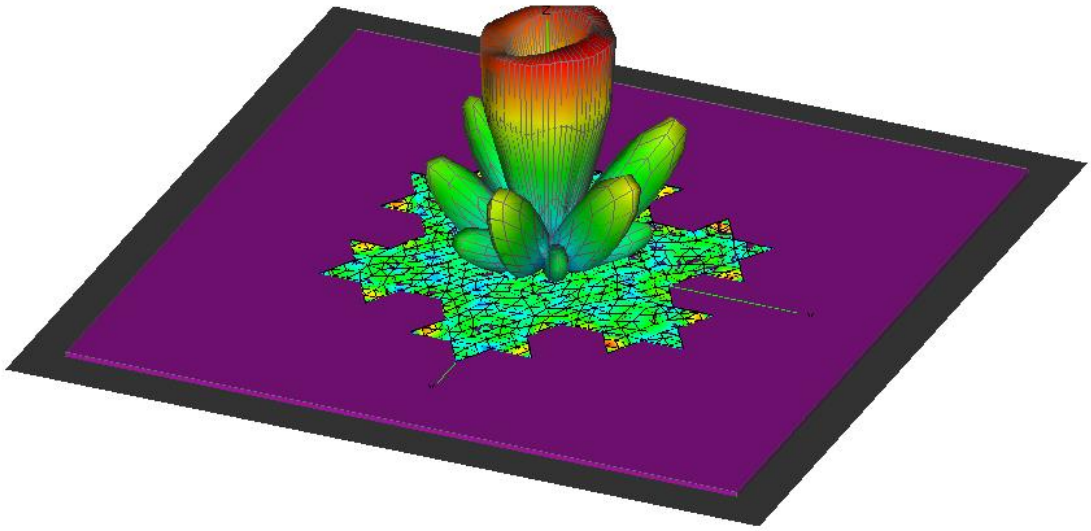

Figure 3-40: 3-D Radiation pattern of 2nd iteration KSF antenna

A frequency response with high gain was obtained by this antenna as demonstrated in Table 3.8.

Table 3-8: 2nd iteration KSF antenna performance

Band no.	Center freq. (GHz)	Ref. coeff. (dB)	Upper freq. (GHz)	Lower freq. (GHz)	Bandwidth (MHz)	Radiation Pattern (dB)	
						Gain	Attenuation
1	8.33	-25.55	8.34	8.31	36	7.45	--------
2	9.43	-11.27	9.44	9.42	19	6.027	--------
3	9.98	-14.35	10.02	9.96	66	3.84	--------
4	10.25	-31.34	10.31	10.17	142	8.77	--------
5	11.55	-18.41	11.59	11.35	248	3.526	---------

2-D antenna gain graph is drawn in Figure 3.41 below.

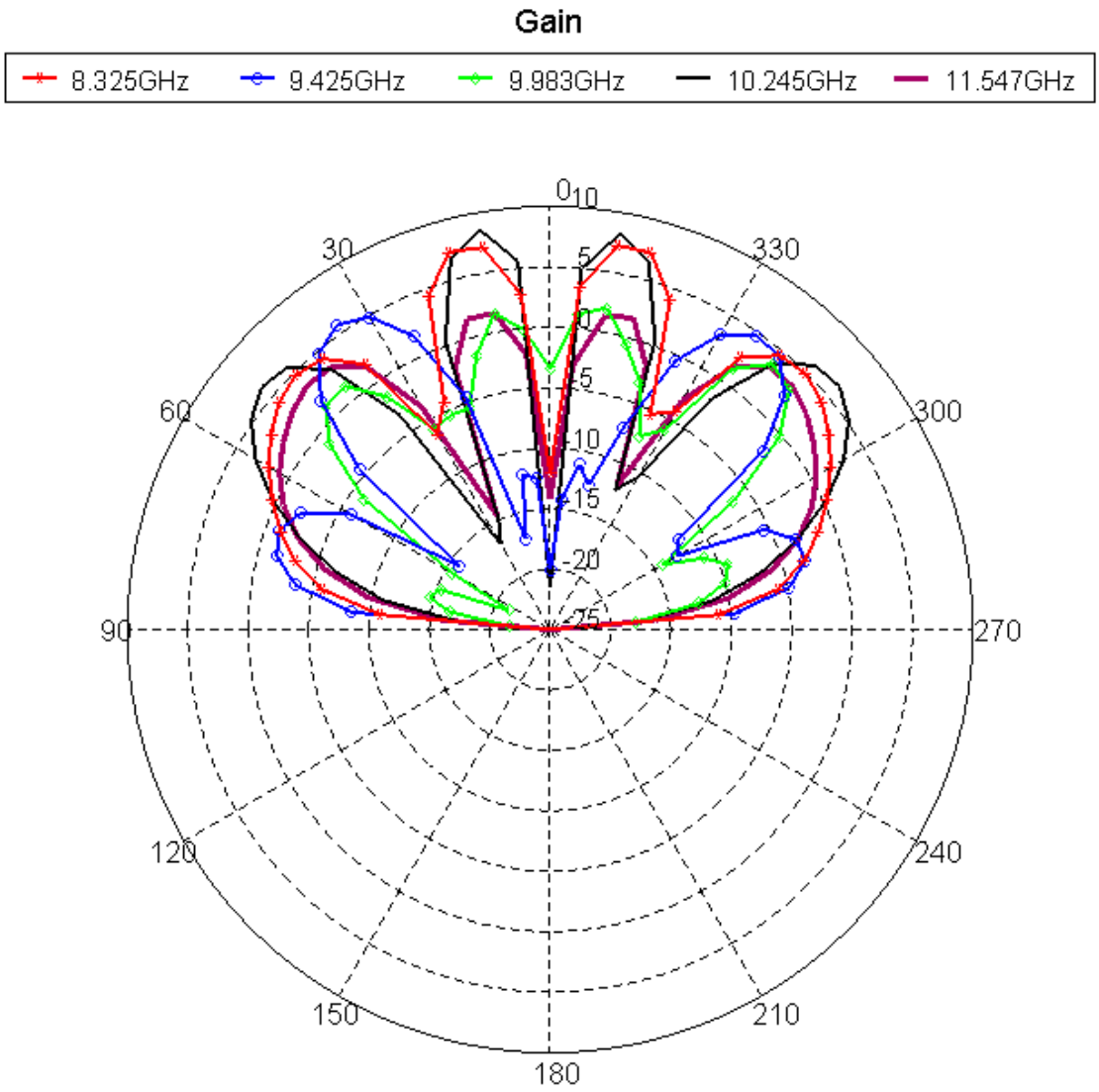

Figure 3-41: 2nd iteration KSF antenna gain

3.2.2.4 3rd Iteration KSF Antenna

3rd iteration Hoch snowflake is discussed in this section; Figure 3.42 shows the geometry of this antenna.

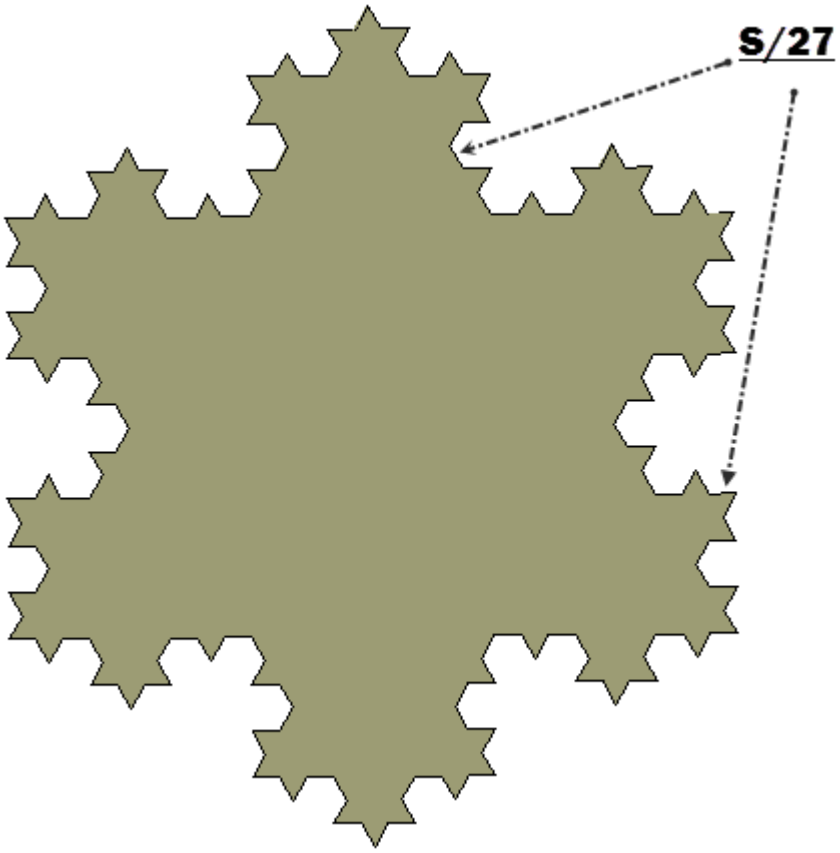

Figure 3-42: 3rd iteration KSF antenna layout with pin feed

All the segment lengths are equal to S/27. The simulation process has been carried out for this step too. The real and imaginary parts of the input impedance are described in Figure 3.43. Reflection coefficients calculations are shown in Figure 3.44, where 8 resonance frequencies are suitable for the antenna operations.

Antenna radiation pattern at 8.156 GHz resonance frequency and gain are demonstrated in Figures 3.45 and 3.46 respectively calculated by FEKO.

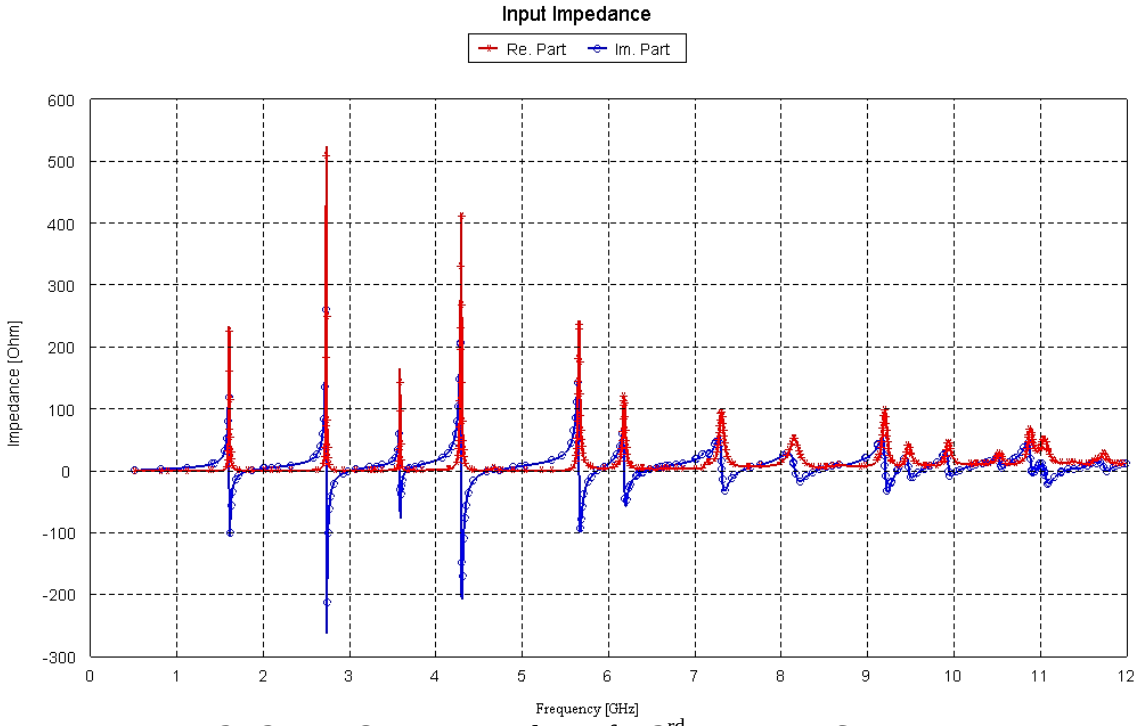

Figure 3-43: FEKO input impedance for 3rd Iteration KSF antenna

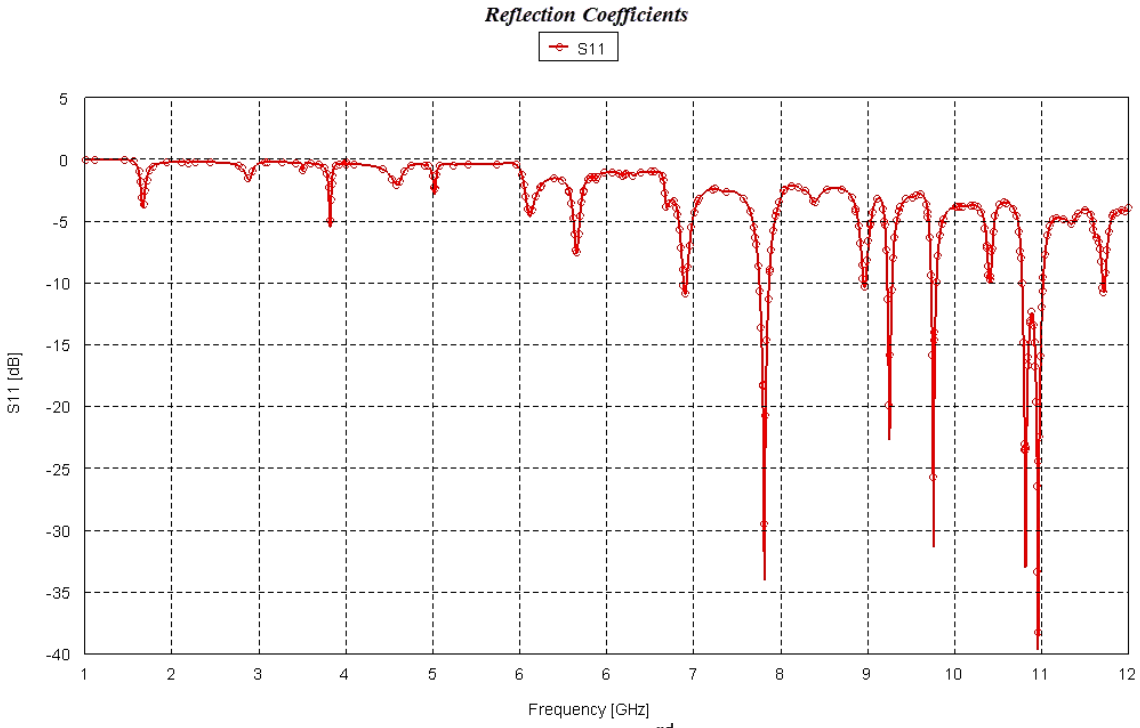

Figure 3-44: Reflection coefficients of 3rd iteration KSF antenna

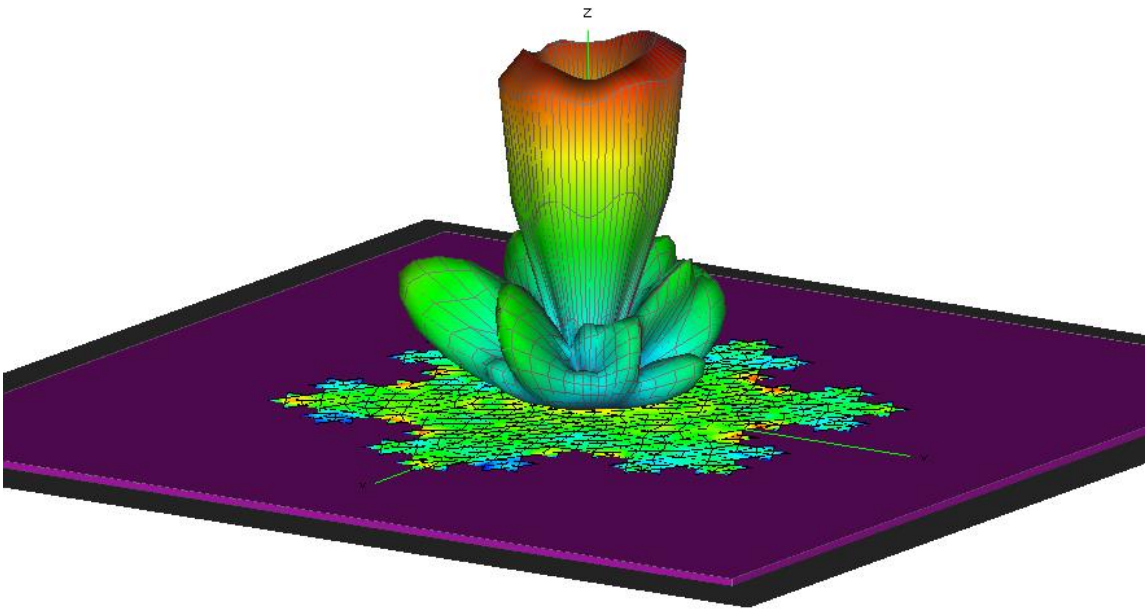

Figure 3-45: 3-D Radiation pattern of 3rd iteration KSF antenna

Table 3.9 summarizes the performance of the antenna over the range of frequencies 1-12 GHz.

Table 3-9: 3rd iteration KSF antenna performance

Band no.	Center freq. (GHz)	Ref. coeff. (dB)	Upper freq. (GHz)	Lower freq. (GHz)	Bandwidth (MHz)	Radiation Pattern (dB)	
						Gain	Attenuation
1	7.32	-11.02	7.342	7.303	41	4.88	--------
2	8.16	-33.84	8.214	8.103	111	11.005	--------
3	9.22	-10.55	9.232	9.196	36	8.543	--------
4	9.48	-22.85	9.508	9.451	57	6.002	--------
5	9.94	-31.44	9.976	9.912	64	1.033	--------
6	10.54	-10.28	-------	------	-------	7.31	--------
7	11.04	-39.94	11.106	10.870	235	2.92	--------
8	11.74	-11.02	11.757	11.713	44	4.033	--------

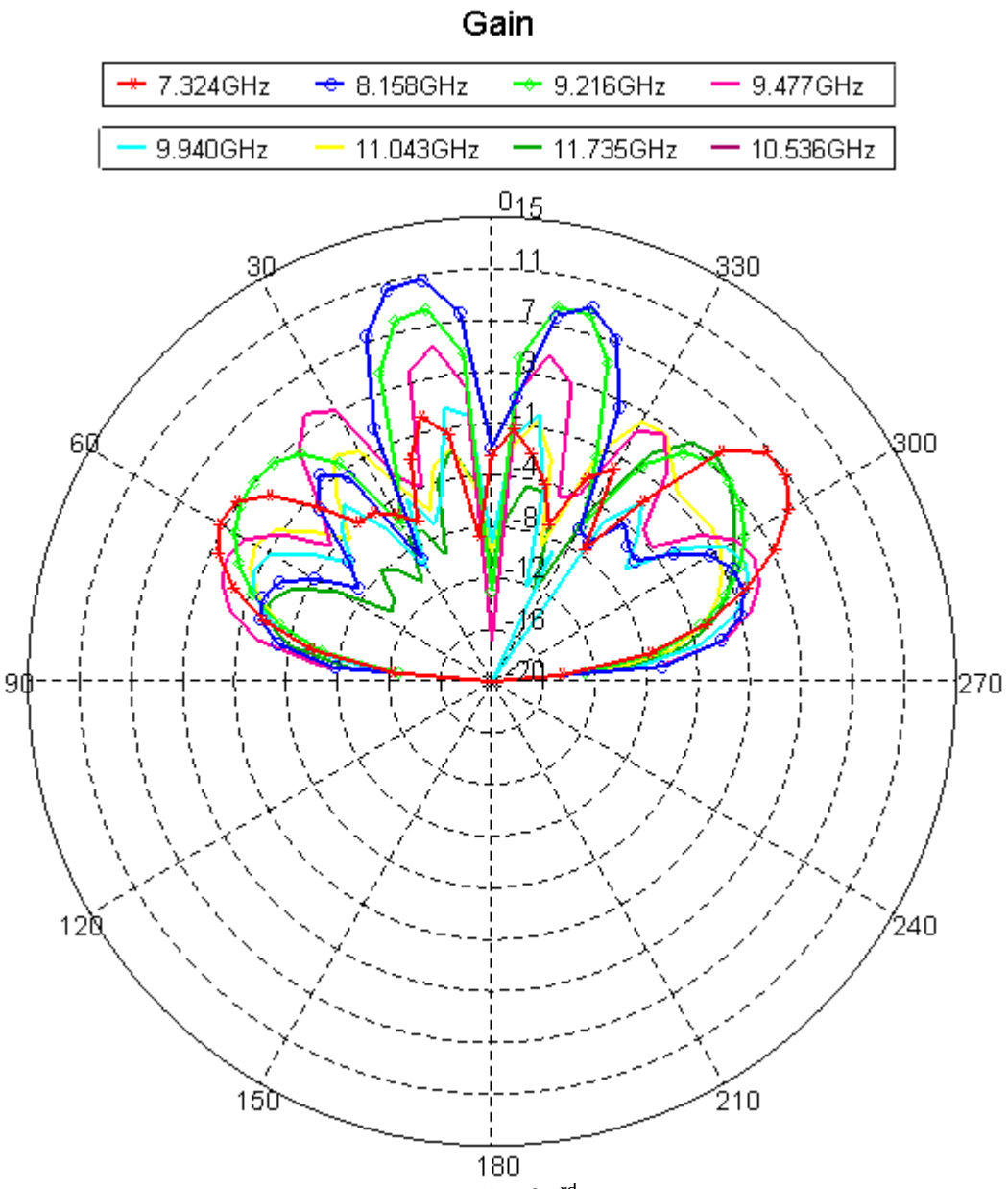

Figure 3-46: 2-D Gain graph of 3rd iteration KSF antenna

The combination of KSF and SGF geometries will be presented in the next section to maximize the antenna gain with multiband response.

3.2.2.5 3rd Iteration KSF with 4th Iteration SGF Shape Slots Antenna (KS-SGF)

The proposed antenna geometry is demonstrated in Figure 3.47 below, the 3rd iteration KSF with SGF shape slots are introduced to improve the gain of the last antenna.

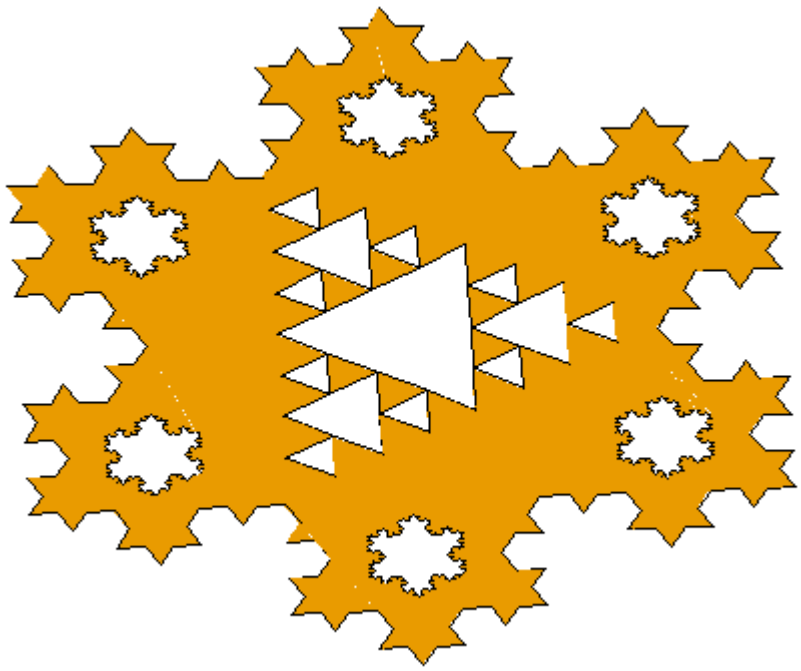

Figure 3-47: KS-SGF antenna configuration with pin feed

This antenna is also implanted on FR4 substrate of 1.59 mm thickness and fed by coaxial cable. FEKO simulation shows that the antenna has multiband behavior with high dB level of gain.

Input impedance and reflection coefficients are shown in Figure 3.48 and 3.49 respectively which has been calculated by FEKO. Table 3.10 summarizes the antenna performance over the frequency range 1-11GHz. 3-D radiation pattern for the antenna was also calculated and presented in Figure 3.50 below.

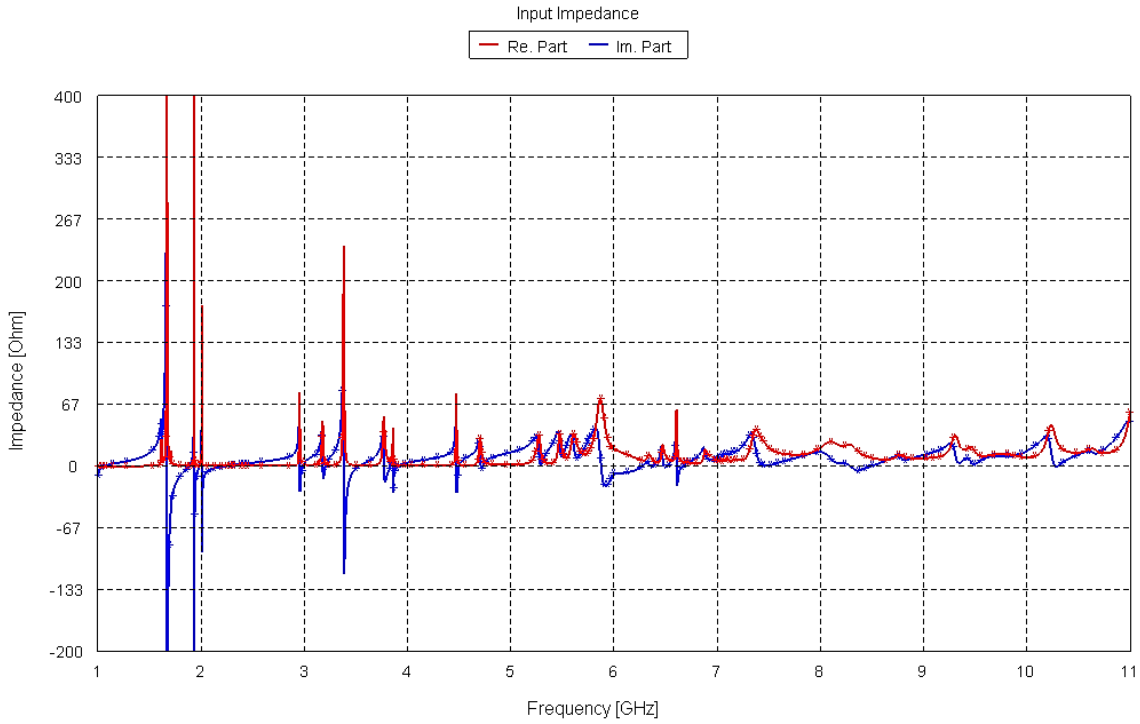

Figure 3-48: KS-SGF antenna input impedance

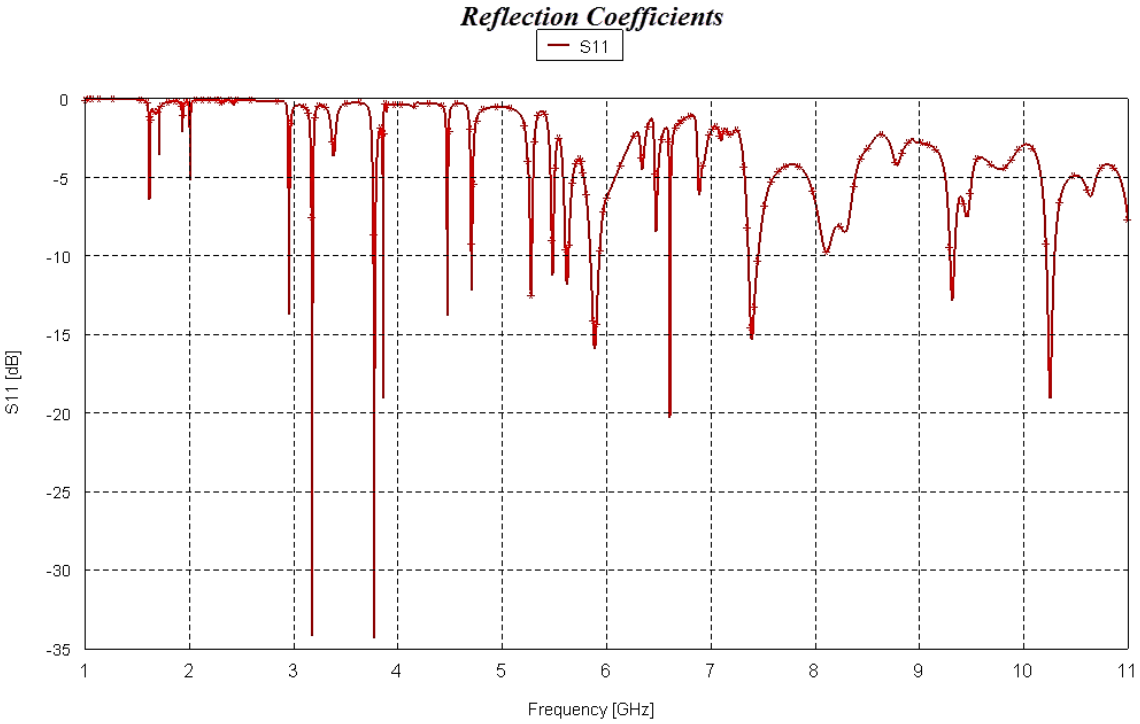

Figure 3-49: KS-SGF antenna reflection coefficients

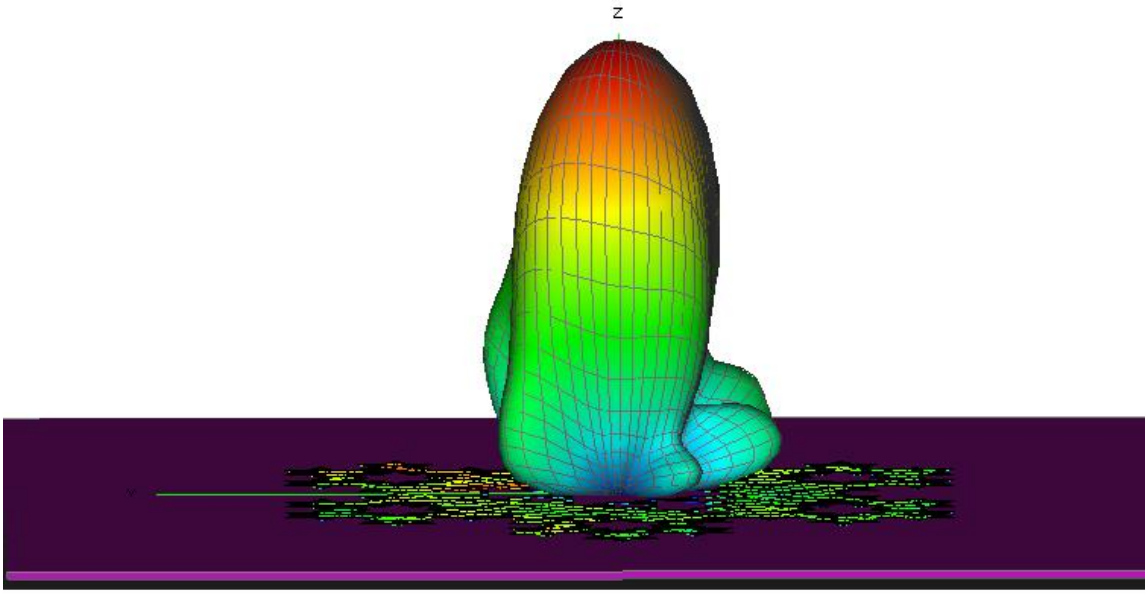

Figure 3-50: KS-SGF antenna 3-D radiation pattern

Table 3-10: KS-SGF antenna performance

Band no.	Center freq. (GHz)	Ref. coeff. (dB)	Upper freq. (GHz)	Lower freq. (GHz)	Bandwidth (MHz)	Radiation Pattern (dB)	
						Gain	Attenuation
1	2.96	-13.94	2.96	2.95	15.0	1.77	---------
2	3.18	-34.36	3.18	3.17	19.3	7.02	---------
3	3.77	-34.49	3.79	3.76	27.9	3.89	---------
4	3.86	-19.26	3.86	3.85	5.3	10.32	--------
5	4.47	-13.87	4.48	4.47	10.76	4.27	---------
6	4.71	-12.41	4.72	4.69	12.91	8.52	--------
7	5.28	-12.89	5.29	5.27	19.37	-------	-0.298
8	5.48	-11.43	5.49	5.47	16.14	9.71	---------
9	5.62	-11.99	5.64	5.60	33.3	8.06	--------
10	5.88	-16.11	5.93	5.84	92.5	2.73	--------
11	6.61	-20.46	6.61	6.60	12.9	-------	-3.79
12	7.39	-15.48	7.46	7.36	99.0	5.95	--------
13	8.11	-10.14	------	-------	-------	4.97	--------
14	9.31	-12.96	9.34	9.29	47.67	7.60	--------
15	10.25	-19.24	10.29	10.21	88.84	5.64	--------

The antenna gain is presented in Figures 3.51, 3.52, and 3.53.

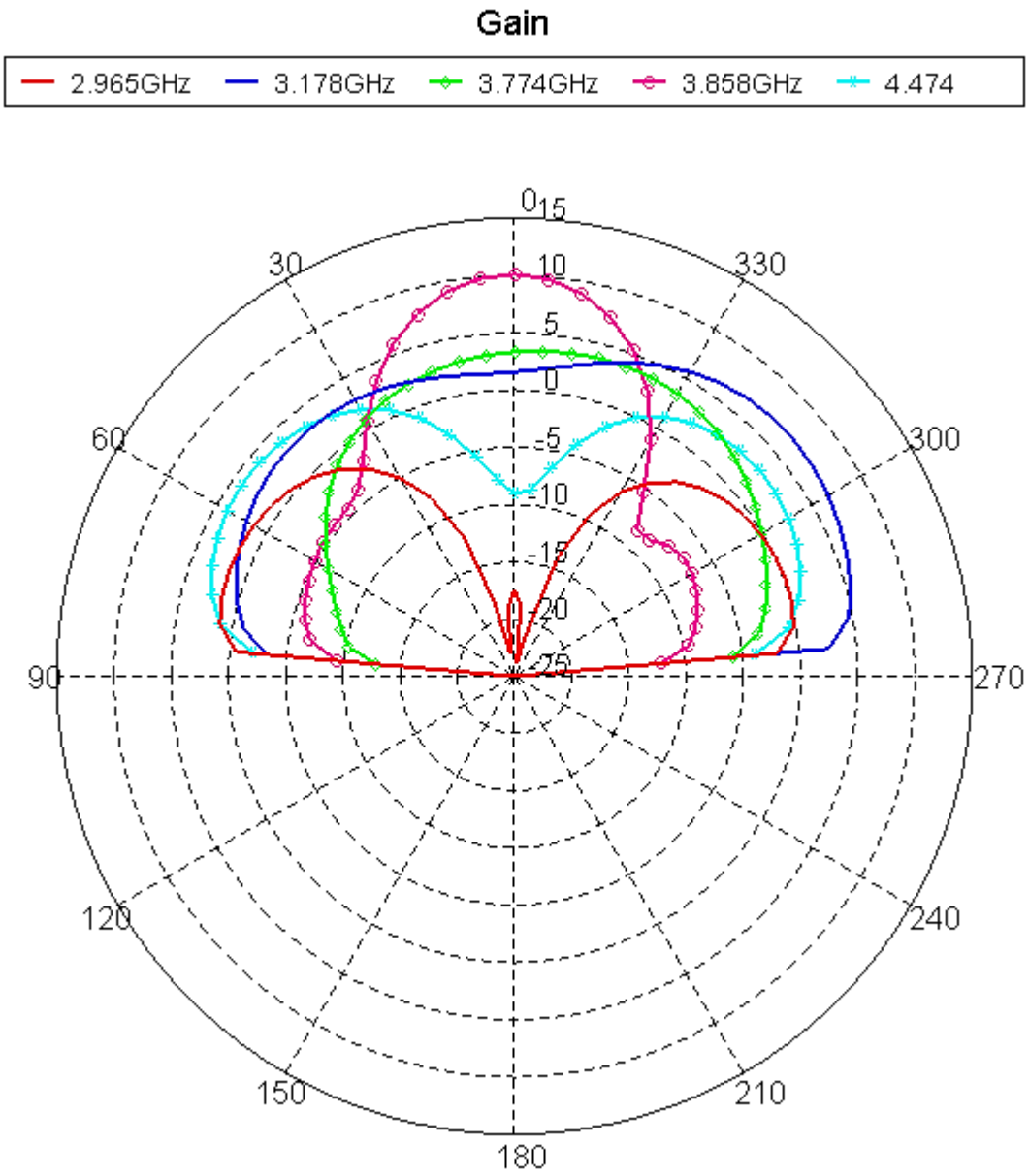

Figure 3-51: KS-SGF antenna gain for the resonance frequencies 2.96-4.474 GHz

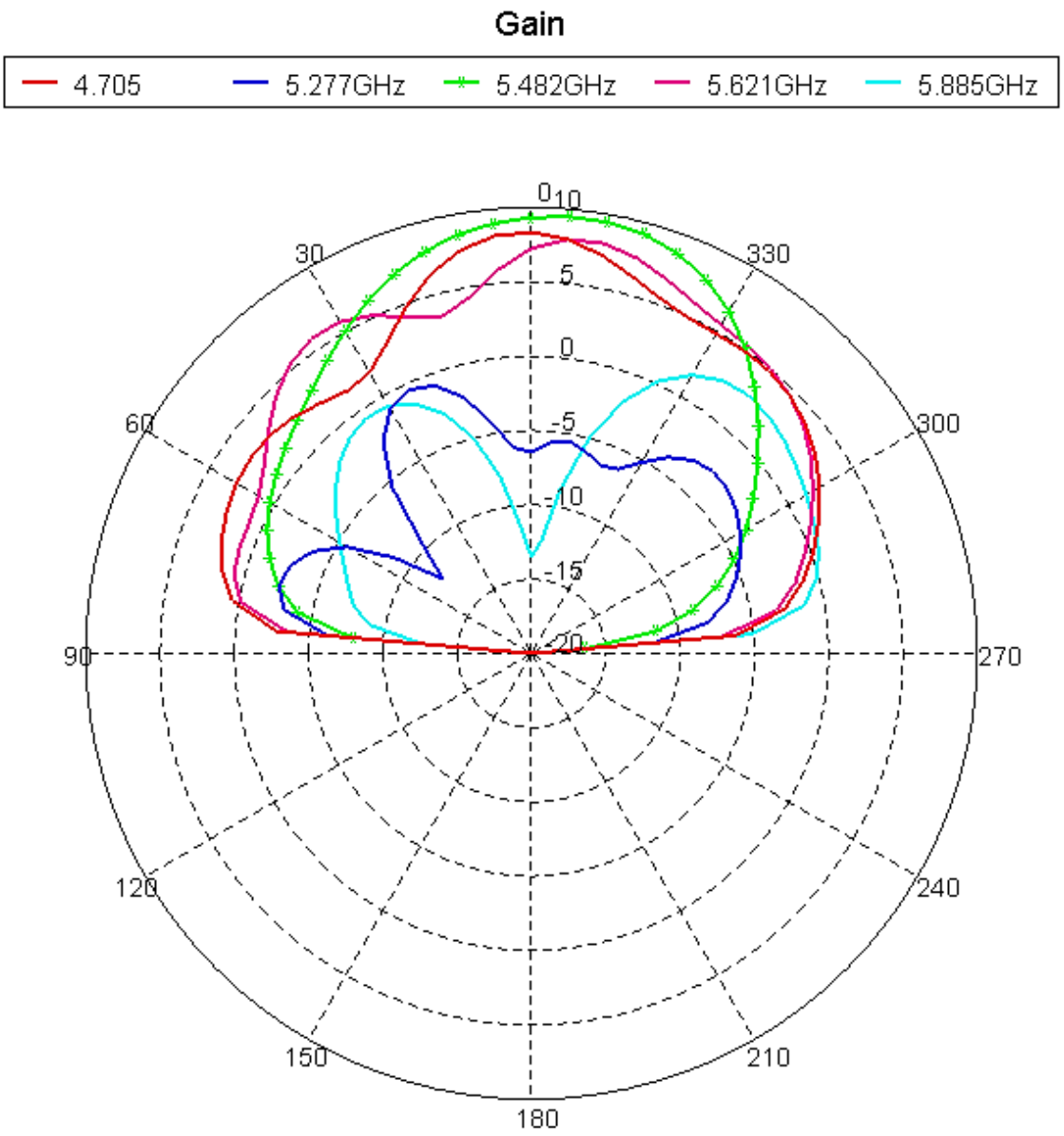

Figure 3-52: KS-SGF antenna gain for the resonance frequencies 4.705-5.885 GHz

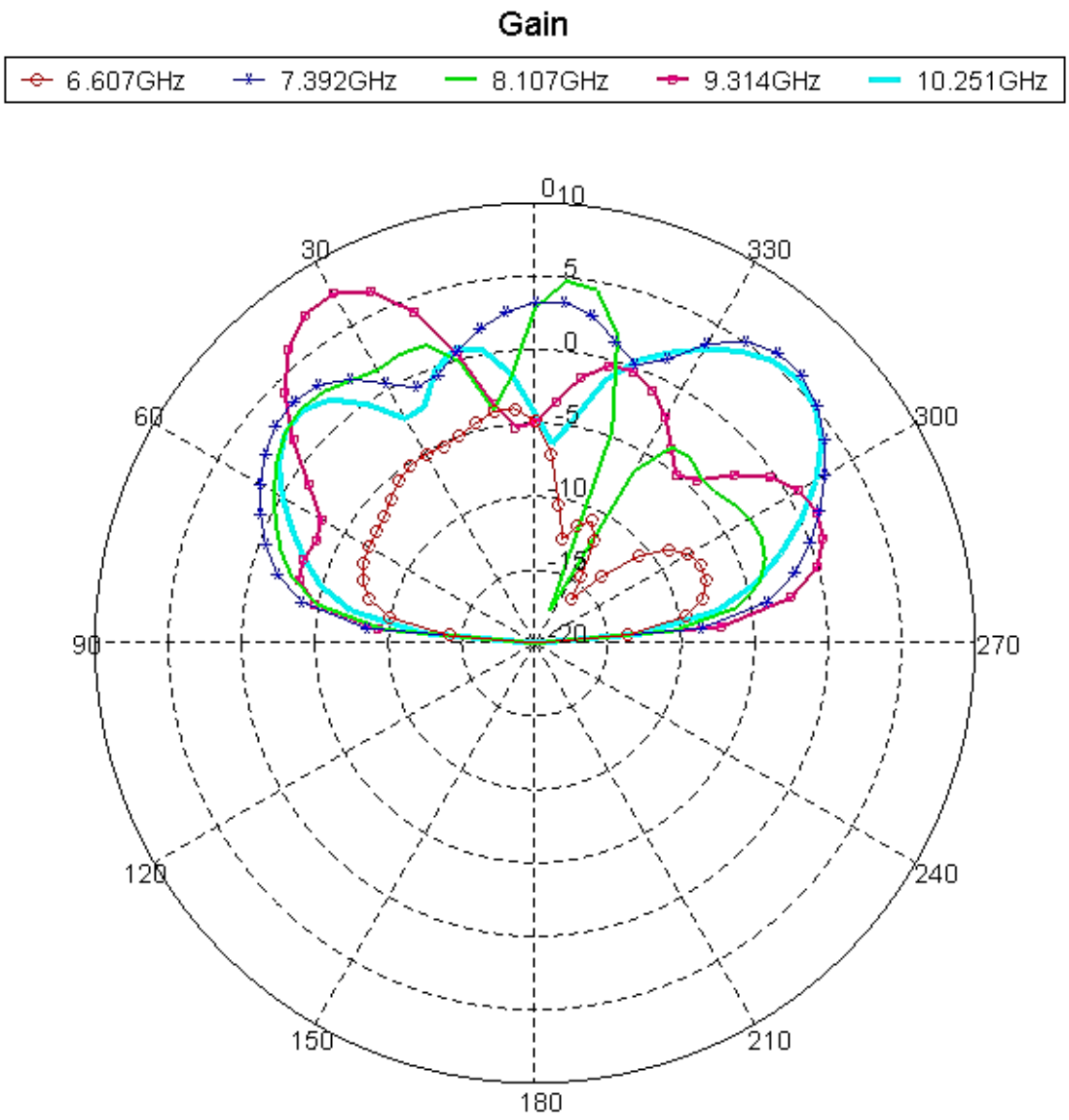

Figure 3-53: KS-SGF antenna gain for the resonance frequencies 6.607-10.251 GHz

The stacking of SC-MKF antenna obtained in section 3.2.1.5 and KS-SGF antenna obtained in section 3.2.2.5 is presented in the next section.

3.2.3 Multilayer Stacked Antenna

The proposed antenna is demonstrated in Figure 3.54. It consist of two layers, the top layer is the KS-SGF antenna, placed on FR4 substrate of 1.59 mm thickness, 4 mm air layer is placed under the substrate layer, then layer 1 which is SC-MKF antenna is attached under the air and above second 1.59 mm FR4 substrate layer. This antenna has been fed by proximity coupled method using 50 Ω MSL that placed under the substrate of the bottom layer.

The air layer has been added in the middle of the antenna in order to reduce the surface waves, where the surface waves are non-radiating energy.

Input impedance of the proposed antenna is shown in Figure 3.55, reflection coefficients are also calculated and displayed in Figure 3.56; from these results the proposed antenna has 11 resonance frequencies (center frequency) with wide bandwidth.

Figure 3.57 shows the 3-D radiation pattern at 2.317 GHz operating frequency, 2-D polar graph for the gain is demonstrated in Figures 3.58 and 3.59 for all resonance frequencies.

Table 3.11 summarizes the stack antenna performance, where gain, bandwidth, resonance frequencies, and reflection coefficients are all listed.

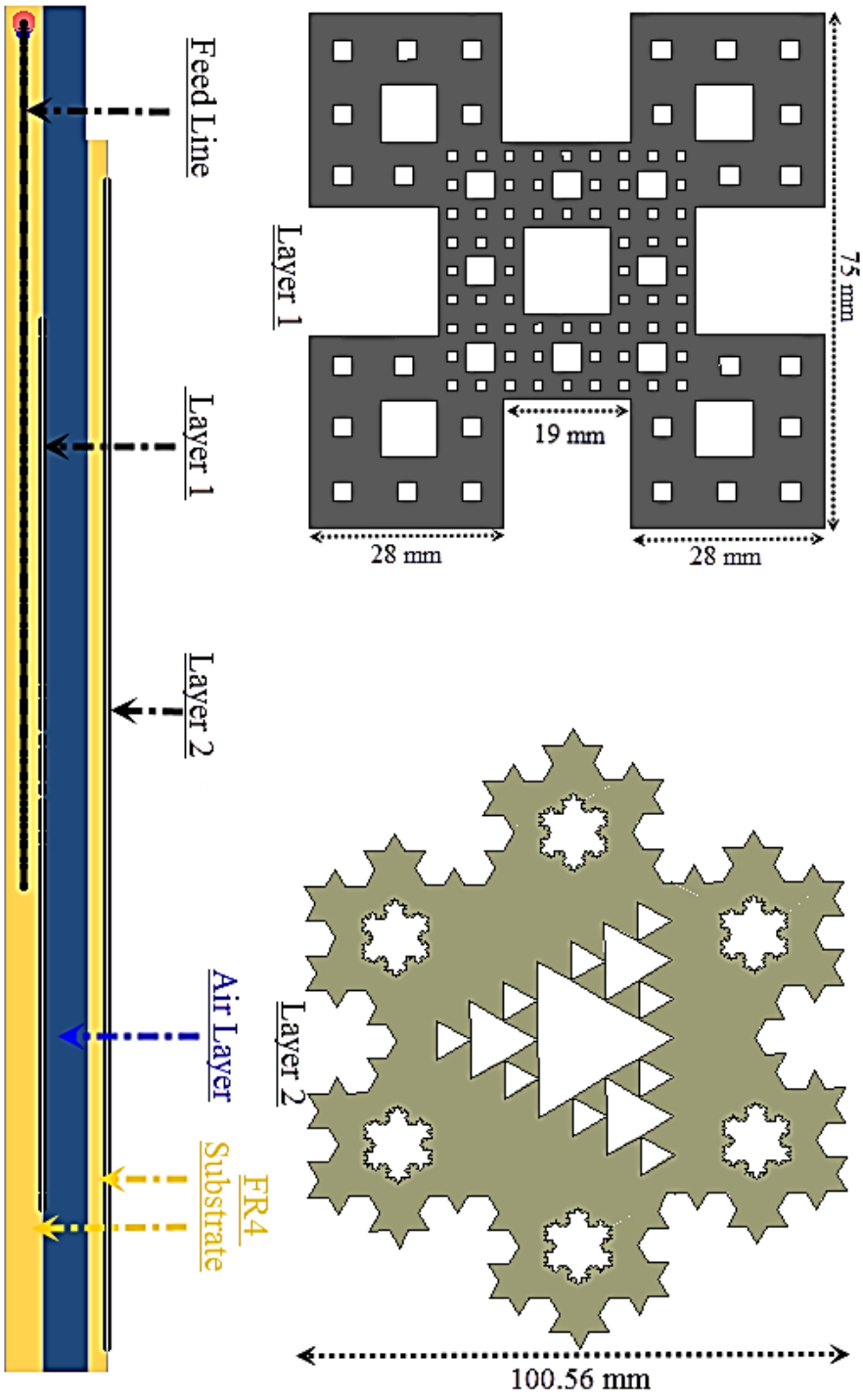

Figure 3-54: Multilayer fractal antenna configuration

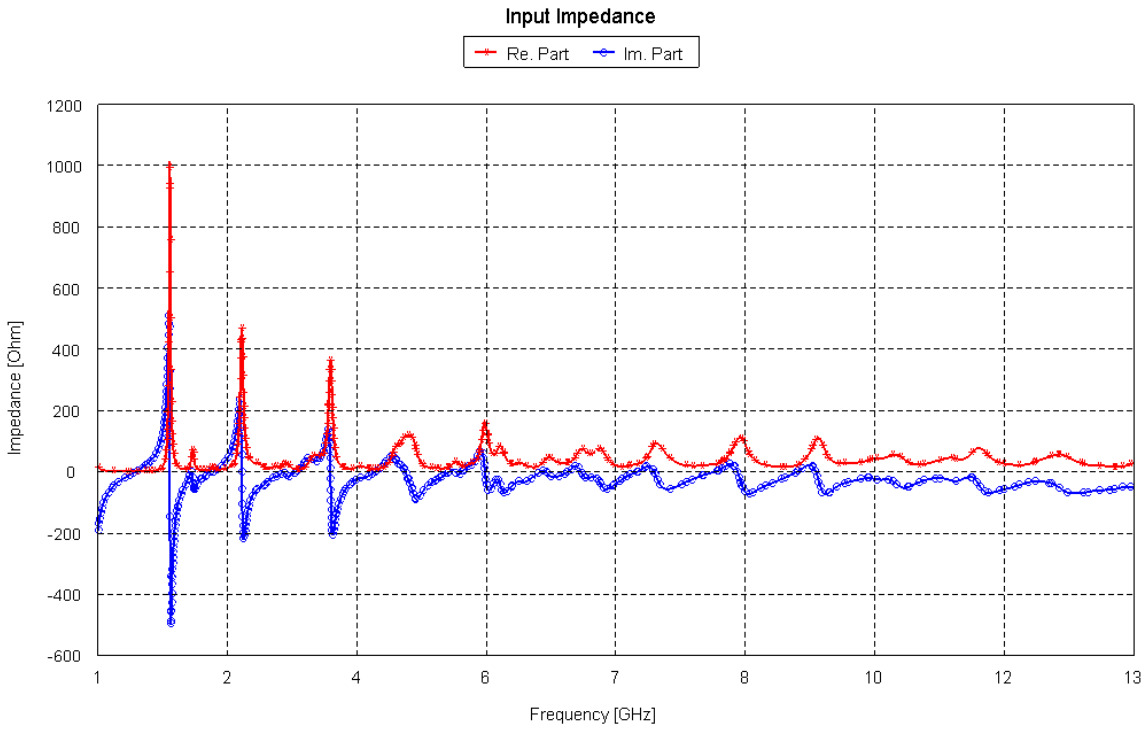

Figure 3-55: FEKO input impedance calculation for the multilayer fractal antenna

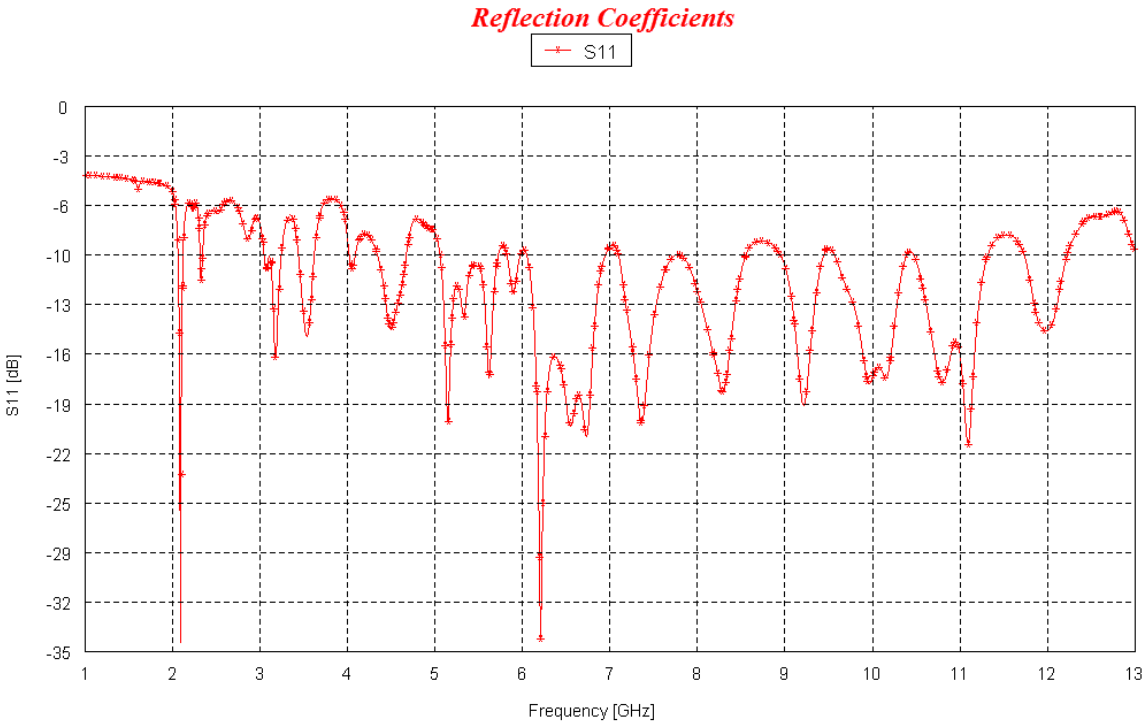

Figure 3-56: Multilayer fractal antenna reflection coefficients simulated by FEKO

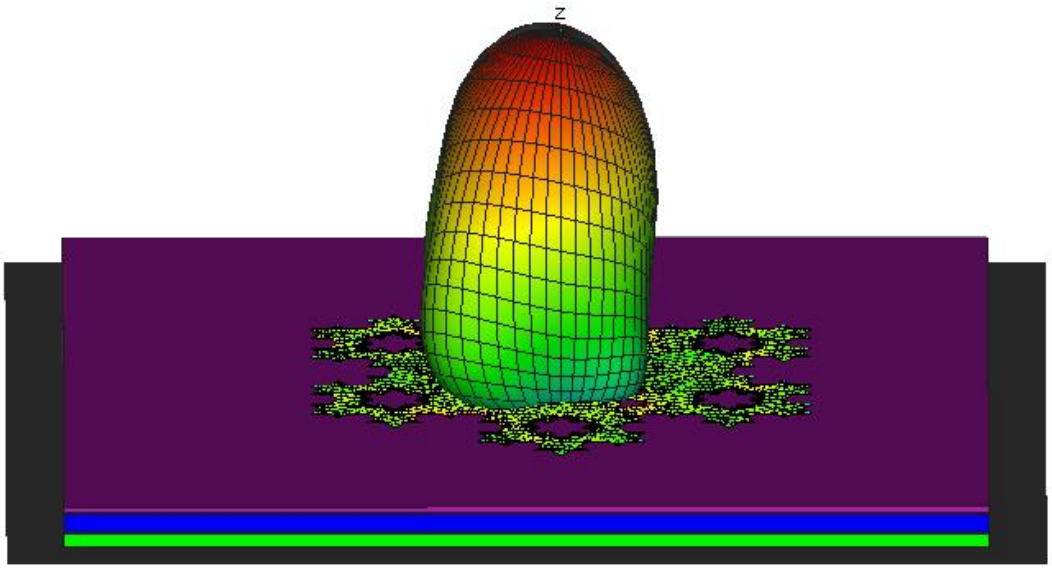

Figure 3-57: 3-D radiation pattern of the multilayer antenna

Table 3-11: Multilayer fractal antenna performance

Band no.	Center freq. (GHz)	Ref. coeff. (dB)	Upper freq. (GHz)	Lower freq. (GHz)	Band-width (MHz)	Radiation Pattern (dB)	
						Gain	Attenuation
1	2.081	-34.60	2.11	2.05	61.78	-------	-4.0896
2	2.31	-11.32	2.34	2.30	36.853	4.37	-------
3	3.16	-16.41	3.24	3.03	204.86	4.36	-------
4	4.04	-10.74	4.09	4.01	82.378	4.78	-------
5	4.49	-14.38	4.67	4.32	349.02	4.04	-------
6	5.14	-20.56	5.71	5.04	673.11	6.09	-------
7	6.203	-34.52	6.95	5.81	1142.9	5.51	-------
8	7.35	-20.71	8.56	7.09	1481.6	4.67	-------
9	9.22	-19.40	9.45	8.94	507.99	5.22	-------
10	11.09	-21.87	11.32	9.55	1770.1	3.13	-------
11	11.98	-14.60	12.25	11.72	530.25	4.63	-------

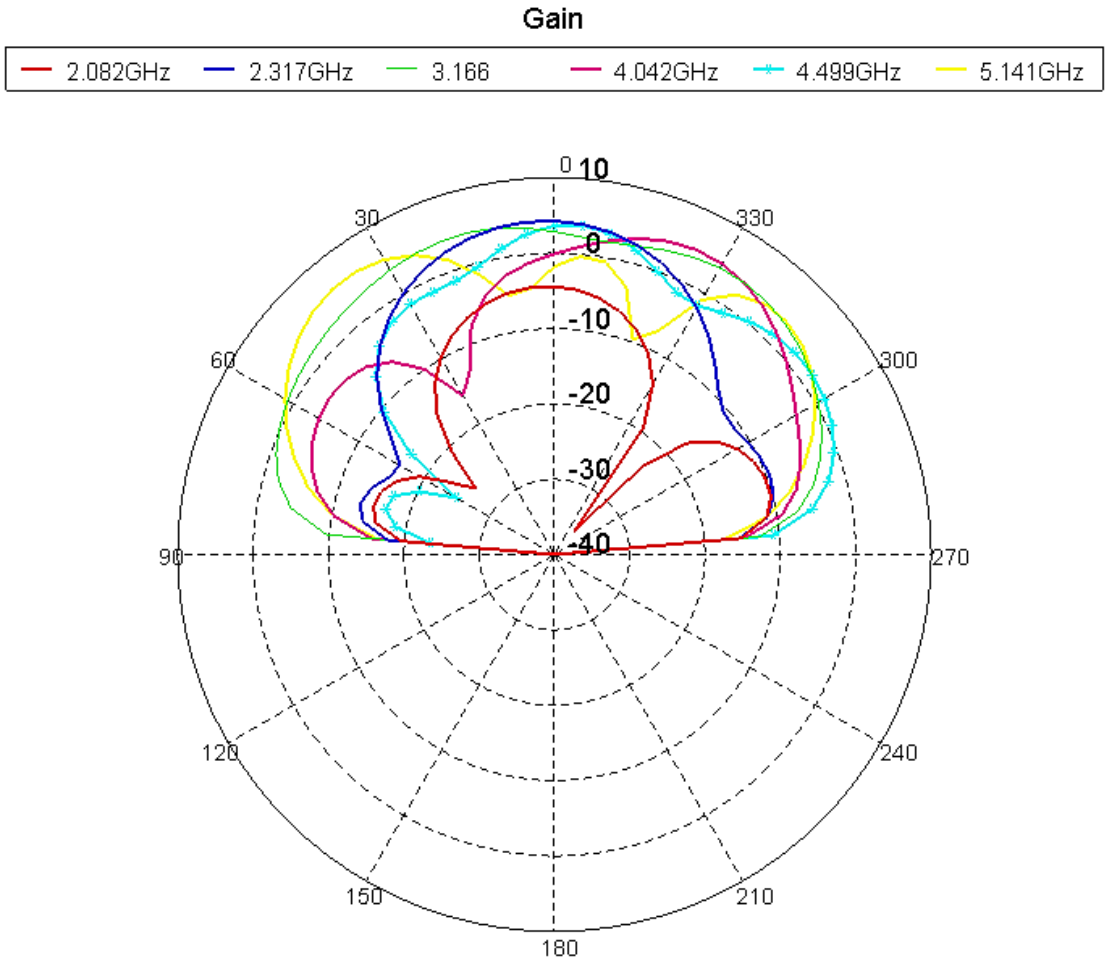

Figure 3-58: Multilayer antenna gain for the frequencies 2.08-5.141 GHz

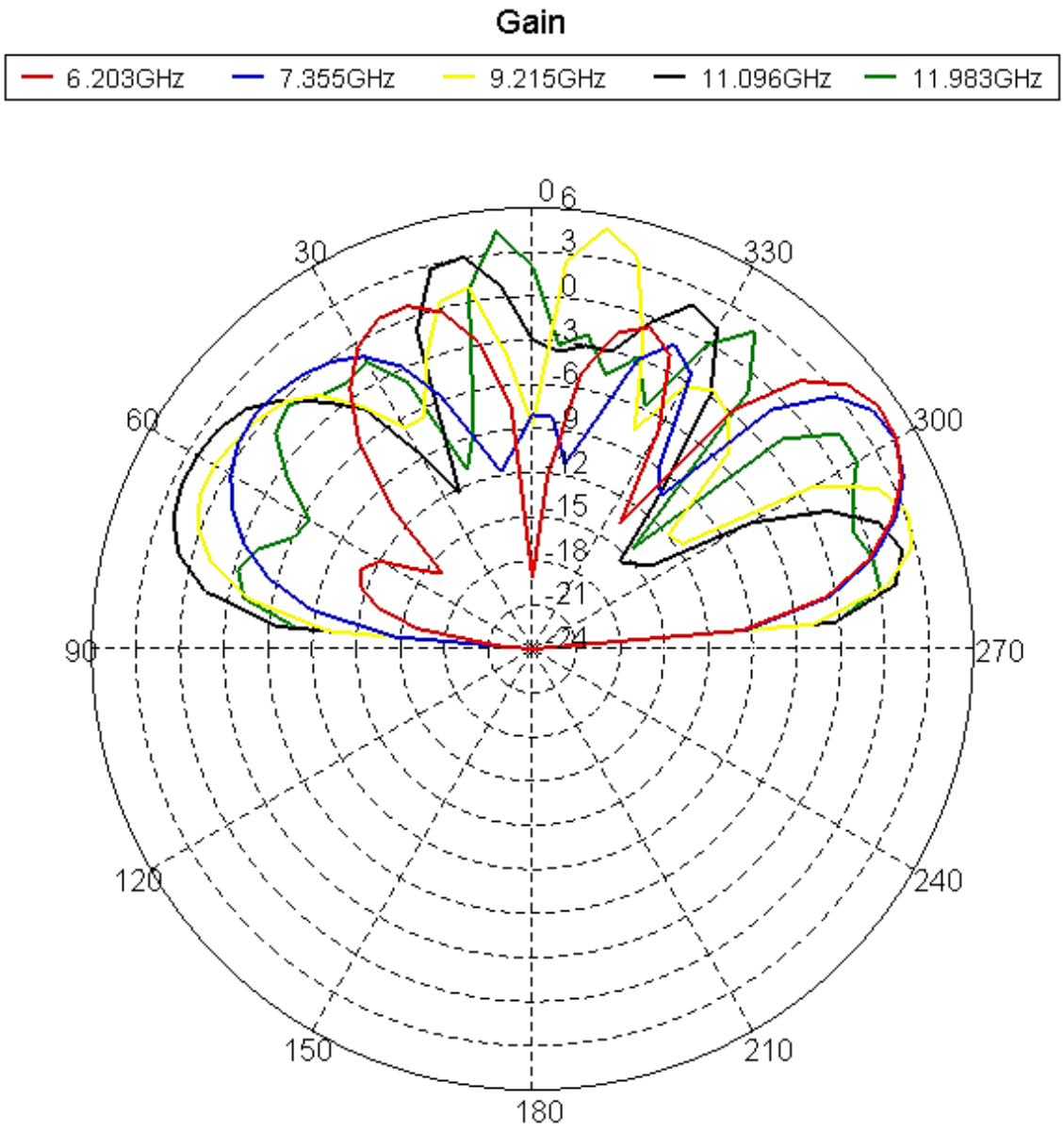

Figure 3-59: Multilayer antenna gain for the frequencies 6.203-11.983 GHz

From these results we can conclude that the proposed multilayer antenna has multiband behavior with high gain and wide bandwidth.

The proposed antenna can operate on the listed applications shown in Table 3.12, according to the Federal Communications Commission and Electronic Communications Committee for the frequency allocation bands [27] [28].

Table 3-12: Suitable applications for the proposed antenna

Band no.	Center freq. (GHz)	Applications
1	2.317090	Land mobile. Aeronautical telemetry. Tactical radio relays. Amateur.
2	3.166425	Active sensors. Defense systems. Radio location (civilian).
3	4.041774	FSS earth station.
4	4.493769	Passive sensors. Fixed satellite. Defense systems.
5	5.140703	Microwave landing systems. Radio determination applications. Aeronautical telemetry. Feeder links. Radio LANs. Broadband disaster relief. Active sensors. Defense systems. Maritime radar. Weather radar.
6	6.203384	FSS earth station. Passive filters. UWB applications. Radio astronomy. Feeder links. Radio determination applications.
7	7.354520	Passive sensors. UWB applications. Radio determination applications. Mobile satellite service earth station. Defense systems. Weather satellite. Earth exploration satellite. Land mobile. Radio astronomy. Space research. Aeronautical navigation. Radio location (civilian).
8	9.214898	Aeronautical navigation. Radio location (civilian). Defense systems. Radio determination applications. UWB applications. Weather radar.
9	11.096067	Active sensors. Aeronautical navigation.

		Radio location (civilian). Defense systems. Radio determination applications. Tactical radio relays. Broadband wireless access. Passive sensors. Radio astronomy. High EIRP satellite terminals. Low EIRP satellite terminals. Fixed satellite service earth station.
10	11.983124	Broadcasting satellite receivers. High EIRP satellite terminals. Low EIRP satellite terminals.

Chapter 4

CONCLUSION AND FUTURE WORK

4.1 Conclusion

A compact fractal antenna has been modeled and simulated in this thesis. The proposed antenna utilizes a novel geometrical combination of fractal shapes arranged in two layers. Multiband antenna behavior has been achieved through the capacitive and inductive loads introduced by the cavities on the patch surface and the added conducting plates to the patch edges. The selection of antenna operating frequency has been successfully achieved and shown in the FEKO simulation results; eleven different resonance frequencies with bandwidth of 1770 MHz and up to 6.09 dB gain are obtained. The proposed antenna is suitable for space research, defense systems, weather radars and many other applications according to the federal communications committee.

4.2 Suggested Future Work

Antenna bandwidth can be improved by using dielectric substrate layers with different dielectric constant such as Roger Duroid ($\mathcal{E}_r$ =2.2), Roger ultrom ($\mathcal{E}_r$ =2.5), Benzocylob uten ($\mathcal{E}_r$ =2.6), and Liquid crystal polymer ($\mathcal{E}_r$ =2.85).

Multi feeder can be employed here with matching network for better bandwidth.

REFERENCES

[1] G. A. Deschamps, "Third Symposium on the USAF Microstrip Microwave Antennas Research and Development Program," *University of Illinois*, pp. 18-22, Oct. 1953.

[2] R. E. MUNSON, "Conformal Microstrip Antennas and Microstrip Phased Arrays," *IEEE Transactions on Antennas and Propagation*, vol. 22, no. 1, pp. 74-78, Jan. 1974.

[3] B. B. Mandelbrot, The Fractal Geometry of Nature, New York: Library of Congress CaWogtllg in Publicatkin Data, 1983.

[4] A. Muscat, "The design of low gain wideband multiband antennas employing optimization techniques," PhD Thesis, Queen Mary University of London, Aug. 2011.

[5] M. Konca, and S. Uysal, "Multi-beam Patch Antenna Design," Master's thesis , Eastern Mediterranean University, Cyprus, May 2010.

[6] R. Mohanam and T. Shanmuganantham, "Sierpinski Carpet Fractal Antenna for Multiband Appllications," *Internotional Journal of Computer Applications*, vol. 39, pp. 19-23, Feb. 2012.

[7] W. Chen and G. M. Wang, "Small Size Edge-Fed Sierpinski Carpet Microstrip Patch Antenna," *Progress in Electromagnetics Researches,* vol. 3, pp. 195-202, 2008.

[8] S. Wang, B. L. Ooi, "Analysis and Bandwidth Enhancement of Sierpinski Carpet Antenna," *Microwave and Optical Technology Letters,* vol. 31, no. 1, pp. 13-18, Oct. 2001.

[9] V. Radonic, K. Plamer and Stojanovic, "Flexible sierpinski carpet fractal antenna on hilbert slot patterned," *International Journal of Antennas and Propagation,* pp. 1-7, 2012.

[10] R. Mishra, R. Ghatak and D. Poddar, "Design formula for sierpinski gaket pre-fractal planar monopole antennas," *IEEE Antennas and Propagation Magazine,* vol. 50, no. 3, pp. 104-107, 2008.

[11] Y. Kumer, S. Kumer and R. Jyoti, "Sectoral sierpinski gasket fractal antenna for wireless LAN applications," *International Journal of RF and Microwave Computer Aided Engineering,* vol. 22, no. 1, pp. 68-74, 2012.

[12] H. Oraizi and S. Hedayati, "Miniturzation of microstrip antennas by the novel application of the giuseppe peanno fractal geometries," *IEEE Transaction on Antennas and Propagation,* vol. 60, no. 8, pp. 3559-356, Aug. 2012.

[13] H. Oraizi and S. Hedayati, "Circular polarized microstrip antennas using the square and giuseppe peano fractals," *IEEE Transaction on Antennas and Propagation*, vol. 60, no. 8, pp. 3466-3567, Jul. 2012.

[14] L. Chen, Y. Chang and H. Xie, "Minkowski fractal patch antenna for size and radar cross section reduction," *IEEE CIE International Conference*, vol. 2, pp. 1406-1409, Oct. 2011.

[15] P. Dalsania, B. Saha and V. Dwivedi, "Analysis of multiband behavior on square patch fractal antenna," *Communication Systems and Network Technologies (CSNT) International Conference*, pp. 76-78, May 2012.

[16] A. Azari, "A new ultra-wideband fractal monopole antenna," *International Journal of Electronics*, vol. 99, no. 2, pp. 295-303, Feb. 2012.

[17] J. Burke, K. Miller and I. Poggio, "Numerical electromagnetic code NEC," *IEEE Antennas and Propagation Society International Symposium*, vol. 3, pp. 2871-2874, Jun. 2004.

[18] W. Chen, G. Wang and C. Zhang, "Bandwidth enhancement of a microstrip line fed wide-slot antenna with fractal-shaped slot," *IEEE Transactionon Antennas and Propagation*, vol. 57, no. 7, pp. 2176-2179, Jul. 2009.

[19] A. Younas, "A new directivity fractal antenna based on modified koch snowflake geometry," *Asia-Pacific Microwave Conference Proceedings*

(APMC) , pp. 191-194, Dec. 2010.

[20] H. Zhang, H. Xu, B. Tian and X. Zeng, "CPW-Fed fractal solt antenna for UWB application," *International Journal of Antenna and Propagation,* pp. 1-4, 2012.

[21] R. Kumar, D. Magar and K. Sawant, "On the design of inscribed triangle circular fractal antenna for UWB applications," *International Journal of Electronics and Communications,* vol. 6, pp. 68-75, 2011.

[22] O. Kaka, M. Toycan and V. Bashiry, "Modified hilbert fractal geometry, multiservice, miniaturized patch antenna for UWB wireless communication," *The International Journal for Computation and Mathematics in Electrical and Electronic Engineering,* vol. 31, no. 6, pp. 1835-1849, 2012.

[23] [Online]. Available: http://feko.info/applications..

[24] B. Madhave, K. Sarat, P. Kumer, K. Kumer, N. Ramesh and M. Kumer, "Substrate permitivity effects on the performance of microstrip elliptical patch antenna," *Journ. of Emerg. Tren. in CIS,* vol. 2, no. 3, pp. 122-125, 2011.

[25] A. Balanis, Antenna Theory Analysis and Design (3rd ed.), New york: New Jersey: John Wiley & Sons, Inc., 2005.

[26] W. Rotman, "Wide-angle microwave lens for line source applications," *IEEE*

Tranactions on Antennas and Propagation, vol. 11, no. 6, pp. 623-632, 1963.

[27] "FCC Table of Frequency Allocations," Federal Register, USA, Aprile. 2013.

[28] "European FCC Table Frequency Alloc.," ECC within CEPT, Europ, Feb. 2013.

APPENDICES

Appendix A: Rectangular Patch Antenna Design

** PREFEKO input file generated by CADFEKO version 5.0.124623
** Work in mm
SF: 1: : : : : : : : : 0.001
** Import mesh model
IN 8 31 "Rectangular patch.cfm"
** End of geometry
EG: 1 : 0 : 0 : : : 1e-06 : 1 : 1 : : 0 : 0 : 0 : 1
** Planar substrate
GF: 10 : 1 : : : 0 : : 1 : 1 : 0 : 0 : 0 : 0 : 1000 : : : : : : : : : : : : : : : : : 1.59 : 4.6 : 1 : : 0.012 : : 0 : 1000
** Set frequency
FR: : 2 : : : : 1000000000 : : 12000000000
** Sources
DP: Port2_Start_S : : : : : 28.5 : 7.65626244468 : 0
DP: Port2_End_S : : : : : 28.5 : 4.73026244468 : 0
AE: 0 : Port2_Start_S : Port2_End_S : 3 : : 1 : 0 ** VoltageSource1
** Total source power
** use defaults
** Requested output
DA: : : : 0
** Far fields: FarField1
DA: : : 0 : : : : 0
OF: 1 : 0 : : : : 0 : 0 : 0
FF: 1 : 19 : 73 : 0 : : 0 : 0 : 5 : 5 ** FarField1
** End of file
EN
** CADFEKO Checksum: 54556f5dc28ef0685b102b702a8cd610

Appendix B: 1st Iteration SCF Antenna Design

** PREFEKO input file generated by CADFEKO version 5.0.124623
** Work in mm
SF: 1 : : : : : 0.001
** Import mesh model
IN 8 31 "1st SCA.cfm"
** End of geometry
EG: 1 : 0 : 0 : : : 1e-06 : 1 : 1 : : 0 : 0 : 0 : 1
** Planar substrate
GF: 10 : 1 : : : 0 : : 1 : 1 : 0 : 0 : 0 : 0 : 1000 : : : : : : 1.59 : 4.6 : 1 : : 0.012 : : 0 : 1000
** Set frequency
FR: : 2 : : : : 1000000000 : : 12000000000
** Sources
DP: Port1_Start_S : : : : : 28.5 : 8.4446667 : 0
DP: Port1_End_S : : : : : 28.5 : 5.5186667 : 0
AE: 0 : Port1_Start_S : Port1_End_S : 3 : : 1 : 0 ** VoltageSource1
** Total source power
** use defaults

** Requested output
DA: : : : 0
** Far fields: FarField1
DA: : : 0 : : : : 0
OF: 1 : 0 : : : : 0 : 0 : 0
FF: 1 : 37 : 73 : 0 : : -90 : 0 : 5 : 5
** FarField1
** End of file
EN
** CADFEKO Checksum: 775d341ef88d05f6375c5ebeca14b7a1.

Appendix C: 2nd Iteration SCF Antenna Design

** PREFEKO input file generated by CADFEKO version 5.0.124623
** Work in mm
SF: 1 : : : : : 0.001
** Import mesh model
IN 8 31 "2nd SCA.cfm"
** End of geometry
EG: 1 : 0 : 0 : : : 1e-06 : 1 : 1 : : 0 : 0 : 0 : 1
** Planar substrate
GF: 10 : 1 : : : 0 : : 1 : 1 : 0 : 0 : 0 : 0 : 1000; : : : : 1.59 : 4.6 : 1 : : 0.012 : : 0 : 1000
** Set frequency
FR: : 2 : : : : 1000000000 : : 12000000000
** Sources
DP: Port1_Start_S : : : : : 28.5 : 6.58666666667 : 0
DP: Port1_End_S : : : : : 28.5 : 6.16666666667 : 0
AE: 0 : Port1_Start_S : Port1_End_S : 3 : : 1 : 0 ** VoltageSource1
** Total source power
** Requested output
DA: : : : 0
OS: 1 : : 1 ** Currents1
** Far fields: FarField1
DA: : : 0 : : : : 0
OF: 1 : 0 : : : : 0 : 0 : 0
FF: 1 : 19 : 73 : 0 : : 0 : 0 : 5 : 5
** FarField1
** End of file
EN
** CADFEKO Checksum: f38ec243b04b93542c74a060652ac493.

Appendix D: 3rd Iteration SCF Antenna Design

** PREFEKO input file generated by CADFEKO version 5.0.124623
** Work in mm
SF: 1 : : : : : 0.001
** Import mesh model
IN 8 31 "3rd SCA.cfm"
** End of geometry
EG: 1 : 0 : 0 : : : 1e-06 : 1 : 1 : : 0 : 0 : 0 : 1
** Planar substrate
GF: 10 : 2 : : : 0 : : 1 : 1 : 0 : 0 : 0 : 0 : 1000 : : : : : : 1.59 : 4.6 : 1 : : 0.012 : : 0 : 1000
: : : : : : 1.59 : 4.4 : 1 : : 0.012 : : 0 : 1000
** Set frequency
FR: : 2 : : : : 100000000 : : 12000000000
** Sources
DP: Port1_Start_S : : : : : 40 : 1.463 : -1.59
DP: Port1_End_S : : : : : 40 : -1.463 : -1.59
AE: 0 : Port1_Start_S : Port1_End_S : 3 : : 1 : 0
** VoltageSource1
** Total source power
** use defaults
** Requested output
DA: : : : 0
OS: 0 ** Currents1
FF: 1 : 19 : 73 : 0 : : 0 : 0 : 5 : 5
** End of file
EN
** CADFEKO Checksum: 39a4762ad086a4e9480a5c1628064815.

Appendix E: Combination of 3rd Iteration SCF and 1st Iteration MKF Antenna

** PREFEKO input file generated by CADFEKO version 5.0.124623
** Work in mm
SF: 1 : : : : : 0.001
** Import mesh model
IN 8 31 "3rd SCA and 1st MKA"
** End of geometry
EG: 1 : 0 : 0 : : : 1e-06 : 1 : 1 : : 0 : 0 : 0 : 1
** Planar substrate
GF: 10 : 1 : : : 0 : : 1 : 1 : 0 : 0 : 0 : 0 : 1000 : : : : : : 3.18 : 4.6 : 1 : : 0.012 : : 0 : 1000
** Set frequency
FR: : 2 : : : : 1000000000 : : 11000000000
** Sources
DP: Port2_Start_S : : : : : 71.833335 : 1.5 : -1.59
DP: Port2_End_S : : : : : 71.833335 : -1.5 : -1.59
AE: 0 : Port2_Start_S : Port2_End_S : 3 : : 1 : 0
** VoltageSource1

** Total source power
** use defaults
** Requested output
DA: : : : 1
OS: 0 ** Currents1
FF: 1 : 19 : 73 : 0 : : 0 : 0 : 5 : 5
** End of file
EN
** CADFEKO Checksum: 421c2f50786157be187a100b413bc178.

Appendix F: Triangular Patch Antenna

** PREFEKO input file generated by CADFEKO version 5.0.124623
** Work in mm
SF: 1 : : : : : 0.001
** Import mesh model
IN 8 31 "Triangular Patch Antenna .cfm"
** End of geometry
EG: 1 : 0 : 0 : : : 1e-06 : 1 : 1 : : 0 : 0 : 0 : 1
** Planar substrate
GF: 10 : 1 : : : 0 : : 1 : 1 : 0 : 0 : 0 : 0 : 1000 : : : : : : : 1.59 : 4.6 : 1 : : 0.002 : : 0 : 1000
** Set frequency
FR: : 2 : : : : 1200000000 : : 2000000000
** Sources
A4 0 -1 0 1 0 0 0 0 1.12 50
** Total source power
** use defaults
** Requested output
DA: : : : 0
OS: 1 : : 1 ** Currents1
** Far fields: FarField1
DA: : : 0 : : : : 0
OF: 1 : 0 : : : : 0 : 0 : 0
FF: 1 : 37 : 73 : 0 : : -90 : 0 : 5 : 5 ** FarField1
** End of file
EN
** CADFEKO Checksum: 47701aedcd8e7657d8632b94b8349ec5.

Appendix G: 1st Iteration KSF Antenna

** PREFEKO input file generated by CADFEKO version 5.0.124623
** Work in mm
SF: 1 : : : : : 0.001
** Import mesh model
IN 8 31 "1st KSF Antenna .cfm"

** End of geometry
EG: 1 : 0 : 0 : : : 1e-06 : 1 : 1 : : 0 : 0 : 0 : 1
** Planar substrate
GF: 10 : 1 : : : 0 : : 1 : 1 : 0 : 0 : 0 : 0 : 1000 : : : : : : : 1.59 : 4.5 : 1 : : 0.002 : : 0 : 1000
** Set frequency
FR: : 2 : : : : 500000000 : : 12000000000
** Sources
A4 0 -1 0 1 0 0 0 0 1.12 50
** Total source power
** use defaults
** Requested output
DA: : : : 0
OS: 1 : : 1 ** Currents1
** Far fields: FarField1
DA: : : 0 : : : : 0
OF: 1 : 0 : : : : 0 : 0 : 0
FF: 1 : 37 : 73 : 0 : : -90 : 0 : 5 : 5 ** FarField1
** End of file
EN
** CADFEKO Checksum: c815064e70e983cfaf7392012bbdd9cd.

Appendix H: 2nd Iteration KSF Antenna

** PREFEKO input file generated by CADFEKO version 5.0.124623
** Work in mm
SF: 1 : : : : : 0.001
** Import mesh model
IN 8 31 "2nd KSF Antenna .cfm"
** End of geometry
EG: 1 : 0 : 0 : : : 1e-06 : 1 : 1 : : 0 : 0 : 0 : 1
** Planar substrate
GF: 10 : 1 : : : 0 : : 1 : 1 : 0 : 0 : 0 : 0 : 1000 : : : : : : : 1.59 : 4.6 : 1 : : 0.002 : : 0 : 1000
** Set frequency
FR: : 2 : : : : 500000000 : : 12000000000
** Sources
A4 0 -1 0 1 0 0 0 0 1.12 50
** Total source power
** use defaults
** Requested output
DA: : : : 0
OS: 1 : : 1 ** Currents1
** Far fields: FarField1
DA: : : 0 : : : : 0
OF: 1 : 0 : : : : 0 : 0 : 0
FF: 1 : 37 : 73 : 0 : : -90 : 0 : 5 : 5 ** FarField1
** End of file
EN
** CADFEKO Checksum: 834dd6f24f3332e280f99872a0f904f3.

Appendix I: 3rd Iteration KSF Antenna

** PREFEKO input file generated by CADFEKO version 5.0.124623
** Work in mm
SF: 1 : : : : : 0.001
** Import mesh model
IN 8 31 "3rd KSA .cfm"
** End of geometry
EG: 1 : 0 : 0 : : : 1e-06 : 1 : 1 : : 0 : 0 : 0 : 1
** Planar substrate
GF: 10 : 1 : : : 0 : : 1 : 1 : 0 : 0 : 0 : 0 : 1000
: : : : : : 1.59 : 4.6 : 1 : : 0.002 : : 0 : 1000
** Set frequency
FR: : 2 : : : : 500000000 : : 12000000000
** Sources
A4 0 -1 0 1 0 0 0 0 1.12 50
** Total source power
** use defaults
** Requested output
DA: : : : 0
OS: 1 : : 1 ** Currents1
** Far fields: FarField1
DA: : : 0 : : : : 0
OF: 1 : 0 : : : : 0 : 0 : 0
FF: 1 : 37 : 73 : 0 : : -90 : 0 : 5 : 5 ** FarField1
** End of file
EN
** CADFEKO Checksum: 8bf759a4ae6357944b0feaafaee9e839.

Appendix J: 3rd Iteration KSF and 4th Iteration SGF Antenna (KS-SGF)

** PREFEKO input file generated by CADFEKO version 5.0.124623
** Work in mm
SF: 1 : : : : : 0.001
** Import mesh model
IN 8 31 "3rd KSF Antenna+ 4th Iteration SGF Antenna .cfm"
** End of geometry
EG: 1 : 0 : 0 : : : 1e-06 : 1 : 1 : : 0 : 0 : 0 : 1
** Planar substrate
GF: 10 : 1 : : : 0 : : 1 : 1 : 0 : 0 : 0 : 0 : 1000 : : : : : : 1.59 : 4.6 : 1 : : 0.002 : : 0 : 1000
** Set frequency
FR: : 2 : : : : 500000000 : : 12000000000
** Sources
A4 0 -1 0 1 0 0 0 0 1.12 50
** Total source power
** use defaults
** Requested output
DA: : : : 0

OS: 1 : : 1 ** Currents1
** Far fields: FarField1
DA: : : 0 : : : : 0
OF: 1 : 0 : : : : 0 : 0 : 0
FF: 1 : 37 : 73 : 0 : : -90 : 0 : 5 : 5 ** FarField1
** End of file
EN
** CADFEKO Checksum: c7acbf2cd568e8a04bb14372e71760f8.

Appendix K: Stacked Antenna Design

** PREFEKO input file generated by CADFEKO version 5.0.124623

** Work in mm
SF: 1 : : : : : 0.001

** Import mesh model
IN 8 31 "Stacked Antenna .cfm"
** End of geometry
EG: 1 : 0 : 0 : : : 1e-06 : 1 : 1 : : 0 : 0 : 0 : 1
** Planar substrate
GF: 10 : 3 : : : 0 : : 1 : 1 : 0 : 0 : 5.59 : 0 : 1000 : : : : : : 1.59 : 4.5 : 1 : : 0.012 : : 0 : 1000
: : : : : : 4 : 1.07 : 1 : : 0 : : 0 : 1000 : : : : : : 3.18 : 4.5 : 1 : : 0.012 : : 0 : 1000
** Set frequency
FR: : 2 : : : : 1000000000 : : 15000000000
** Sources
DP: Port2_Start_S : : : : : 64.44445 : 1.5 : -1.59
DP: Port2_End_S : : : : : 64.44445 : -1.5 : -1.59
AE: 0 : Port2_Start_S : Port2_End_S : 3 : : 1 : 0 ** VoltageSource1
** Total source power
** use defaults
** Requested output
DA: : : : 1
OS: 0 ** Currents1
** Far fields: FarField1
DA: : : 0 : : : : 0
OF: 1 : 0 : : : : 0 : 0 : 0
FF: 1 : 37 : 73 : 0 : : -90 : 0 : 5 : 5 ** FarField1
** End of file
EN
** CADFEKO Checksum: 658ea8be78985c04849ec36ec37647a8.